Title
Developing New Spectroscopic Techniques to Study Carotenoid-Dependent Non-Photochemical Quenching in Plants and Algae

Author
Fischer, Alexandra L

Publication Date
2018

Peer reviewed|Thesis/dissertation

Developing New Spectroscopic Techniques to Study Carotenoid-Dependent Non-Photochemical Quenching in Plants and Algae

By

Alexandra Lee Fischer

A dissertation submitted in partial satisfaction of the
requirements for the degree of

Doctor of Philosophy

in

Chemistry

in the

Graduate Division

of the

University of California, Berkeley

Committee in charge:

Professor Graham R. Fleming, Chair
Professor Krishna K. Niyogi
Professor Ronald C. Cohen

Spring 2018

Developing New Spectroscopic Techniques to Study Carotenoid-Dependent Non-Photochemical Quenching in Plants and Algae

By

Alexandra Lee Fischer

Abstract

Developing New Spectroscopic Techniques to Study Carotenoid-Dependent Non-Photochemical Quenching in Plants and Algae

by

Alexandra Lee Fischer

Doctor of Philosophy in Chemistry

University of California, Berkeley

Professor Graham R. Fleming, Chair

Photosynthetic organisms live in environments with highly variable light conditions. In order to survive, they must maximize photosynthetic production while at the same time minimizing photodamage caused by excess absorbed sunlight. To prevent this photodamage, photosynthetic organisms have developed a suite of mechanisms called non-photochemical quenching (NPQ) mechanisms which dissipate excess excitation energy as heat. However, little is known about the specific molecular mechanisms that convert excitation energy to heat or how these mechanisms are activated and de-activated.

NPQ mechanisms have previously been characterized according to their timescale of activation, with the fastest group, referred to as qE mechanisms, responding within 30 s to a few minutes to increases in light intensity. As the fastest responders, these mechanisms are responsible for the largest portion of the energy quenching. Previous work has shown that these mechanisms require the carotenoid zeaxanthin (Zea) in order to fully function. There have been two types of proposed molecular mechanisms by which this carotenoid could be directly involved in excitation energy quenching, and this thesis describes the development of new spectroscopic techniques that are capable of tracking intermediate species associated with each of these mechanisms as samples acclimate to high light conditions. These techniques were then used to determine the role of each of these quenching mechanisms in several photosynthetic organisms.

The first molecular mechanism of interest is called charge transfer (CT) quenching. This mechanism involves a chlorophyll (Chl) –Zea dimer, which accepts excitation energy from light-harvesting chlorophylls, then undergoes charge separation, and finally charge recombination to complete the cycle. Previous transient absorption (TA) experiments found that an intermediate Zea cation species formed selectively in light-acclimated plant thylakoid samples, but did not determine at what point during the light acclimation process the Zea cation began forming. The difficulty lies in tracking sub-microsecond processes, such as Zea cation absorption, which evolve over seconds to minutes in real time. Combining these two timescales into one measurement has previously been developed in fluorescence lifetime snapshots, which measure quenching by following fast changes in the Chl fluorescence lifetime as a function of

high-light acclimation. This thesis will discuss the development of a new transient absorption technique, called snapshot transient absorption, capable of tracking signals that change on the same timescale as qE, seconds to minutes. Development of this technique required numerous changes to the instrumental setup as well as optimization of sample preparation and data collection to obtain a sufficient signal-to-noise ratio to accurately track Zea cation signals in spinach photosynthetic membranes.

This technique, combined with previously established fluorescence lifetime snapshots as well as time-resolved HPLC measurements, determined that the timing and intensity of the Zea cation signal observed in spinach membranes is consistent with CT quenching acting as a qE quenching mechanism. However, results indicated that CT quenching only utilized a small percentage of the overall Zea concentration, implying that Zea may also participate in the second theorized quenching mechanism, excitation energy transfer (EET) quenching. The EET quenching mechanism involves energy transfer from excited Chl to the dark S1 state of Zea, which then rapidly relaxes down to the ground state.

To determine the feasibility of the EET quenching mechanism, snapshot TA technique was adapted to track the population of the Car S1 state in photosynthetic samples. Zea cations absorption occurs at a wavelength where the underlying Chl excited state dynamics are largely constant throughout the experiment, but the same is not true for Car S1 absorption. Therefore in order to collect data on Car S1 absorption, the snapshot TA was adjusted to account for changes in the Chl ESA background. These experiments determined that in spinach photosynthetic membranes, EET quenching likely occurs in tandem with CT quenching, though its activation time is slightly longer. Snapshot TA spectroscopy was also used to study a series of *Nannochloropsis oceanica* mutants. *N. oceanica* is a small ocean algae which appears to rely on Zea, as well as its epoxidized forms, for much of its quenching ability. While this research is still in progress, results thus far are discussed. It appears that the EET quenching signal in *N. oceanica* is highly dependent on the Zea concentration, and that *lhcx1*, a suspected quenching protein, does not perform EET quenching. Future work should focus on determining the relationship between the EET and CT quenching mechanisms in *N. oceanica* mutants.

For my wonderful husband Nathan,
who gives the best hugs and makes truly spectacular veggie lasagna

Acknowledgements

First, I would like to thank my adviser, Graham Fleming, for his support at every stage of graduate school. From enlightening scientific discussions to career advice, Graham has helped me grow tremendously, both academically and personally.

Additionally, my Fleming lab-mates have always very generous with their time and knowledge. Thank you especially to Emily Jane Sylak-Glassman, Tom Oliver, Nicholas Lewis, Michelle Leuenberger, Daniele Monahan, and Jonathan Morris. I would also like to thank Soomin Park in particular for being the best collaborator a scientist could ask for.

I would also like to thank my extremely knowledgeable collaborators, including Professor Kris Niyogi, Alizée Malnoë, Zhirong Li, and Masakazu Iwai. Your patient and thorough explanations as well as your willingness to answer endless questions about genetics were always much appreciated.

I would also like to thank my delightful friends and family. My parents and my sister have listened to me complain about esoteric technical problems for countless hours and are always ready with words of encouragement and love. Of my friends, I would like to give specific shout outs to Tamara, Alexis, and Sumana for their endless emotional support, great jokes, and excellent taste in distracting media.

Lastly, I would like to thank my husband Nathan. Thank you for always taking my thoughts, opinions, and ideas so seriously. Even when deadlines loom, you can always make me smile.

Table of Contents

Table of Contents Continued…

Chapter 1: Introduction

Photosynthesis is the process by which plants, as well as other organisms, harvest light energy from the sun and convert it into storable chemical energy. This process supports the vast majority of multi-cellular organisms on earth and is essential for human survival. Though photosynthesis is an intricate and dynamic process, for brevity's sake only the very early steps will be discussed here.

The Machinery of Photosynthesis

Though photosynthesis occurs in a variety of organisms, including plants, algae, and bacteria, I will largely focus on plants. Within land plants, photosynthetic processes take place in an organelle called the chloroplast.[1] Within the chloroplast the photosynthetic proteins are localized to two types of membranes. One type of membrane, called grana stacks, consists of closed, flattened bubbles stacked on top of one another. The space inside each grana bubble is called the lumen. The space outside the membranes, but within the chloroplast, is called the stroma. The second type of membrane are tube-like membranes that connect the grana membranes to each other, and are called stroma lamellae.[2] This structure is shown in figure 1.1.

The grana membranes house the majority of the proteins involved in the early steps of photosynthesis. Grana membranes are very densely packed with protein; as much as 80% of the membrane surface area is covered by protein.[3] The most abundant type of protein present in the grana membrane is light-harvesting complex II (LHCII). LHCII is responsible for the first step in photosynthesis, the initial absorption of sunlight. LHCII monomers are densely packed with pigments and each one contains 14 chlorophyll molecules and 4 carotenoid molecules.[4] The majority of LHCII proteins in the thylakoid membrane assemble into trimers. Due to the dense packing and high pigment concentration, LHCIIs can absorb light and then transfer this collected excitation energy to the pigment of a protein complex where the next step of photosynthesis takes place, photosystem II (PSII).

PSII complexes' main function is to take excitation energy and use it to perform charge separations, i.e. the first chemical reaction in photosynthesis. The core of PSII is a pair of proteins called D1 and D2, which are together called the reaction center (RC). There are additional light-harvesting monomers and trimers surrounding each RC. This set of proteins associates with an identical set of RC and light harvesting proteins forming a PSII supercomplex. Within each RC protein, there is a special pair of closely-spaced chlorophyll molecules called P680. Once excitation energy reaches P680, the two chlorophylls undergo charge separation. To prevent recombination, the electron and the hole are then quickly separated from one another. The electron rapidly transfers to a nearby pheophytin pigment, which is a Chl sans magnesium ion. Next, it is moved even further away from P680 to a charge carrier called plastoquinone (PQ), which will move the charge to the next location through the thylakoid membrane itself. Meanwhile, the hole is moved towards the lumenal-side of the protein to an

oxidize-able tyrosine residue. Then the hole makes its way even closer to the lumen, to a manganese cluster called the oxygen evolving complex (OEC). Here, the holes from repeated charge splitting events will be used to oxidize water into oxygen and protons.[5] These steps are illustrated in figure 1.2. Ultimately, these electrons will be used to make useful chemical products NADPH, ATP, and sugars that the plant can use as fuel for biomass production.

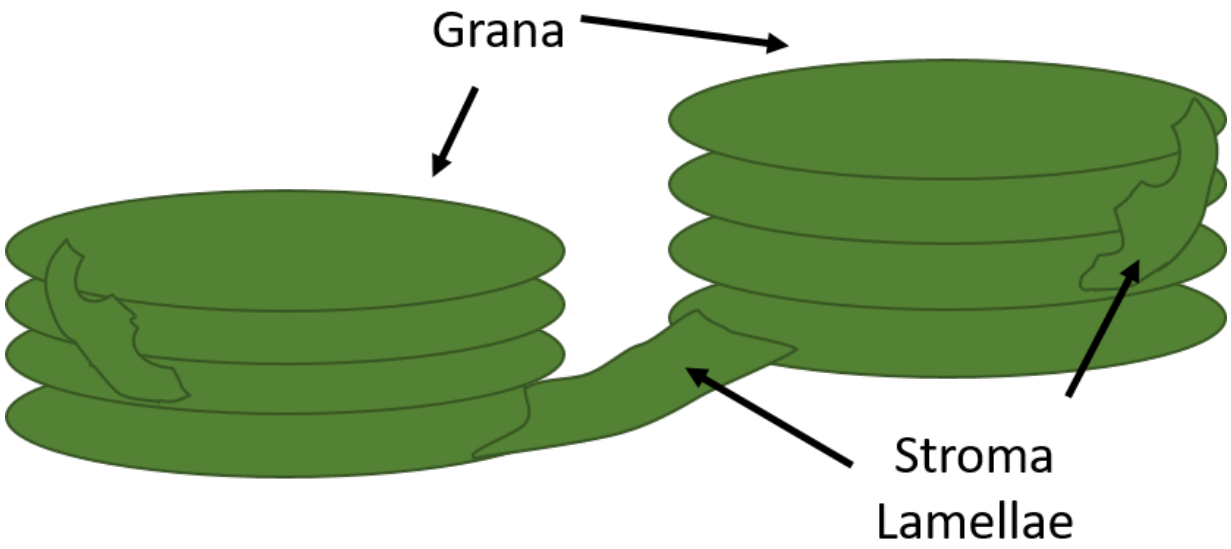

Figure 1.1: Schematic depiction of thylakoid membrane structure.

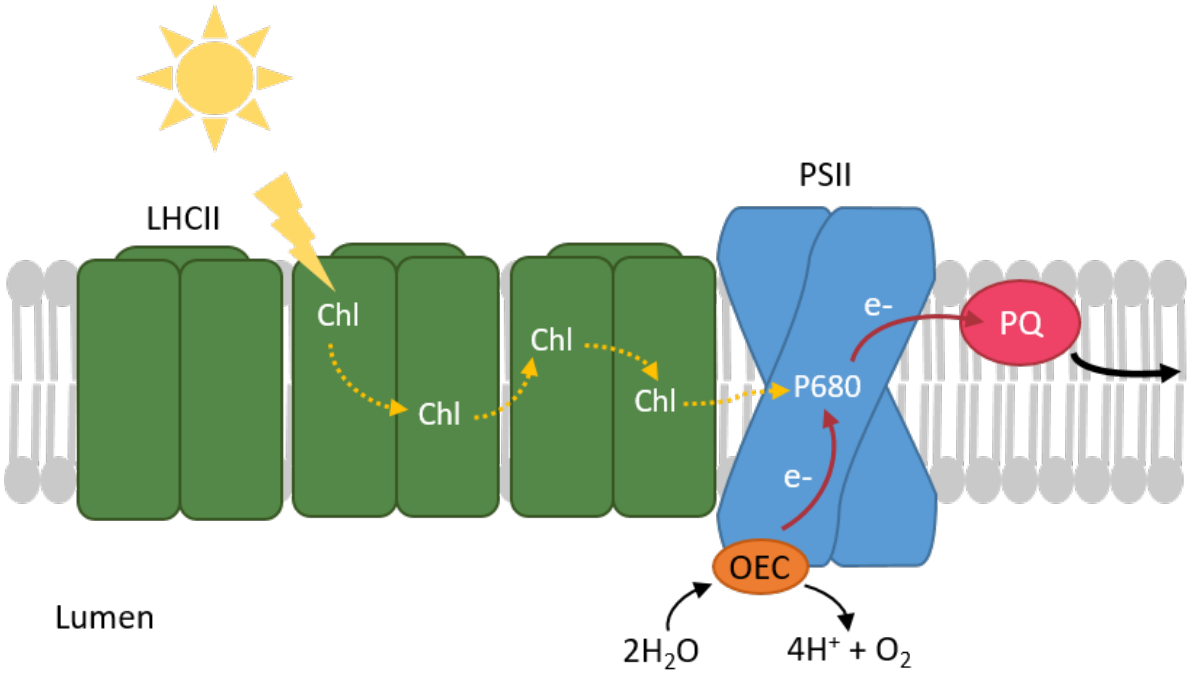

Figure 1.2: Side view of the grana membrane, showing the initial steps in photosynthesis. Initial light absorption most likely to occur in light-harvesting complex II (LHCII). Excitation energy can then 'hop' from chlorophyll to chlorophyll until it reaches the special pair (P680) of photosystem II (PSII). On P680 a charge separation occurs. The electron is moved to plastoquinone (PQ) for transport to the next step, while the hole is filled at the oxygen evolving complex (OEC) where electrons are stripped from water molecules, which become protons and molecular oxygen.

The Utility of Quenching

As they are literally rooted to the ground, plants have very little control over the amount of sunlight that shines on them. They also have a limited capacity as to the number of photons that can be used productively, and in fact, they can receive enough sunlight to reach maximum production even during an overcast day. So on sunny days, they cannot move out of the way and must instead use other measures to protect themselves.

Under excess light conditions the light-harvesting proteins do not stop absorbing photons and directing them towards PSII, and PSII continues to generate electrons and holes. Unfortunately, there is a limited number of plastoquinones available to move electrons away from PSII. When there is no plastoquinone available, PSII is considered "closed" and cannot perform any additional charge separation. Under these conditions, the electron remains on PSII and often will return to P680 and recombine with the hole. This charge re-combination process can lead to the formation of triplet chlorophyll (^{3}Chl*). If triplet chlorophyll encounters triplet molecular oxygen ($^3O_2$), triplet-triplet energy transfer can occur, forming singlet oxygen ($^1O_2$).[6] Alternatively, under closed reaction center conditions the transfer of excitation energy to PSII for electron production is halted, which increases the amount of time the average chlorophyll molecule remains electronically excited. The longer the excitation energy remains on a chlorophyll molecule, the more likely it is for that chlorophyll to undergo intersystem crossing, forming ^{3}Chl,* which can then form $^1O_2$. Singlet oxygen can damage photosynthetic proteins, and if PSII itself is damaged can be especially debilitating for the plant, as the repair process is very time consuming and can take hours.[7,8] For more information on singlet oxygen formation in photosynthetic systems, see Krieger-Liszkay.[9]

In order to repair a damaged PSII protein, the DI sub-protein, which holds the special pair Chls in place, must be removed and degraded. Then a completely new DI protein must be transcribed and re-inserted into the membrane. This process takes approximately two hours.[7] Thus it is extremely important to prevent this damage from happening in the first place. Dame if of the D1 protein is strongly light-dependent, and plants that can turn quenching on quickly are better able to protect these essential photosynthetic proteins and can avoid the costly repair process.[10] However, quenching must also turn off rapidly once the excess light is gone. It would be highly inefficient for the plant if quenching mechanisms were still active and excitation energy was being dissipated that could have been used for productive photosynthesis. This would prevent maximum chemical energy storage and inhibit organism growth.

In order to prevent photooxidative damage, photosynthetic organisms have developed a set of processes known as non-photochemical quenching (NPQ) mechanisms. These mechanisms turn on in response to light stress and turn off when the stress is over. Functionally, all of these mechanisms involve converting excess excitation energy into heat before the excitation energy can reach PSII. Historically, NPQ mechanisms have been categorized by the amount of time they take to turn on and off.[11] However, as knowledge of the mechanisms improves, quenching mechanisms are increasingly grouped by trigger or triggering process. The fastest of these categories is called qE, or energy-dependent quenching.

qE mechanisms are triggered by a sharp drop in pH within the lumen which occurs immediately after initial high light stress. Given the near-immediate trigger, these processes turn on within seconds to minutes. qE quenching is extremely important for plant fitness, as these mechanisms are responsible for the largest portion of total energy quenched. The next-fastest quenching mechanisms are called qZ, and are thought to depend on the population of the pigment zeaxanthin. Zeaxanthin (Zea) is a carotenoid that is only present in its epoxidized form, violaxanthin (Vio), in dark-acclimated conditions. The pool of Vio is only de-epoxidized into Zea once high light acclimation begins. This process will be discussed further in the next section. Another type of quenching, called qT, activates in tens of minutes and is related to the phosphorylation of LHCII. Finally, qI quenching turns on within hours of bright light exposure and is related damage of PSII. The large variety of timescales and mechanisms allow photosynthetic organisms to respond efficiently to their dynamic environments and to prevent damage while allowing productive reactions to continue.[12] The timescales of these types of quenching and other relevant processes are summarized in figure 1.3. For the purposes of this thesis I will largely focus on qE, or energy-dependent quenching.

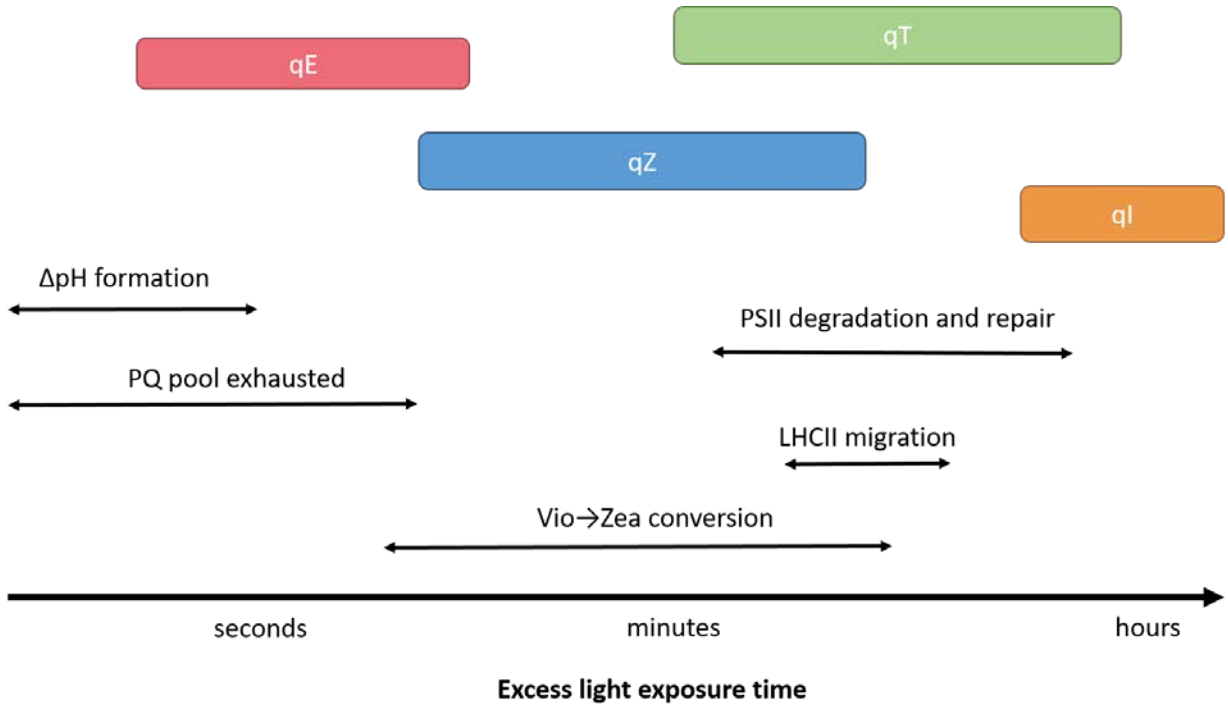

Figure 1.3: Timescales of quenching types as well as several processes integral to quenching and photosynthetic function.

Important Components of qE Quenching

Though all types of NPQ play important roles in plant photoprotection, qE quenching is arguably the most important for plant fitness due to its fast response time to changes in light intensity. While there are no confirmed molecular mechanisms of qE quenching, there is still some information known about the necessary components for maximum qE quenching.

One of the most integral components of qE quenching is the formation of the pH gradient across the thylakoid membrane in response to excess light, hereafter referred to as ΔpH. There are several individual reactions in photosynthesis that cause protons to build up in the lumen, but in a non-quenched system, there are also several reactions that are fueled by the proton motive force and will push protons through the membrane to the outside of the lumen, re-equilibrating the system.[13] Under excess-light conditions however, the protons build up on the inside of the lumen faster than they can be pushed outside the lumen, causing a large drop in pH within the lumen. This results in a spike in the difference between the outside of the lumen and the inside of the lumen, and is known to be the key driver of qE quenching.[11] The complete mechanistic influence of the change in ΔpH is unknown, but it is the focus of much study. There is also some evidence that ΔΨ, the electrical potential across the thylakoid membrane which includes ΔpH, may actually be influencing quenching.[14–16]

Another important factor in qE quenching is the previously mentioned carotenoid Zeaxanthin (Zea). Zea is a molecule consisting of a functionalized 6-membered ring on each end of a conjugated chain, the length of which changes depending on the epoxidation state.[17] In non-quenching conditions, Zea is not present in plants. Instead, it is present in its epoxidized form, violaxanthin (Vio). Once a plant begins to experience excess light, the formation of ΔpH triggers the enzyme violaxanthin de-epoxidase (VDE) to begin converting Vio into Zea, through the intermediate pigment antheraxanthin (Anth). Once quenching is no longer needed, another triggering pathway activates the enzyme zeaxanthin epoxidase, which converts Zea back into Vio. These three pigments are collectively known as the xanthophyll cycle, and are often quantified as the sum of all three pigment concentrations. The light-dependent conversion process is depicted in figure 1.4 along with the chemical structures of each carotenoid. The forward conversion process from Vio to Zea is known to be approximately twenty times faster than the reverse process.[18] Zea specifically is known to be necessary in order for plants to have maximum qE quenching.[19,20]

The last key player known to influence qE quenching in plants is the protein PsbS. PsbS is a pH-sensitive protein that does not contain pigments, and therefore cannot directly quench excitation energy.[21] Instead it is thought to act as a catalyst, increasing the speed with which quenching mechanisms activate in response to a bright light stimulus [15]. It is currently unclear how PsbS increases the speed of quenching, or if it increases the activation time of one mechanism or multiple quenching mechanisms.[22]

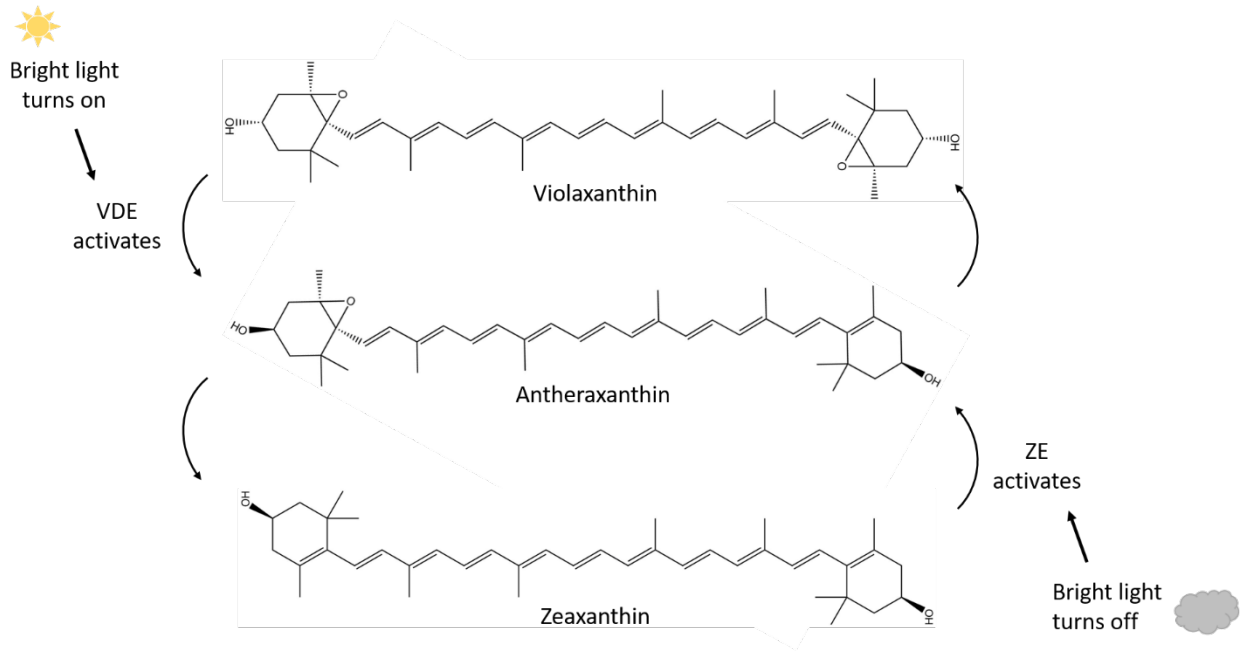

Figure 1.4: Conversion of violaxanthin to zeaxanthin in response to bright light exposure. Upon experiencing excess light, ΔpH activates the enzyme violaxanthin de-epoxidase (VDE) which begins to de-epoxidize Vio into Zea, via the intermediate antheraxanthin (Anth). Once the excess light is gone, the enzyme zeaxanthin epoxidase (ZE) is activated, which epoxidizes zeaxanthin back into violaxanthin.

Proposed Zea-Chl quenching mechanisms

Though it has been known for quite some time that Zea is necessary for qE quenching, there is currently no confirmed molecular mechanism for Zea-dependent quenching. There are however, two prominent proposed mechanisms that may occur exclusively or in tandem. Both mechanisms require the Zea molecule to be in close proximity to a Chl molecule. The first mechanism involves excitation energy transfer from the general pool of excited Chl to a Chl-Zea dimer. Once excited, this dimer undergoes charge separation, forming a Chl^- and a Zea^+. After some time the charges recombine, forming ground state Chl-Zea once again. This mechanism will be referred to as charge transfer (CT) quenching.[23] This mechanism is discussed extensively in chapter 2 and 3. The second mechanism involves energy transfer from Chl Q_y state to the Zea S_1 excited state, then Zea relaxes quickly back to the ground state. This mechanism is called excitation energy transfer (EET) quenching.[24] Greater detail about this mechanism can be found in chapter 4. These two mechanisms are shown in figure 1.5.

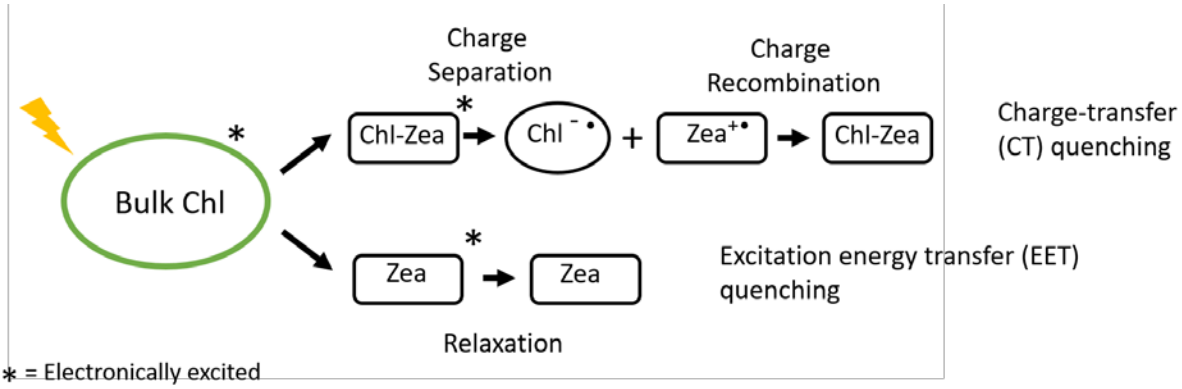

Figure 1.5: Two possible direct-quenching mechanisms for Zea.

Conventional spectroscopic tools for studying quenching

Given that photosynthetic membranes by nature interact strongly with visible light, spectroscopic tools are a very appealing means of studying their quenching dynamics. Many different spectroscopic techniques have been used to try to gain information about quenching dynamics as well as the formation of quenching species, but for this thesis I will largely focus on two types of techniques which approach quenching from opposing viewpoints. Chlorophyll fluorescence techniques are designed to study the dynamics and intensity of the quenching itself and do not directly give any information about the specifics of the molecular quenching mechanisms.[25] On the other side, transient absorption spectroscopy can be used to try to detect the presence of species thought to be involved in quenching, but does not give information about the quenching behavior.[26] However, when used in combination, they can give information on both the molecular mechanism and the effect that mechanism has on overall quenching.

When measuring processes related to NPQ it is important to note that processes and changes occur on a large range of timescales. Some events occur in less than 100 femtoseconds, such as energy transfer between neighboring pigments in LHCII.[27] Other events, such as charge recombination of Chl^- and a Zea^+, take approximately 150 picoseconds, over one thousand times slower.[28] Yet both of these processes are still fast enough that they would need to be measured using pulsed femtosecond lasers rather than a mechanically-pulsed continuous light source. However, if one zooms out to consider larger population-level changes due to quenching turning on, timescales are even longer. qE quenching activates within seconds to minutes, but qI quenching only activates after longer periods of high light exposure. Thus, many of the spectroscopic studies of quenching mentioned in this thesis will study sub-nanosecond processes that evolve over minute timescales.

Measuring changes in Chl fluorescence is one of the oldest methods of studying NPQ as well as photosynthesis in general.[25] Chl fluorescence is useful as an indicator of quenching, but it does have limitations. The foremost is that because Chls are so abundant in photosynthetic

organisms and are housed in a wide variety of environmental conditions, measurements of Chl fluorescence are always inherently the result of many different relaxation processes. For example, a single excitation on one Chl in an LHCII trimer has a variety of ways it can relax down to the ground state.[11] Of course, fluorescence is one such pathway. Other possible pathways include internal conversion down to the ground state, or intersystem crossing, creating ^{3}Chl,* which could transfer energy to $^3O_2$, then form $^1O_2$. The excitation energy could also transfer to a neighboring pigment. This energy transfer (and additional subsequent transfers) could lead to PSII, where the excitation energy could be used for a charge separation. Or, the energy transfer could ultimately lead to a quenching site, where the excitation energy could be dissipated. These pathways are illustrated in figure 1.6. Though we are only observing the fluorescence (with the exception of quenching in dark-acclimated membranes), all of these pathways are still taken by different Chls in the photosynthetic membrane. When the quenching pathway opens up, the amount of fluorescence is reduced because some portion of the Chls are now taking that route to the ground state instead of the fluorescent route. However, when analyzing Chl fluorescence data, one must be cognizant of the fact that it is always a reflection of many possible relaxation pathways and timescales, not just those related to quenching.[25]

Additionally, there are two methods of measuring fluorescence, and each has its benefits. One method involves monitoring changes in the fluorescence yield to indicate changes in NPQ. In dark-acclimated samples, the fluorescence yield is very high, and as the samples are adapted to bright light, the yield shrinks. By comparing the fluorescence yield from the light-acclimated sample to that of the dark-acclimated, the amount of quenching can be quantified. There are commercially available instruments using this method, and each measurement is relatively quick to perform. Lastly, this method is non-invasive and non-destructive, so samples can be characterized and then used for other experiments. The second method of measuring fluorescence involves measuring Chl fluorescence lifetimes.[29,30] This method involves a pulsed laser, which excites the Chl. After each laser pulse interacts with the sample, the arrival time of individual fluorescent photons is recorded at the detector, then graphed as a histogram. This histogram can be fitted to exponential decays to give a fluorescence lifetime, which will shorten as quenching intensifies. This method offers several advantages over collecting fluorescence yield, largely, that fluorescence lifetime is insensitive to changes in fluorescence yield not caused by Chl excited state decay.[31] Changes in fluorescence yield can also be caused by damage or chloroplast shielding, which is where one chloroplast moves over another to block it from absorbing light.[30] Both of these can artificially inflate the amount of quenching in yield measurements. Unfortunately, fluorescence lifetime measurements require extensive equipment and lab space.

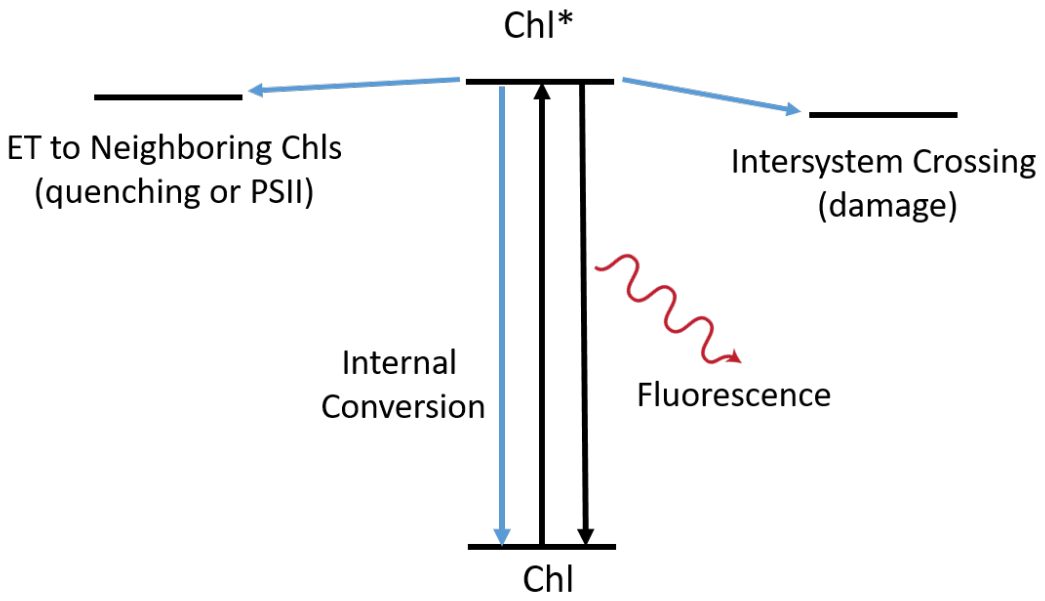

Figure 1.6: Predominant relaxation pathways for an excited chlorophyll molecule in a photosynthetic membrane.

The second type of spectroscopy that is often use to study quenching is transient absorption (TA) spectroscopy. TA spectroscopy is not often used to study the amount of quenching in a plant, instead it is used to look for the appearance of species involved in quenching.[32] In TA spectroscopy, two laser beams interact with the sample. The first beam is called the pump beam; it is very intense and has a narrow bandwidth and is used to excite the sample. The second beam is called the probe beam; it is much less intense and is often a broad spectrum of white light. After the pump beam excites the sample, the probe beam then re-excites the sample, and then the transmitted beam is detected. In brief, the probe beam is used to measure the changes in absorption caused by the pump beam. By delaying the probe beam in time, one can measure where the energy from the pump beam went and how long it took to get there.[26] This technique is discussed in further detail in chapter 2.

References

(1) Blankenship, R. E. *Molecular Mechanisms of Photosynthesis*, 2nd ed.; Wiley-Blackwell, 2014.

(2) Daum, B.; Kühlbrandt, W. Electron Tomography of Plant Thylakoid Membranes. *J. Exp. Bot.* **2011**, *62* (7), 2393–2402.

(3) Kirchhoff, H.; Haferkamp, S.; Allen, J. F.; Epstein, D. B. A.; Mullineaux, C. W. Protein Diffusion and Macromolecular Crowding in Thylakoid Membranes 1[W]. *Plant Physiol.* **2008**, *146*, 1571–1578.

(4) Liu, Z.; Yan, H.; Wang, K.; Kuang, T.; Zhang, J.; Gui, L.; An, X.; Chang, W. Crystal Structure of Spinach Major Light- Harvesting Complex at 2.72 Å Resolution.

(5) Cady, C. W.; Crabtree, R. H.; Brudvig, G. W. Functional Models for the Oxygen-Evolving Complex of Photosystem II. *Coord. Chem. Rev.* **2008**, *252*, 444–455.

(6) Telfer, A. Singlet Oxygen Production by PSII Under Light Stress: Mechanism, Detection and the Protective Role of B-Carotene. *Plant Cell Physiol.* **2014**, *55* (7), 1216–1223.

(7) Melis, A. Photosystem-II Damage and Repair Cycle in Chloroplasts: What Modulates the Rate of Photodamage in Vivo? *Trends Plant Sci.* **1999**, *4* (4), 130–135.

(8) Järvi, S.; Suorsa, M.; Aro, E.-M. Photosystem II Repair in Plant Chloroplasts — Regulation, Assisting Proteins and Shared Components with Photosystem II Biogenesis ☆*BBA - Bioenerg.* **2015**, *1847*, 900–909.

(9) Krieger-Liszkay, A. Singlet Oxygen Production in Photosynthesis. *J. Exp. Bot.* **2005**, *56* (411), 337–346.

(10) Park, Y.-L.; Chow, W. S.; Anderson, J. M. Light Inactivation of Functional Photosystem II in Leaves of Peas Grown in Moderate Light Depends on Photon Exposure. *Planta* **1995**, *196*, 401–411.

(11) Müller, P.; Li, X.-P.; Niyogi, K. K. Non-Photochemical Quenching. A Response to Excess Light Energy 1. *Plant Physiol.* **2001**, *125*, 1558–1566.

(12) Zaks, J.; Amarnath, K.; Sylak-Glassman, E. J.; Fleming, G. R. Models and Measurements of Energy-Dependent Quenching. *Photosynth. Res.* **2013**, *116* (2–3), 389–409.

(13) Takizawa, K.; Cruz, J. A.; Kanazawa, A.; Kramer, D. M. The Thylakoid Proton Motive Force in Vivo. Quantitative, Non-Invasive Probes, Energetics, and Regulatory Consequences of Light-Induced Pmf. *Biochim. Biophys. Acta - Bioenerg.* **2007**, *1767* (10), 1233–1244.

(14) Cruz, J. A.; Sacksteder, C. A.; Kanazawa, A.; Kramer, D. M. Contribution of Electric Field (Δψ) to Steady-State Transthylakoid Proton Motive Force (Pmf) in Vitro and in Vivo. Control of Pmf Parsing into Δψ and ΔpH by Ionic Strength. *Biochemistry* **2001**, *40*, 1226–1237.

(15) Sylak-Glassman, E. J.; Malnoë, A.; De Re, E.; Brooks, M. D.; Fischer, A. L.; Niyogi, K. K.; Fleming, G. R. Distinct Roles of the Photosystem II Protein PsbS and Zeaxanthin in the Regulation of Light Harvesting in Plants Revealed by Fluorescence Lifetime Snapshots. *Proc. Natl. Acad. Sci.* **2014**, *111* (49), 17498–17503.

(16) Avenson, T. J.; Cruz, J. A.; Kramer, D. M.; Croteau, R. B. Modulation of Energy-Dependent Quenching of Excitons in Antennae of Higher Plants. *Proc. Natl. Acad. Sci.* **2004**, *101* (15), 5530–5535.

(17) Polívka, T.; Sundström, V. Ultrafast Dynamics of Carotenoid Excited States−From Solution to Natural and Artificial Systems. *Chem. Rev.* **2003**, *104*, 2021–2071.

(18) Yamamoto, Y. A Random Walk To and Through the Xanthophyll Cycle. In *Photoprotection, Photoinhibition, Gene Regulation, and Environment*; Demmig-Adams, B., Adams, W. W., Mattoo, A. ., Eds.; 2008; pp 1–10.

(19) Demmig-Adams, B. Carotenoids and Photoprotection in Plants: A Role for the Xanthophyll Zeaxanthin. *Biochim. Biophys. Acta* **1990**, *1020* (1), 1–24.

(20) Adams, W. W.; Demmig-Adams, B.; Winter, K.; Winter, K. Relative Contributions of Zeaxanthin-Related and Zeaxanthin-Unrelated Types of ;high-Energy-State' Quenching of Chlorophyll Fluorescence in Spinach Leaves Exposed to Various Environmental Conditions. *Plant Physiol.* **1990**, *92* (2), 302–309.

(21) Li, X.-P.; Muller-Moule, P.; Gilmore, A. M.; Niyogi, K. K. PsbS-Dependent Enhancement of Feedback de-Excitation Protects Photosystem II from Photoinhibition. *Proc. Natl. Acad. Sci.* **2002**, *99* (23), 15222–15227.

(22) Correa-Galvis, V.; Poschmann, G.; Melzer, M.; Stühler, K.; Jahns, P. PsbS Interactions Involved in the Activation of Energy Dissipation in Arabidopsis. *Nat. Plants* **2016**, *2* (2), 15225.

(23) Andreas Dreuw, *; Graham R. Fleming, and; Head-Gordon, M. Charge-Transfer State as a Possible Signature of a Zeaxanthin−Chlorophyll Dimer in the Non-Photochemical Quenching Process in Green Plants. **2003**.

(24) Ruban, A. V.; Berera, R.; Ilioaia, C.; Van Stokkum, I. H. M.; Kennis, J. T. M.; Pascal, A. A.; Van Amerongen, H.; Robert, B.; Horton, P.; Van Grondelle, R. Identification of a Mechanism of Photoprotective Energy Dissipation in Higher Plants. *Nature* **2007**, *450* (7169), 575–578.

(25) Krause, G. H.; Weis, E. Chlorophyll Fluorescence as a Tool in Plant Physiology. II. Interpretation of Fluorescence Signals. *Photosynth. Res.* **1984**, *5* (2), 139–157.

(26) Berera, R.; van Grondelle, R.; Kennis, J. T. M. Ultrafast Transient Absorption Spectroscopy: Principles and Application to Photosynthetic Systems. *Photosynth. Res.* **2009**, *101* (2–3), 105–118.

(27) Croce, R.; Mü, M. G.; Bassi, R.; Holzwarth, A. R. Carotenoid-to-Chlorophyll Energy

Transfer in Recombinant Major Light-Harvesting Complex (LHCII) of Higher Plants. I. Femtosecond Transient Absorption Measurements. *Biophys. J.* **2001**, *80*, 901–915.

(28) Holt, N. E.; Zigmantas, D.; Valkunas, L. Carotenoid Cation Formation and the Regulation of Photosynthetic Light Harvesting. **2005**, *307* (January), 433–437.

(29) Amarnath, K.; Zaks, J.; Park, S. D.; Niyogi, K. K.; Fleming, G. R. Fluorescence Lifetime Snapshots Reveal Two Rapidly Reversible Mechanisms of Photoprotection in Live Cells of Chlamydomonas Reinhardtii.

(30) Sylak-Glassman, E. J.; Zaks, J.; Amarnath, K.; Leuenberger, M.; Fleming, G. R. Characterizing Non-Photochemical Quenching in Leaves through Fluorescence Lifetime Snapshots. *Photosynth. Res.* **2016**, *127* (1), 69–76.

(31) Noomnarm, U.; Clegg, R. M. Fluorescence Lifetimes: Fundamentals and Interpretations. **2009**.

(32) Wasielewski, M. R.; Kispert, L. D. Direct Measurement of the Lowest Excited Singlet State Lifetime of All-Trans-β-Carotene and Related Carotenoids. *Chem. Phys. Lett.* **1986**, *128* (3), 238–243.

Chapter 2: Development of Snapshot Transient Absorption Spectroscopy

Note: Portions of this chapter are adapted from work published in J. Phys. Chem. Lett., co-authored with Soomin Park, Zhirong Li, Roberto Bassi, Krishna K. Niyogi, and Graham R. Fleming. Soomin Park contributed equally to authorship.

Full Citation: Park, Soomin; Fischer, Alexandra L.; Li, Zhirong; Bassi, Roberto; Niyogi, Krishna K.; Fleming, Graham R. Snapshot Transient Absorption Spectroscopy of Carotenoid Radical Cations in High-Light-Acclimating Thylakoid Membranes. *J. Phys. Chem. Lett.* **2017**, *8* (22), 5548-5554.

Introduction

Photosynthetic organisms have developed a series of mechanisms called nonphotochemical quenching (NPQ) mechanisms which turn on under high-light conditions to prevent photodamage.[1] These mechanisms are typically categorized by the speeds with which they respond to initial high light stress. The fastest set of mechanisms is called qE, or energy-dependent quenching, and these turn on within seconds to minutes of initial light exposure. qE quenching is responsible for the largest portion of excitation energy quenching in plants as it is the most responsive to changes in light intensity.[2] However, there are no confirmed molecular mechanisms for qE quenching, though there are several proposed mechanisms.

One of the necessary components for maximum qE quenching is the carotenoid zeaxanthin (Zea), but it is not present in dark-acclimated plants.[3–5] Once the high light acclimation begins, the enzyme violaxanthin de-epoxidase is activated, which converts the carotenoid violaxanthin (Vio) into Zea. Zea is also thought to be necessary for qZ quenching, or Zea-dependent quenching.[6] qZ mechanisms respond more slowly to light acclimation, within tens of minutes of initial light exposure. Zea may participate in different molecular mechanisms with different timescales of activation, a faster one corresponding to qE quenching, and a slower one corresponding to qZ quenching.

There are several proposed molecular mechanisms describing how Zea may directly participate in excitation energy quenching (see Figure 1.5). This chapter will focus on a mechanism called charge-transfer quenching, or CT quenching. This mechanism requires Zea to be in such close proximity to a Chl molecule that they form a dimer. Then, this dimer is excited via excitation energy transfer from other, previously excited Chls. The Zea and Chl then undergo charge separation, becoming Zea^+ and Chl^-. The Zea^+ and Chl^- pair then undergo a charge-recombination, returning to the ground state dimer. Additionally, It is also possible that another carotenoid, Lutein (Lut), can substitute for Zea in CT quenching when no Zea is present, or may be the primary carotenoid involved in CT quenching in certain organisms.[7]

To investigate whether CT quenching occurs in plants, Holt et al. performed transient absorption (TA) experiments on light-acclimated and dark-acclimated thylakoids by pumping Chl b at 650 nm and probing the maximum absorption peak of Zea^+ (1000 nm).[8] See figure 2.1. Holt and coworkers found a significant difference between the dark- and light-acclimated decays, including a distinct rise component exclusive to the light-acclimated trace. They attributed the difference in signal to Zea^+ formation, possibly as a part of a light-dependent quenching mechanism. However, this experiment did not provide information as to whether Zea^+ appearance is co-incident with fluorescence quenching, or how many minutes of light acclimation are required before the Zea^+ signal appears.

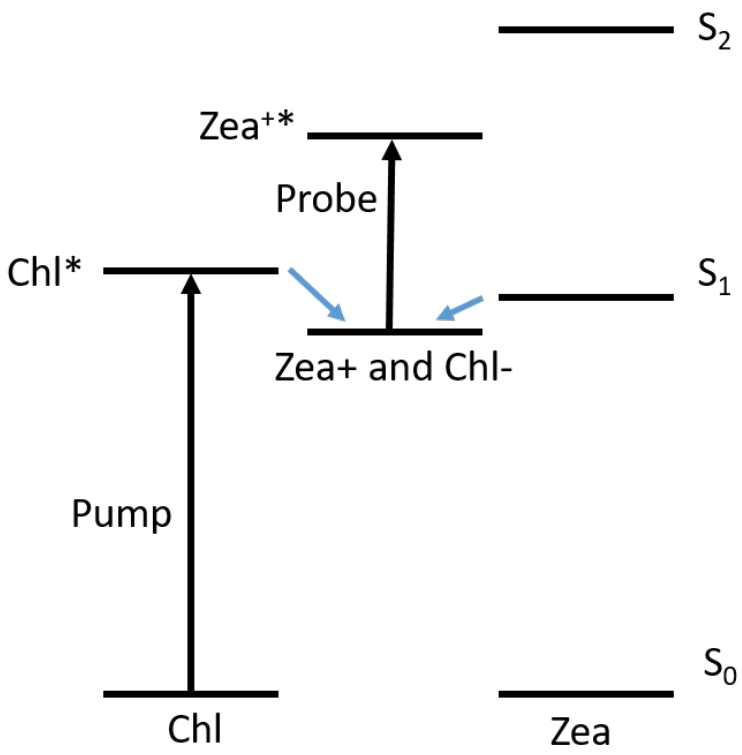

Figure 2.1: Energy level diagram illustrating transitions associated with transient absorption measurements of Zea^+. The pump wavelength is 650nm, the energy of the S_0 to Q_y transition for Chl b.[9] The probe wavelength is 1000nm, the wavelength of maximum absorption of Zea^+.[10] * indicates electronic excitation.

To determine if the carotenoid cation signal shown in Holt et al. was directly tied with quenching, it was necessary to observe the dynamics of the carotenoid cation signal over the course of the bright-light acclimation, rather than only before and after. This ties into a common issue inherent to studying NPQ dynamics and mechanisms, namely the large difference in timescales between individual molecular processes compared to the timescales of overall membrane adaptations (see figure 1.3). Experiments such as fluorescence lifetime

measurements or transient absorption measurements are designed to follow <μs molecular processes, and often are not capable of also tracking the more slowly changing membrane-scale processes, which change over seconds- to hour-long timescales. Considering that both the molecular and membrane scale changes influence overall quenching behaviors, ideally experiments would be designed to measure changes in both the <μs and the s-to-hours timescales.

For measuring Chl fluorescence quenching, this experiment already exists. Fluorescence lifetime snapshots involve rapid (1 s long) individual measurements of the Chl fluorescence decay of a photosynthetic sample, repeated at 10-30 s intervals over the course of a bright light acclimation sequence lasting tens of minutes to hours.[11,12] Each individual fluorescence decay is then fitted to a multi-exponential decay and can be represented by a single number, the amplitude-weighted average lifetime. After plotting these lifetimes over the actinic light sequence time, it is then possible to observe the changes in fluorescence behavior as a function of the actinic light sequence. Of course, the presence of individual molecular quenching mechanisms cannot be discerned using only changes Chl fluorescence.[13,14] Transient absorption spectroscopy is typically used to determine the presence of individual transient species in photosynthetic samples, but until now, no transient absorption experiment had been developed with sufficient resolution to track changes in both the molecular (<μs) and organism-level (s to hours) timescales.

In order to determine if CT quenching is a qE quenching mechanism, we needed to develop a transient absorption technique analogous to fluorescence lifetime snapshots. This would potentially involve repeated transient absorption measurements of a photosynthetically active sample as it adapts to a light condition over the course of minutes to hours. However, since CT quenching is a possible qE quenching mechanism, the experiment needs to be able to follow changes in signal on a timescale relevant to qE, ie seconds to minutes.

Results and Discussion

To measure the evolution of the Zea^+ in light-acclimating photosynthetic membranes, we needed to drastically decrease the data acquisition time of the transient absorption setup such that we could monitor changes in the Zea^+ decay faster than the timescale of qE quenching. Ultimately, this meant eliminating the slowest components of the existing transient absorption setup, the movement of the delay stage. In a conventional transient absorption experiment, the delay time between the pump and probe pulses is set using a motorized delay stage, data is collected, then stage is moved to a new delay time, and the process is repeated until the entire time range of the decay has been explored. Eliminating the necessity of a moving delay stage is not a new idea, and several novel but technically difficult methods have been developed.[15–17] Instead of relying on a difficult to align singe-shot method, we fixed the delay stage at a 20 ps delay between pump and probe, the time delay where there was a maximum difference between the light- and dark-acclimated Zea^+ excited state absorption (ESA) decays observed in Holt et al.[10] This removes the time required for the delay stage to physically move from one delay time to another.

Similar to the fluorescence lifetime snapshots, snapshot transient absorption involves collecting data in short time windows (10 s) in approximately 30 second intervals as a sample changes from dark-acclimated to light-acclimated. In snapshot TA, the signal collected during the initial dark adaptation period is averaged and then subtracted from each subsequent data point. Then, these difference points are graphed as a function of light-acclimation time (see figure 2.2). This gives a snapshot of how the difference between the dark-acclimated and light-acclimating sample changes over the course of the light acclimation.

Further experimental depth can be achieved by adding a second dark to light cycle, the experiment can test the responsiveness of a species to a repeated dark-light cycling, as is often the case for plants in natural environments.[18] When investigating CT quenching and Zea^+ specifically, repeated dark-light cycling also removes the time it takes for Vio to convert to Zea from influencing the overall quenching activation time. Conversion from Vio to Zea is between 20 and 300 times faster than conversion of Zea to Vio, so there should be little to no back conversion within a short (~5 min) dark-acclimation period.[19] After the first light acclimation period, the sample should have converted a significant portion of the Vio pool into Zea. The next dark period may be too short a time for significant Zea to Vio conversion, but it is sufficient time for other physical changes to occur, such as pigment movement out of pigment-protein pockets, or the conformational changes of proteins. When the light comes back on then, the time it takes for the Zea^+ signal to re-appear is indicative of the time it takes for CT quenching to turn on without regard to the timescale of the xanthophyll cycle.

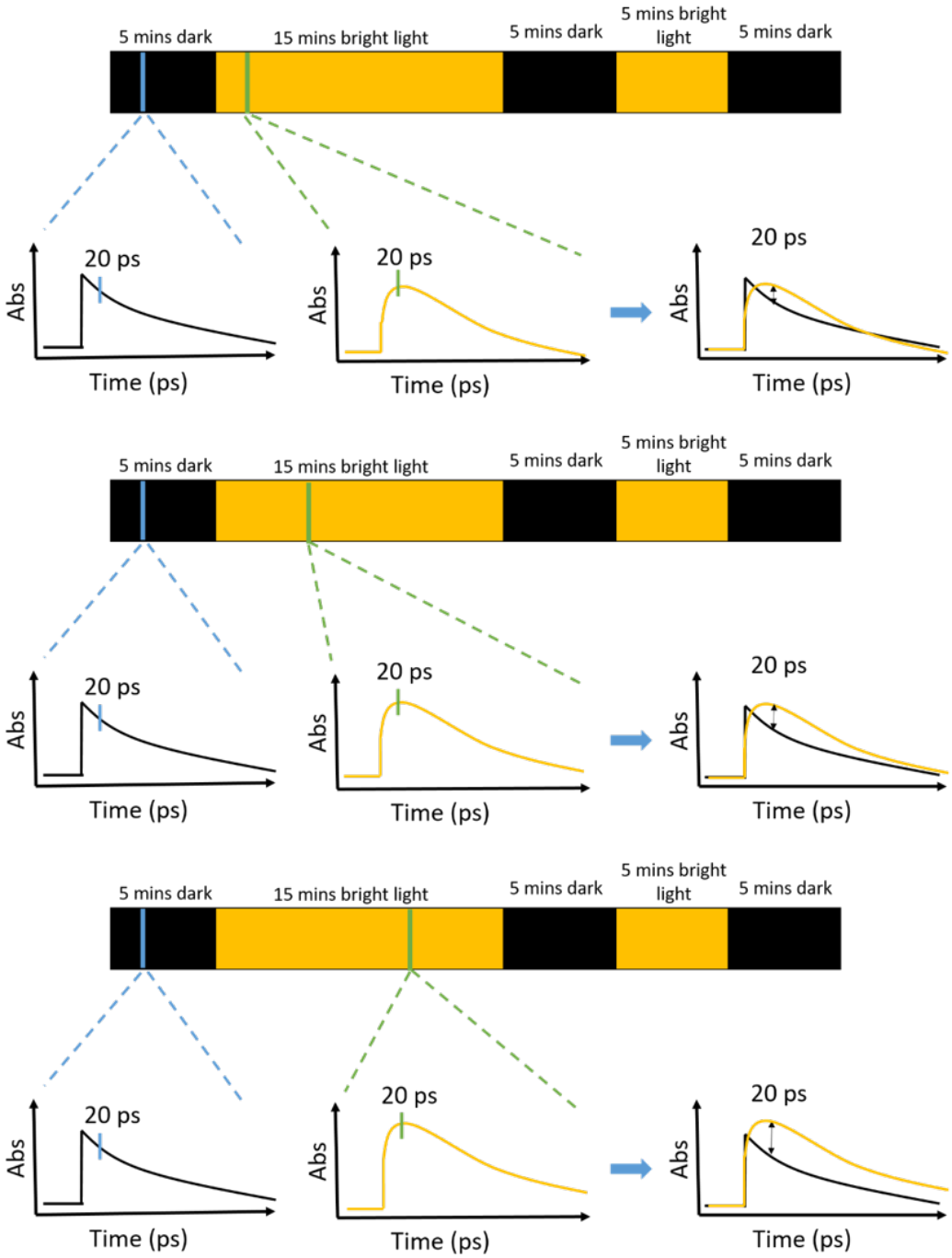

Figure 2.2: Schematic of snapshot transient absorption data collection for tracking Zea^+ ESA in photosynthetic samples. The black and yellow bars represent the time over which the bright actinic light is turned on and off. The pump-probe delay time is fixed at 20 ps throughout the experiment. Data is collected in 10 s windows at 30 second intervals over the course of the experiment. The average initial dark-acclimated signal is subtracted from the signal at each subsequent time point, giving the difference between light- and dark-acclimated signals. This difference should grow over the course of the initial light-acclimation period, as the sample transitions from fully dark-acclimated to fully light-acclimated.

A second important consideration when developing the snapshot TA experiment was the fragility of photosynthetic samples, particularly isolated thylakoid membranes. Isolated membranes are very sensitive to photodamage and cannot tolerate the high laser intensities that some inorganic samples can tolerate. Therefore, the intensity of the pump beam must be limited to a power which will not cause significant damage over the timescale of the experiment (~40 mins). Additionally, these samples are very sensitive to damage due to overheating, and ideally they are kept on ice. In order to perform this experiment at the required speed, light-acclimation must occur while the sample is in the setup. To do this, a large actinic light was added in close proximity to the sample position to allow for intense, even illumination of the entire sample cell. Unfortunately, commercial actinic lamps with both a broad spectrum and high intensity are often tungsten halogen lamps, which generate a significant amount of heat in addition to visible light. In our setup, the close position of the actinic light to the sample and the long light acclimation time results in the sample heating up by approximately 20° C over the course of the measurement. This heating almost certainly jeopardizes the structural integrity of the thylakoid membranes and changes the chemistry occurring inside of them, causing them to deteriorate faster. To reduce this heating, an infrared filter was placed between the actinic light and the sample (see figure 2.3). This filter allows the desired, visible light through while blocking the IR light that causes much of the sample heating.

Unfortunately, not only are thylakoid membrane samples delicate, they are also highly scattering. As discussed in the introduction, thylakoid membranes have a complex structure and are folded many times within the chloroplast.[20] This means that when a beam of light passes through a cuvette containing these membranes, it will encounter many medium changes and surfaces for possible scattering. Further complicating matters is the fact that each disk of a grana membrane is approximately 300-600nm in diameter, which is the same order of magnitude as the wavelength of the pump beam, and only slightly smaller than the probe wavelength.[21] This means that the thylakoids can very effectively scatter both the pump and the probe, which could reduce the amount of signal observed while increasing the amount of noise. As we cannot alter the shape of the membranes themselves without potentially altering the quenching dynamics and moving farther from *in vivo* conditions, other external measures were taken to minimize the effects of membrane scattering.

Several important changes were made to the setup and sample preparation process to reduce the signal loss due to sample scattering. The first important change was to improve the sample preparation procedure. After membrane isolation, the samples were filtered and washed twice before dilution for the experiment.[22] This step removes debris remaining in the sample and partially reduces the scattering. However, the majority of the changes were made to the setup itself. One such change was the addition of an 850 nm longpass filter after the sample and before the spectrometer to remove errant pump light as well as probe wavelengths below 850 nm (See figure 2.3). Though the spectrometer will also remove a large portion of this light, it is prudent to reduce the intensity beforehand.

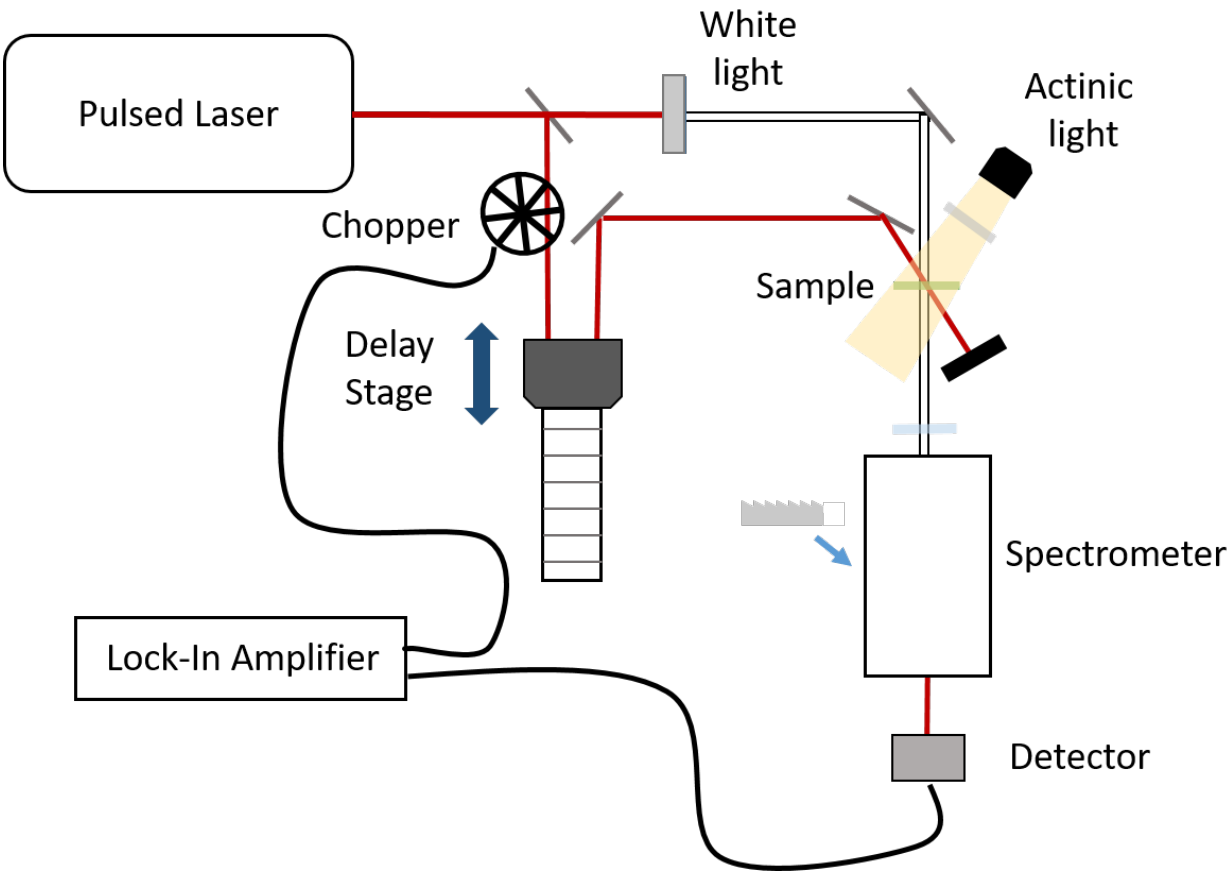

Figure 2.3: Schematic of snapshot transient absorption setup. The red line represents the pump beam path, while the white line represents the probe beam path. The sample is represented by a green line.

By far the most important component of the setup with regards to improving the signal to noise ratio was the lock-in amplifier. A lock-in amplifier is a device used for electronic signal filtration. There are two required inputs, one is the electronic signal to be filtered and the other is a reference signal. In our case, the electronic signal comes from a photodiode detecting the probe intensity and the reference signal is the frequency of an optical chopper put in the path of the pump beam (see figure 2.3). Then using these two inputs, the amplifier "locks" into the reference frequency and then looks for changes in the signal that occur at same frequency as the reference. This is of course a very simplified version of the process, for further explanation and details see the SR 830 product manual.[23] In this experiment, the lock-in will isolate only signals that are coincident with both the pump and probe interacting with the sample. This removes a significant portion of probe-dependent scatter and gives a much higher signal-to-noise ratio.

However, there are additional ways to improve lock-in signal filtration even further. The method described above is known as "single-modulation," wherein only one of the two beams is chopped and used as a reference frequency. There is another method called double-modulation, wherein both the pump and the probe are chopped at different frequencies and the sum frequency is used as the reference, theoretically resulting in higher signal-to-noise ratios.[24] Yet when we applied this signal filtering method to our setup, the reduction in signal was not in proportion to the reduction in noise (see table 2.1). In fact, single-modulation sampling gave much higher signal-to-noise ratios (S/N) at all three frequencies tested. In single-modulation sampling, we had chopped the pump line, which is most helpful in controlling for probe inconsistencies. In our setup, the probe intensity is much less stable than the pump intensity, so moving from single-modulation where only the pump was chopped to double-modulation where both beams were chopped had less of an effect as we were trying to account for instabilities in an already-stable beam. Additionally, there was a change in the S/N ratio that varied by sampling frequency. Lower frequencies (~210 Hz) had lower S/N ratios than higher frequencies (~1700) but medium frequencies (~1000 Hz) had the highest S/N ratios (see table 2.1). Higher chopping frequencies should allow the lock-in to filter out faster changes in the probe intensity, but at a certain point the chopper itself becomes unstable. Thus, the optimum sampling frequency for our setup is at approximately 1 kHz rather than a higher frequency.

	Single-modulation			Double-modulation		
Frequency (Hz)	213	997	1710	213	997	1710
S/N	1238	**1550**	1409	24	61	151

Table 2.1: Comparison of the signal-to-noise ratio (S/N) using single-modulation vs. double-modulation signal filtering at varying chopper frequencies. Frequencies are rounded to the nearest whole number. S/N ratios derived by comparing the average maximum signal intensity to the noise at negative delay times. Data taken on a laser dye in ethanol.

Despite these changes to the setup, the signal intensity was still too low for reliable measurements. According to theoretical studies, photosynthetic membranes can have a very low density of quenching sites while still maintaining strong overall quenching, so the signal itself is potentially very small as CT quenching likely is only responsible for a portion of overall quenching.[1,25] Previously, this transient absorption setup had been primarily used for experiments with pump and probe wavelengths in the visible range. As this experiment requires a near IR (NIR) probe, there were several modifications needed to increase the intensity of the probe beam before it interacts with the sample, as well as the intensity of the transmitted probe that reaches the detector.

The primary modification was to change the type of crystal used to generate the white light of the probe beam, a process called supercontinuum generation. The process of supercontinuum generation spectrally broadens a narrow bandwidth laser source to such a

degree that it becomes broad-spectrum white light. Previously, when this setup was used for experiments requiring a visible probe, supercontinuum generation was performed by focusing the probe line through a sapphire crystal, which generates a broad spectrum of visible light but does not provide much NIR light. As thylakoid membranes are highly scattering, a large percentage of the probe intensity at 1000 nm could potentially be lost before reaching the detector. To improve this, the sapphire crystal was replaced with a YAG crystal, which can generate higher intensities in the NIR. This improvement increased the intensity of 1000 nm probe light by an order of magnitude, substantially increasing S/N.

Despite the increase in the intensity of the probe beam, there was still a large loss in probe intensity before reaching the detector. As the setup had been designed for use with a visible probe, the grating in the spectrometer was chosen to favor retention of visible light. In fact, the older grating was designed for highest efficiency at 500 nm light, and was only about 30% efficient at 1000 nm.[26] To improve the versatility of the setup, we installed a grating designed for optimum efficiency at 750 nm (see figure 2.3). Compared to the 500 nm grating, this new grating was more than doubly efficient at retaining 1000 nm light. This combination of improvements to the probe line was instrumental to the success of the experiment, the results of which will be discussed in detail in chapter 3.

Though the pump intensity required also caused significant exciton-exciton annihilation, experimental data indicated that the degree of annihilation was consistent throughout the course of the experiment (see chapter 3). Of course, this annihilation may also cause physical changes to the energy landscape within the thylakoid membrane, and ideally would be minimized. However, that would require a significantly higher signal-to-noise ratio which may not be possible with thylakoid membrane samples.

Conclusions

Ultimately, tracking signal at only one pump-probe delay time as well at the numerous improvements and adjustments to the instrument and sample preparation method allowed us to collect data with sufficient time resolution to answer our scientific question. Snapshot transient absorption is capable of tracking qE-timescale changes in thylakoid membranes as they acclimate to intense light. This technique is analogous to and works well in concert with the fluorescence lifetime snapshot technique for summarizing the slow evolution of fast processes in photosynthetic samples. Though there are still improvements to be made, snapshot transient absorption is a versatile technique that may be used to inform many debates in the field of NPQ.

References

(1) Müller, P.; Li, X.-P.; Niyogi, K. K. Non-Photochemical Quenching. A Response to Excess Light Energy 1. *Plant Physiol.* **2001**, *125*, 1558–1566.

(2) Külheim, C.; Agren, J.; Jansson, S. Rapid Regulation of Light Harvesting and Plant Fitness in the Field. *Science* **2002**, *297* (5578), 91–93.

(3) Demmig-Adams, B. Carotenoids and Photoprotection in Plants: A Role for the Xanthophyll Zeaxanthin. *Biochim. Biophys. Acta* **1990**, *1020* (1), 1–24.

(4) Yamamoto, H. Y.; Nakayama, T. O. M.; Chichester, C. O. Studies on the Light and Dark Interconversions of Leaf Xanthophylls. *Arch. Biochem. Biophys.* **1962**, *97* (1), 168–173.

(5) Niyogi, K. K.; Bjorkman, O.; Grossman, A. R.; Niyogi, K. K.; Fleming, G. R. The Roles of Specific Xanthophylls in Photoprotection. *Proc. Natl. Acad. Sci.* **1997**, *94* (25), 14162–14167.

(6) Nilkens, M.; Kress, E.; Lambrev, P.; Miloslavina, Y.; Müller, M.; Holzwarth, A. R.; Jahns, P. Identification of a Slowly Inducible Zeaxanthin-Dependent Component of Non-Photochemical Quenching of Chlorophyll Fluorescence Generated under Steady-State Conditions in Arabidopsis. *BBA - Bioenerg.* **2010**, *1797*, 466–475.

(7) Li, Z.; Ahn, T. K.; Avenson, T. J.; Ballottari, M.; Cruz, J. A.; Kramer, D. M.; Bassi, R.; Fleming, G. R.; Keasling, J. D.; Niyogi, K. K. Lutein Accumulation in the Absence of Zeaxanthin Restores Nonphotochemical Quenching in the Arabidopsis Thaliana npq1 Mutant. *Plant Cell* **2009**, *21*, 1798–1812.

(8) Holt, N. E.; Zigmantas, D.; Valkunas, L.; Li, X. P.; Niyogi, K. K.; Fleming, G. R. Carotenoid Cation Formation and the Regulation of Photosynthetic Light Harvesting. *Science (80-.).* **2005**, *307* (5708), 433–436.

(9) Blankenship, R. E. *Molecular Mechanisms of Photosynthesis*, 2nd ed.; Wiley-Blackwell, 2014.

(10) Holt, N. E.; Zigmantas, D.; Valkunas, L. Carotenoid Cation Formation and the Regulation of Photosynthetic Light Harvesting. **2005**, *307* (January), 433–437.

(11) Amarnath, K.; Zaks, J.; Park, S. D.; Niyogi, K. K.; Fleming, G. R. Fluorescence Lifetime Snapshots Reveal Two Rapidly Reversible Mechanisms of Photoprotection in Live Cells of Chlamydomonas Reinhardtii. *Proc. Natl. Acad. Sci.* **2012**, *109* (22), 8405–8410.

(12) Sylak-Glassman, E. J.; Zaks, J.; Amarnath, K.; Leuenberger, M.; Fleming, G. R. Characterizing Non-Photochemical Quenching in Leaves through Fluorescence Lifetime Snapshots. *Photosynth. Res.* **2016**, *127* (1), 69–76.

(13) Krause, G. H.; Weis, E. Chlorophyll Fluorescence as a Tool in Plant Physiology. II. Interpretation of Fluorescence Signals. *Photosynth. Res.* **1984**, *5* (2), 139–157.

(14) Noomnarm, U.; Clegg, R. M. Fluorescence Lifetimes: Fundamentals and Interpretations.

2009.

(15) Dhar, L.; Fourkas, J. T.; Nelson, K. A. Pulse-Length-Limited Ultrafast Pump–probe Spectroscopy in a Single Laser Shot. *Opt. Lett.* **1994**, *19* (9), 643.

(16) Wakeham, G. P.; Nelson, K. A. Dual-Echelon Single-Shot Femtosecond Spectroscopy. *Opt. Lett.* **2000**, *25* (7), 505.

(17) Harel, E.; Fidler, A. F.; Engel, G. S. Single-Shot Gradient-Assisted Photon Echo Electronic Spectroscopy. *J. Phys. Chem. A* **2011**, *115*, 3787–3796.

(18) Kulheim, C. Rapid Regulation of Light Harvesting and Plant Fitness in the Field. *Science (80-.).* **2002**, *297* (5578), 91–93.

(19) Takizawa, K.; Cruz, J. A.; Kanazawa, A.; Kramer, D. M. The Thylakoid Proton Motive Force in Vivo. Quantitative, Non-Invasive Probes, Energetics, and Regulatory Consequences of Light-Induced Pmf. *Biochim. Biophys. Acta - Bioenerg.* **2007**, *1767* (10), 1233–1244.

(20) Dekker, J. P.; Boekema, E. J. Supramolecular Organization of Thylakoid Membrane Proteins in Green Plants. **2004**.

(21) Dekker, J. P.; Boekema, E. J. Supramolecular Organization of Thylakoid Membrane Proteins in Green Plants. **2004**.

(22) Park, S.; Fischer, A. L.; Li, Z.; Bassi, R.; Niyogi, K. K.; Fleming, G. R. Snapshot Transient Absorption Spectroscopy of Carotenoid Radical Cations in High-Light-Acclimating Thylakoid Membranes. *J. Phys. Chem. Lett.* **2017**, *8* (22), 5548–5554.

(23) Stanford Research Systems. Model SR830 DSP Lock-In Amplifier.

(24) Frolov, S. V; Vardeny, Z. V. Double-Modulation Electro-Optic Sampling for Pump-and-Probe Ultrafast Correlation Measurements. *Cit. Rev. Sci. Instruments Rev. Sci. Instruments Nanoscale Therm. Transp. J. Appl. Phys. J. Chem. Phys. Rev. Sci. Instruments* **1998**, *69* (10), 1257–25102.

(25) Bennett, D. I. G.; Fleming, G. R.; Amarnath, K. Excitation Diffusion Length Controls Photosystem II Light Harvesting during Photoprotection. *Arxhiv eLife Submitt.* **2018**.

(26) Princeton Instruments - Gratings https://www.princetoninstruments.com/products/gratings (accessed Apr 5, 2018).

Chapter 3: Snapshot Transient Absorption Spectroscopy of Carotenoid Radical Cations in High-Light- Acclimating Thylakoid Membranes

Published work: This work has been previously published in J. Phys. Chem. Lett.[1] and was co-authored with Soomin Park, Zhirong Li, Roberto Bassi, Kris Niyogi, and Graham Fleming. Soomin and Zhirong contributed equally to data collection, analysis, and writing.

Full Citation: Park, S.; Fischer, A. L.; Li, Z.; Bassi, R.; Niyogi, K. K.; Fleming, G. R. Snapshot Transient Absorption Spectroscopy of Carotenoid Radical Cations in High-Light-Acclimating Thylakoid Membranes. *J. Phys. Chem. Lett.* **2017**, *8* (22), 5548–5554.

Abstract

Non-photochemical quenching mechanisms regulate light harvesting in oxygenic photosynthesis. Measurement techniques for non-photochemical quenching have typically focused on downstream effects of quenching, such as measuring reduced chlorophyll fluorescence. Here, to directly measure a species involved in quenching, we report snapshot transient absorption (TA) spectroscopy, which rapidly tracks carotenoid radical cation signals as samples acclimate to excess light. The formation of zeaxanthin radical cations, which is possible evidence of zeaxanthin-chlorophyll charge-transfer (CT) quenching, was investigated in spinach thylakoids. Together with fluorescence lifetime snapshot data and time-resolved high-performance liquid chromatography (HPLC) measurements, snapshot TA reveals that Zea·+ formation is closely related to energy-dependent quenching (qE) in non-photochemical quenching. Quantitative and dynamic information on CT quenching discussed in this work give insights into the design principles of photoprotection in natural photosynthesis.

Introduction

Non-photochemical quenching (NPQ) describes a collection of mechanisms that photosynthetic organisms use to control the amount of excitation energy reaching reaction centers and to minimize potential oxidative damage. These mechanisms have typically been divided into groups based on their timescales of activation; the fastest set are known as energy-dependent quenching (qE) mechanisms, and they turn on within seconds to minutes of initial high light exposure.[2] Other types of quenching have activation times varying from tens of minutes to hours. Though all types of quenching protect plants from photoinhibition, the rapid response of qE mechanisms makes them responsible for the majority of quenching in the early stages of light

acclimation, allowing for higher seed production under fluctuating light conditions.[3] The carotenoid zeaxanthin (Zea) is required for full qE quenching, but the production of the majority of Zea requires enzymatic conversion from violaxanthin (Vio) in high light.[4–6] It is still unknown exactly how Zea participates in qE quenching, but two possible and non-mutually exclusive mechanisms have been suggested. One involves charge-transfer quenching (CT quenching), in which Zea and a neighboring chlorophyll (Chl) molecule accept excitation energy as a dimer and undergo charge separation followed by recombination, transiently forming a Zea cation and Chl anion.[7] The second mechanism involves excitation energy transfer from an excited Chl Q_y state to Zea S_1 state, which then rapidly relaxes with a lifetime of ~ 9 ps.[8,9] In addition to Zea, the carotenoid lutein (Lut) is thought to be directly involved in quenching *via* similar mechanisms.[10,11]

In previous work, the Zea radical cation (Zea·+) was observed in high-light-acclimated plant thylakoids using transient absorption (TA) spectroscopy.[7] However, these thylakoids had been high-light-acclimated for over 30 min before measurement, which does not indicate whether CT quenching is activated within the first few minutes of high light exposure, the timescale of qE activation. Zea·+ has also been observed in isolated minor (monomeric) light-harvesting complexes containing Zea,[12,13] but these protein conditions may not be indicative of *in vivo* behavior, and once again, do not give information about when CT quenching turns on during light acclimation. In a recent study, Dall'Osto and coworkers concluded that the trimeric light-harvesting complex II (LHCII) is the location of a more slowly activated (several minutes) quenching mechanism that does not involve formation of Zea·+ *in vivo*.[14] This implies that CT quenching may be one of multiple quenching (qE) mechanisms.

Results and Discussion

In order to obtain direct evidence on the timescale of CT quenching, we developed a technique we call snapshot TA spectroscopy, which uses a TA setup at a fixed time delay to allow for data collection within a 10 second window, in intervals as short as a few tens of seconds. Although this method can be exploited to study the formation of other species, our work has specifically focused on the formation of Zea·+ in thylakoid membranes to gather quantitative and dynamic information on the time dependence of Zea-Chl CT quenching. We interpret the snapshot TA data in conjunction with fluorescence lifetime snapshot and time-resolved HPLC data.

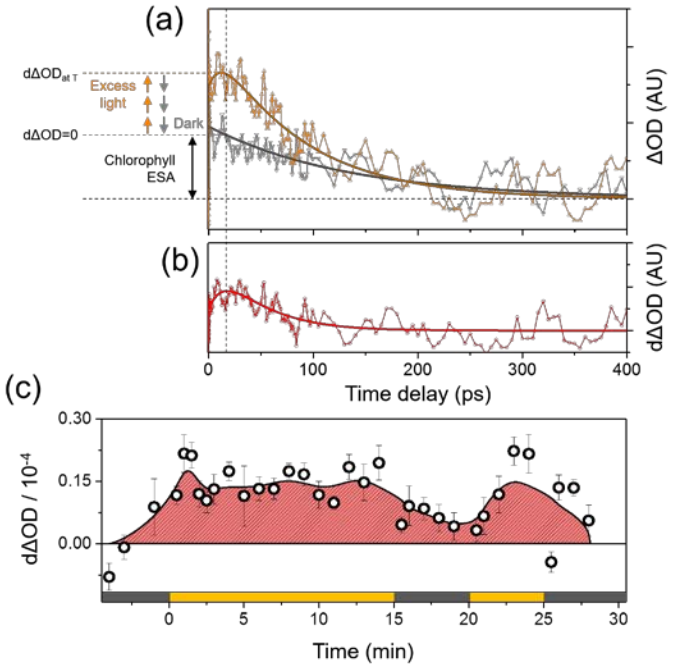

Figure 3.1: (a) Transient absorption kinetics for spinach thylakoid membranes under high-light-acclimated (triangles, yellow) and dark-acclimated (inverted triangles, gray) conditions. (b) Difference between light-acclimated and dark-acclimated kinetic traces. (c) Snapshot TA data obtained 20 ps after excitation with the zero-line representing the averaged signal during the initial dark period. Data are presented as the means $\pm$ SE (n=5), and the solid line represents smoothed curves. Spinach thylakoid membranes were excited and probed at 650 nm and 1000 nm, respectively. The time sequence of actinic light on (yellow) and off (dark gray) is presented in the bottom bar.

Figure 3.1(a) exhibits TA kinetic profiles probed at 1000 nm for dark- and light-acclimated spinach thylakoid membranes upon excitation of the Chl Q_y band. Light acclimation of the thylakoids, induced by continuous irradiation at 850 µmol photons·m^{-2}·s^{-1}, leads to the formation of Zea·+, resulting in additional rise (15.4 ps) and decay (40 ps) components (Figure 3.1(b)). In a previous report,[7] the TA kinetic traces of the Zea·+-depleted *Arabidposis thaliana* (*npq4* mutant) indicated that the Chl excited state absorption (ESA) signal is nearly identical in dark- and light-acclimated samples at 1000 nm. Therefore, Chl ESA dynamics and Chl*-Chl* annihilation were thought to contribute equally to the near-IR TA signals of dark-acclimated and high-light-acclimated thylakoids at the same Chl concentration and excitation laser intensity and the observed difference kinetics directly indicate the population of the charge-separation states (Chl·- and Zea·+).[15] The reconstructed difference spectrum in Figure S3.5 indicates the characteristic Zea·+ absorption, consistent with our previous observations.[7] When following the formation of Zea·+ in spinach thylakoids, the maximum difference in the decay traces of dark-

and light-acclimated samples occurs at a time delay of 20 ps and at a detection wavelength of 1000 nm. By focusing only on that wavelength and delay time, we were able to acquire a data point every 30 seconds, making the snapshot TA method a valuable complement to fluorescence for tracking qE on the seconds to minutes timescale. The duration of the data acquisition window is limited by the signal-to-noise (SN) ratio. To increase the SN ratio, we placed appropriate sets of filters and polarizers, as described in Experimental Methods. Using dark-acclimated samples, we first establish a baseline, corresponding to the ESA of Chl, then began the light acclimation sequence (Figure 3.1(a, c)).

Figure 3.1(c) shows the difference between the TA signal from dark-acclimated sample and the signal at various times during light acclimation. There is a sharp rise in Zea·+ absorption signal within 2 min of the first light acclimation period, supporting the idea that CT quenching is part of a qE mechanism. The signal drops, then plateaus after about 5 min of light exposure. We suggest that this is due to trimeric LHCII migration away from the photosystem II (PSII) supercomplex, which is proposed to occur within 5 min of high light exposure.[16,17] If, as suggested previously,[12,13,18] CT quenching occurs in the monomeric LHCII, this reduces the amount of excitation energy funneled to the CT quenching site. It is noteworthy that the Zea·+ TA signal slowly decreased in dark periods despite the near-constant Zea concentration, indicative of asymmetric induction-relaxation of the CT quenching mechanism. As another possible quencher, Lut·+ exhibits maximum peak absorption at 920 nm which is noticeably blue-shifted relative to the spectrum of Zea·+.[10] We did not observe any positive snapshot TA signal at 920 nm, so it appears that Lut·+ is not involved in this type of quenching in wild-type spinach thylakoids.

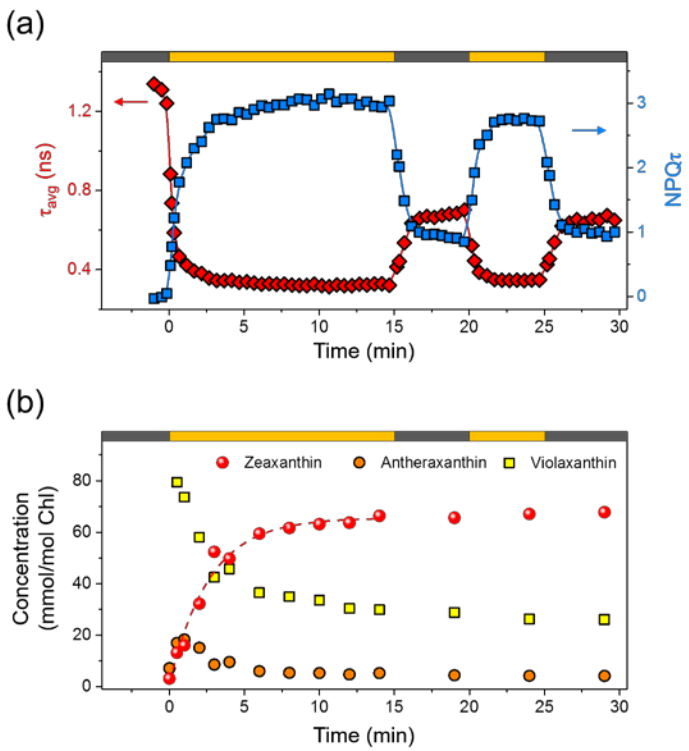

Figure 3.2: (a) The evolution of average Chl fluorescence lifetimes (τ_{avg}) in response to high light illumination and the NPQτ values (see text) calculated using corresponding τ_{avg} values at each time point. (b) The concentrations of zeaxanthin, antheraxanthin and violaxanthin determined by time-resolved HPLC measurements. The dashed line indicates a single exponential fit to Zea accumulation with a time constant of 2.66 min.

Using the same samples, we also conducted fluorescence lifetime snapshot experiments to evaluate Chl quenching behavior. In contrast to fluorescence yields, fluorescence decays of chlorophyll are not dependent upon photobleaching or changes in Chl concentration, which allows for precise evaluation of NPQ originating from the activation of quenchers and related quenching mechanisms.[19–22] Figure 3.2(a) presents amplitude-weighted average lifetimes (τ_{avg}) and corresponding NPQ parameters (NPQτ) extracted from 68 fluorescence decays at 680 nm (Figure S3.6). NPQτ is a lifetime-based parameter analogous to the conventional NPQ value ($= (F_m - F_m')/F_m'$),[19] and details of the calculation of NPQτ are presented in Experimental Methods. When the actinic light was turned on, thylakoid samples showed a rapid decrease in Chl lifetime from 1.3 ns to 0.34 ns, eventually plateauing after 5 min. 90% of maximum NPQτ was achieved within 3 min. This early time period ($\leq$ 3 min) of NPQτ in response to light is similar to both the timing of the appearance of the maximum amount of Zea·+ (Figure 3.1(c)) and the qE timescale.[2] Therefore, this set of data supports the idea that a Zea·+-mediated CT quenching mechanism is a part of qE quenching.

To quantify the Zea conversion in spinach thylakoids, we performed HPLC measurements in parallel on the same batch of thylakoid samples at each time point. As shown in Figure 3.2(b), the violaxanthin de-epoxidase (VDE) converted Vio to Zea exponentially (τ_{rise}=2.66 min). To determine how much Zea is involved in CT quenching (or forms Zea·+), one needs to use the extinction coefficient (ε) of Zea·+. Unfortunately, there is a large variation in the values of ε for carotenoid radical cation reported previously, and none of these studies examined the value in a protein environment (see details in Supporting Information).[23–26] Because we do not know the role of any protein-induced conformational changes on the ε, we decided to use a range of values for ε (53,000-73,000 L mol^{-1} cm^{-1}), centered around ε for β-carotene cation absorption at 970nm (63,000 L mol^{-1} cm^{-1}) to quantify the Zea·+ represented in our TA data.[24] Based on these values of ε, we were able to estimate that after 1 min of light acclimation (maximum Zea·+ signal), only a small portion (≤0.6%) of the Zea pool at that time was observed as the Zea·+ species in the snapshot TA signal. This is approximately equivalent to a Zea·+ in 5-7% of PSII supercomplexes (see Supporting Information for values used in the calculation).[27–29] The bulk of the Zea may facilitate other quenching processes, such as LHCII migration or quenching of reactive oxygen species, as suggested previously.[17,30] Accordingly, we suggest that the Zea·+ formation is not simply proportional to the concentration of Zea, but is rather controlled by ΔpH or ΔpH-triggered mechanisms such as activation of the Photosystem II subunit S (PsbS) protein.[31]

It is well-accepted that qE mechanisms require activation of PsbS, which is initiated by ΔpH across the thylakoid membrane .[32–34] Recently, Correa-Galvis *et al.* reported a crosslinking assay using 3,3′-dithiobis(sulphosuccinimidylpropionate) (DTSSP).[35] For dark-acclimated thylakoids, the DTSSP treatment arrests rearrangement and relocation of membrane proteins, preventing the protein-protein interactions required for qE activation. Although the DTSSP does not specifically target qE-specific PsbS interactions, it is tempting to speculate that the major effects of DTSSP are due to inactivated PsbS as the NPQ activation of DTSSP-treated thylakoid exhibits a very similar time course to that of the PsbS-deficient *npq4* mutant.[35] Therefore, we employed DTSSP treatment of our dark-acclimated thylakoid sample to examine the effect of chemical crosslinking on the CT quenching. In addition, we separately treated samples with 1,4-dithiothreitol (DTT) which is known to inhibit VDE activity and prevent conversion of Vio to Zea.[36,37]

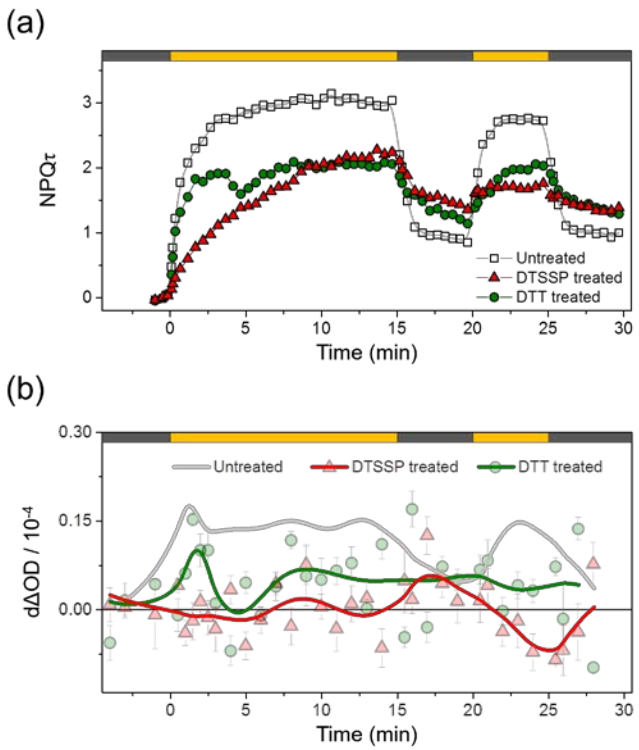

Figure 3.3: (a) The evolution of NPQτ values of DTSSP- and DTT-treated thylakoids in response to high light illumination. (b) Snapshot TA data of DTSSP- and DTT-treated thylakoids. The untreated sample is displayed with a smoothed trajectory (gray curve).

Figure 3.3(a) shows the results of fluorescence lifetime snapshot measurements of DTSSP- and DTT-treated thylakoid samples. In the DTSSP-treated sample, it appears that the chemical crosslinking removed a qE component from the NPQ trace, resulting in slowed quenching and *npq4*-like (*i.e.* absence of PsbS) behavior.[21] Interestingly, the DTSSP treatment had little impact on the activity of VDE and rate of Zea formation (Figure S3.7(a)). The snapshot TA results in Figure 3.3(b) revealed that the DTSSP-treated thylakoids showed no significant Zea·+ in response to light, suggesting that re-arrangement or conformational changes of active PsbS and partner proteins are necessary for Zea·+ formation.[7] This result supports the idea that the CT quenching mechanism is a part of NPQ quenching in higher plants and is triggered by a ΔpH → messenger proteins (e.g. PsbS) pathway,[38,39] and/or the ΔpH and electric potential gradients (Δψ) across the membrane stabilizing the state of CT quenching. In fact, the ΔpH obtained from the model of Zaks *et al.*,[38,39] the rate of quenching and [Zea·+]/[Zea] are well-correlated, as shown in Figure 3.4(a). This ΔpH-dependent CT-quenching mechanism resembles the pH-dependency of quenching in other photosynthetic organisms such as *Physcomitrella patens*[40] and *Chlamydomonas reinhardtii*.[41]

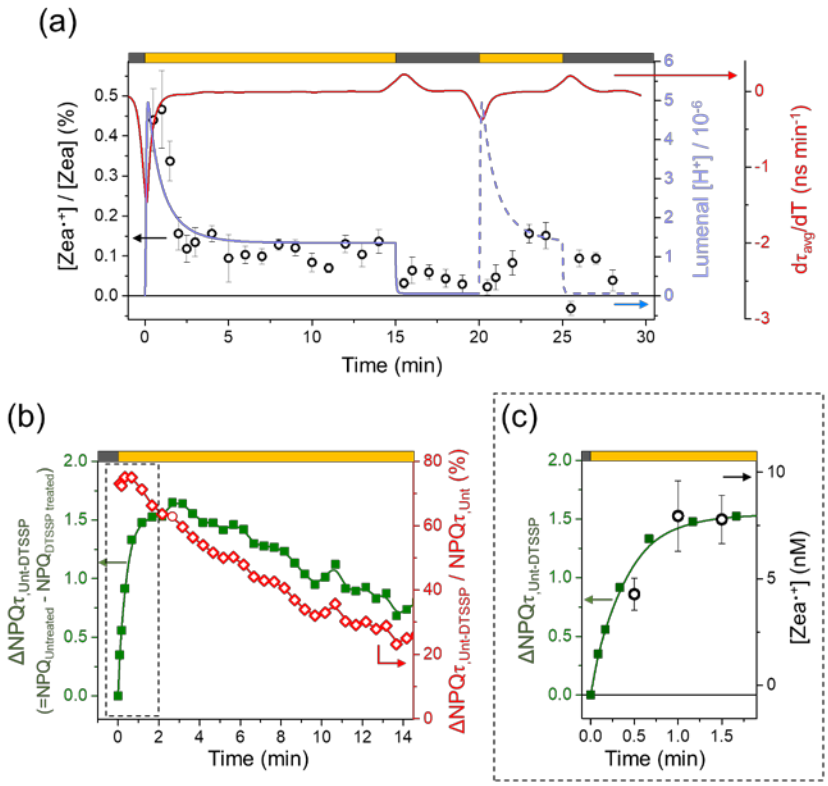

Figure 3.4: (a) The evolution of [Zea·+]/[Zea] (circles), derivative of fluorescence lifetime (τ_{avg}) (red line) and lumenal [H^+] (blue line) in response to high light/dark exposures. The data of lumenal [H^+] were calculated according to the kinetic model developed by Zaks *et al*.[38,39] The dashed blue line indicates significant uncertainty in lumenal [H^+] as the model was designed for the light acclimation of completely dark-acclimated systems. (b) The $\Delta NPQ\tau_{,Unt\text{-}DTSSP}$ (untreated minus DTSSP-treated samples) (green line with squares) and $\Delta NPQ\tau_{,Unt\text{-}DTSSP}$ as a percent of overall NPQ ($NPQ\tau_{,Unt}$) (red line with diamonds) during high-light-acclimation. (c) The rises of $\Delta NPQ\tau_{,Unt\text{-}DTSSP}$ (green line with squares) and [Zea·+] (circles) in the early (≤2 min) stage of high-light-acclimation. Note that the values of [Zea·+] were calculated based on an extinction coefficient of Zea·+ (=63,000 L mol^{-1} cm^{-1}).[24]

If we make the assumption that DTSSP treatment only stops Zea·+ formation, but not Zea-dependent NPQ that does not involve Zea·+ formation, the difference between the quenching behaviors (or decreases in fluorescence lifetime) of the untreated and the DTSSP-treated samples ($\Delta NPQ\tau_{,Unt\text{-}DTSSP}$) corresponds to the contribution of Zea·+ formation to qE. In this case the percentage of qE contributed by Zea·+ formation is simply $\Delta NPQ\tau_{,Unt\text{-}DTSSP}/NPQ\tau_{,Unt}$. As Figure 3.4(b) shows, this percentage is as high as 75% in the first 2 min, falling to 25% by 15 min of high light exposure. Figure 3.4(c) shows that the initial rise in $\Delta NPQ\tau_{,Unt\text{-}DTSSP}$ is consistent with the rise of the Zea·+ signal in the TA snapshot data. If the CT mechanism occurs only in the monomeric (minor) LHCII and the protonation of PsbS leads to dissociation of trimeric LHCIIs from the PSII supercomplexes,[16,17,35] the concomitant reduction in excitation of monomeric LHCIIs could account for the decrease of Zea·+ contribution at longer light acclimation times. To be consistent

with the snapshot TA data of the DTSSP-treated sample, the formation of Zea·+ must also require dissociation of PsbS dimers or some other intermolecular rearrangement limited by DTSSP crosslinking. The present data, based on the assumptions above, suggest, but by no means prove, that CT quenching is one of the first response to excess light, followed by a suite of processes with slower turn on times that involve Zea in a non-CT role,[9] Lut,[11] and possibly other actors.[42]

The DTT-treated thylakoids with inhibited VDE activity showed a lower level of maximum NPQτ (≅2), close to two-thirds the level of untreated samples. As presented in the HPLC data (Figure S3.7(a)), although there is a small increase in Zea concentration at 2 min after high light exposure, there was little to no increase by the end of the light sequence. However, the DTT-treated thylakoids still exhibited a moderate amount of TA signal at 1000 nm (Figure 3.3(b)). Considering that only a small portion of Zea is converted to Zea·+, one possible explanation is that a pre-existing small pool of Zea (≅3 mmol/mol Chl) is responsible for a large fraction of the CT quenching. It is also possible that antheraxanthin is involved in the quenching, as early antheraxanthin levels were similar across untreated, DTT-treated, and DTSSP-treated thylakoids (Figure S3.7(b)).[38,43] It is noteworthy that a dip in the signal was observed at 5 min in both fluorescence and TA snapshot data. This suggests that the CT quenching is still important in the early stages of NPQ even with reduced VDE activity. In addition, as discussed above, it implies that the detachment of trimeric LHCIIs from PSII supercomplex would transiently isolate them from the CT quenching sites on the monomeric LHCIIs.[16,17]

Our calculations indicate that ≤0.6% of Zea is responsible for the maximum Zea·+ signal (Figure 3.4(a)), provided our estimate of ε for Zea·+ is roughly correct. This combined with our estimate that only 5-7% of PSII supercomplexes have Zea·+ molecules present, assuming that Zea·+ is only associated with the monomeric complexes, might be taken to imply a minor role of CT formation in qE. On the other hands the identical rise of Zea·+ and $\Delta NPQ\tau_{,Unt\text{-}DTSSP}$ suggest otherwise (Figure 3.4(c)). A possible resolution is suggested by the work of Walla and coworkers[44,45] and of Dreuw *et al*.[46] Walla and coworkers show that NPQ onset is correlated with increased Car-Chl energy transfer in both directions,[44,45] while Dreuw *et al* show that the nature of electronically excited states of Zea and Chl molecules in close proximity is very sensitive to the spatial separation of the pair.[46] If a range of Zea-Chl separations and a range of energy gaps exist in the thylakoid membrane, some will give energy transfer, some charge transfer. In this scenario the Zea·+ could be taken as a marker of Zea-Chl interaction that leads to quenching *via* both CT and EET routes. We plan future snapshot TA spectroscopy studies to focus on other possible quenching mechanisms, including EET by measuring changes in absorption in the carotenoid S_1 wavelength region.[9] Snapshot TA studies of the wide variety of *Arabidopsis thaliana* photoprotection mutants available should greatly aid the exploration of NPQ mechanisms.

In summary, we have introduced snapshot TA spectroscopy, which allowed us to follow the appearance of a carotenoid radical cation signal as spinach thylakoid membranes acclimate to high light. We observed a maximum Zea·+ signal after 2 min of light acclimation, consistent with observations from fluorescence lifetime measurements and with the timescale of qE. Time-resolved HPLC measurements revealed that Zea·+ formation in spinach is not significantly limited

by Zea accumulation, and the results of DTSSP and DTT treatments of the thylakoids suggests that Zea·+ formation is highly dependent on re-organization or structural change of proteins, initiated by the pH-sensing protein, PsbS. Therefore, it seems likely that Zea is involved in a CT quenching mechanism in higher plants that rapidly responds to changes in light intensity, consistent with qE quenching.

Methods

Preparation of thylakoid membrane. Fresh spinach leaves were acquired the day before preparation and dark acclimated at 4 °C overnight. Spinach thylakoids membranes were isolated by a modified version of the procedure described previously.[47] Crude thylakoids membranes were washed twice with 10 ml of suspension buffer before diluting with reaction buffer. The final concentration of all thylakoid samples was adjusted to 80 nmol Chl/ml before measurement. The working concentrations of DTSSP and DTT were 3 mM and 2 mM, respectively. The Zea accumulation in thylakoid samples was monitored by HPLC as previously described.[48]

Snapshot transient absorption spectroscopy. Pump-probe spectroscopy for transient absorption measurements has been described in previous literature.[7,12] A Ti:sapphire oscillator (Coherent MIRA Seed) was used to seed a regenerative amplifier (Coherent RegA 9050) with an external stretcher/compressor, generating an 800 nm pulse with a repetition rate of 250 kHz. A portion of the pulses pumped an optical parametric amplifier (OPA, Coherent 9450) which is tuned to 650 nm for Chl b Q_y transition. We chose 650 nm as an excitation wavelength because the output power of our OPA was higher there than that at 680 nm (Chl a Q_y transition), yielding higher SN ratios. The pump pulses had a maximum pump energy of 40 nJ/pulse and the FWHM of the autocorrelation trace was 54 fs. NIR continuum probe pulses were produced using a 1 mm yttrium aluminum garnet (YAG) crystal, and an 850 nm long pass filter was placed after continuum generation. The polarizations of the pump and probe were set to the magic angle (54.7°) by placing a half wave plate and a polarizer in the pump path. The diameters of the pump and probe at the sample position were 120 µm and 73 µm, respectively. After the sample, a second polarization filter set to the probe polarization was placed to minimize pump scattering, as well as an 850 nm long pass filter to ensure a clean probe signal. A monochromator (SpectraPro 300i, Acton Research Corp., Action, MA) and a InGaAs photodiode (DET410, Thorlabs, Newton, NJ) were used to monitor the ΔT/T signal. The actinic light was set to an intensity of 850 µmol photons·m^{-2}·s^{-1} at the sample position, with a heat absorbing filter (KG1). For collecting snapshot TA data at a fixed delay time (20 ps) and a wavelength (1000 nm), a pump and probe shutter was controlled to open for 10 seconds at 30 seconds-1 min intervals throughout the light acclimation sequence. The sample cell was moved between measurements to prevent sample damage. The path length of the cuvette was 1 mm.

Fluorescence lifetime snapshot. Fluorescence lifetime snapshot data was collected in a home-built fluorescence lifetime measurement apparatus previously described.[19–22] Briefly, the 840 nm output pulses with a repetition rate of 76 MHz from Ti:sapphire oscillator (Coherent Mira 900f)

were frequency-doubled to generate 420 nm using a beta barium borate (BBO) crystal, which is for excitation of the Soret band of Chl a. Before the sample, one portion is directed into a photodiode to provide SYNC for the time-correlated single photon counting card (Becker-Hickl SPC-630 and SPC-850). The other portion of laser is intermittently blocked by a shutter controlled by a LabVIEW program. The excitation laser power was 1.6 mW (21 pJ/pulse) at the sample. The sample was intermittently exposed to an actinic light (Schott KL1500) with an intensity of 850 μmol photons·m^{-2}·s^{-1}, also controlled by a shutter and LabVIEW program. After the sample, a monochromator set to 680 nm and a MCP PMT detector (Hamamatsu R3809U) were placed for fluorescence detection. The 68 fluorescence decay measurements were made at intervals varying from every 10 seconds to every 30 seconds in complete darkness. In each measurement, the sample was exposed to the laser for 1 second, divided up into five steps of 0.2 second. The step with the longest fluorescence lifetime was selected in data processing to ensure that the PSII reaction centers were closed. Each fluorescence decay curve was fit to a sum of 3 exponential decay components (Picoquant Fluofit Pro-4.6). Following data fitting, the amplitude-weighted average lifetime (τ_{avg}) and NPQτ values were calculated by following equations:[19,21]

$$\tau_{avg} = \frac{\sum_i A_i \tau_i}{\sum_i A_i}$$

where A_i and τ_i are the amplitudes and the fluorescence lifetime components, respectively.

$$NPQ\tau = \frac{\tau_{avg,dark} - \tau_{avg,light}}{\tau_{avg,light}}$$

where $\tau_{avg,dark}$ is the average of three lifetimes measured at initial dark period.

Supporting Information

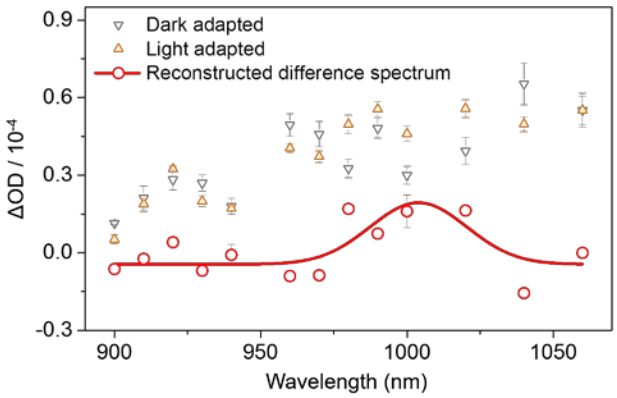

Figure S3.5: Transient absorption spectrum for the dark- and light-acclimated thylakoids. The spectrum was constructed from signals at 20 ps after excitation. Difference spectrum was reconstructed by subtracting dark-acclimated signal from light-acclimated signal. The solid curve represents the Gaussian fit to the difference data. Data are presented as the means ± SE (n=5).

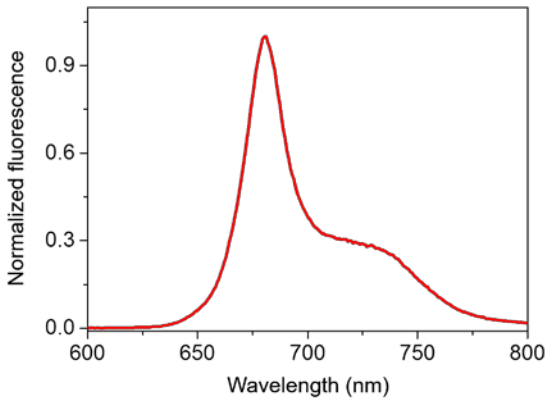

Figure S3.6: Steady-state fluorescence emission spectrum of thylakoid sample. The spectrum was obtained upon excitation of 420 nm and measured at room temperature.

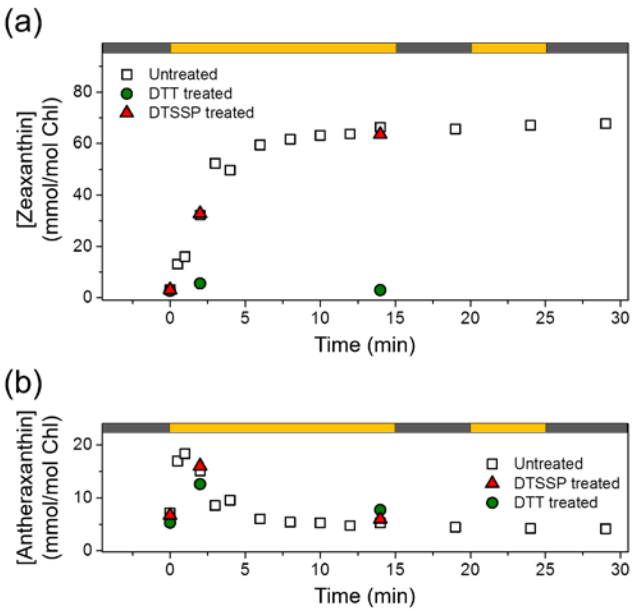

Figure S3.7: The concentrations of (a) zeaxanthin and (b) antheraxanthin as a function of high light exposure time.

Discussion on the previous reports about Zea·+ extinction coefficient

We found a large variation in the values of extinction coefficient (ε) for carotenoid radical cations reported previously. For example, in 1995, T. J. Hill *et al.* conducted pulse radiolysis yielding carotenoid radical cations.[22] Transient absorption after pulse radiolysis of Zea indicated that the ε of Zea·+ at 936 nm is 41,000 L mol^{-1} cm^{-1}. Later, J. A. Jeeravaian and L. D. Kispert reported that ε of β-carotene radical cation at 970 nm equals 63,000 L mol^{-1} cm^{-1}, which was determined *via* a combined electrochemical and chemical study.[23] Meanwhile, Mortensen and Skibsted. used laser photolysis to create Zea·+, and assuming 100% conversion, we calculate ε to be 3125 M^{-1} cm^{-1}.[24] Lastly, Han *et al*. electrochemically created Zea·+ in chloroform.[25] Using their spectroscopic data and their report of 19% conversion to Zea·+, we calculate ε = 3600 M^{-1} cm^{-1}. Additionally, we have attempted to determine this constant by creating Zea·+ *via* I_2 titration, but these experiments indicated that ε is approximately 66,000 M^{-1} cm^{-1} (unpublished).

Quantification of Zea·+ in PSII supercomplex

Values used:

- Extinction coefficient of Zea·+ = 53,000-73,000 L mol^{-1} cm^{-1} (J. A. Jeevarajan *et al.*'s estimate$\pm$10,000).[23]
- The length of overlap between pump and probe pulse along the probing path = 433 μm.
- The concentration of β-carotene measured from thylakoid membrane sample = 94.6 mmol/mol Chl.
- The PSI/PSII ratio in spinach thylakoid membrane = 1.13.[26]
- The number of β-carotene = 24 in PSII (C2S2M2 supercomplex) and in 26 PSI (PSI-LHCI).[27,28]

Acknowledgements

We thank Jonathan M. Morris, Eva M. Nichols, Dr. Lowell D. Kispert, Dr. Masakazu Iwai and Dr. Tae Kyu Ahn for helpful discussions. This work was supported by US Department of Energy, Office of Science, Basic Energy Sciences, Chemical Sciences, Geosciences, and Biosciences Division under Field Work Proposal 449B. K.K.N. is an investigator of the Howard Hughes Medical Institute. S.P. is supported by Basic Science Research Program through the National Research Foundation of Korea funded by the Ministry of Education (NRF-2016R1A6A3A03006768). R.B. thanks the Miller Institute of Berkeley for awarding a visiting professorship grant.

References

(1) Park, S.; Fischer, A. L.; Li, Z.; Bassi, R.; Niyogi, K. K.; Fleming, G. R. Snapshot Transient Absorption Spectroscopy of Carotenoid Radical Cations in High-Light-Acclimating Thylakoid Membranes. *J. Phys. Chem. Lett.* **2017**, *8* (22), 5548–5554.

(2) Müller, P.; Li, X.-P.; Niyogi, K. K. Non-Photochemical Quenching. A Response to Excess Light Energy 1. *Plant Physiol.* **2001**, *125*, 1558–1566.

(3) Kulheim, C. Rapid Regulation of Light Harvesting and Plant Fitness in the Field. *Science (80-.).* **2002**, *297* (5578), 91–93.

(4) Demmig-Adams, B. Carotenoids and Photoprotection in Plants: A Role for the Xanthophyll Zeaxanthin. *Biochim. Biophys. Acta* **1990**, *1020* (1), 1–24.

(5) Yamamoto, H. Y.; Nakayama, T. O. M.; Chichester, C. O. Studies on the Light and Dark Interconversions of Leaf Xanthophylls. *Arch. Biochem. Biophys.* **1962**, *97* (1), 168–173.

(6) Niyogi, K. K.; Grossman, A. R.; Björkman, O. Arabidopsis Mutants Define a Central Role for the Xanthophyll Cycle in the Regulation of Photosynthetic Energy Conversion. *Plant Cell* **1998**, *10* (7), 1121–1134.

(7) Holt, N. E.; Zigmantas, D.; Valkunas, L. Carotenoid Cation Formation and the Regulation of Photosynthetic Light Harvesting. **2005**, *307* (January), 433–437.

(8) Dariusz M. Niedzwiedzki; James O. Sullivan; Tomáš Polívka; Robert R. Birge; Harry A. Frank. Femtosecond Time-Resolved Transient Absorption Spectroscopy of Xanthophylls. *J. Phys. Chem. B* **2006**, *110* (45), 22872-22885.

(9) Ma, Y.-Z.; Holt, N. E.; Li, X.-P.; Niyogi, K. K.; Fleming, G. R. Evidence for Direct Carotenoid Involvement in the Regulation of Photosynthetic Light Harvesting. *Proc. Natl. Acad. Sci.* **2003**, *100* (8), 4377–4382.

(10) Li, Z.; Ahn, T. K.; Avenson, T. J.; Ballottari, M.; Cruz, J. A.; Kramer, D. M.; Bassi, R.; Fleming, G. R.; Keasling, J. D.; Niyogi, K. K. Lutein Accumulation in the Absence of Zeaxanthin Restores Nonphotochemical Quenching in the Arabidopsis Thaliana npq1 Mutant. *Plant Cell Online* **2009**, *21* (6), 1798–1812.

(11) Ruban, A. V.; Berera, R.; Ilioaia, C.; Van Stokkum, I. H. M.; Kennis, J. T. M.; Pascal, A. A.; Van Amerongen, H.; Robert, B.; Horton, P.; Van Grondelle, R. Identification of a Mechanism of Photoprotective Energy Dissipation in Higher Plants. *Nature* **2007**, *450* (7169), 575–578.

(12) Ahn, T. K.; Avenson, T. J.; Ballottari, M.; Cheng, Y.-C.; Niyogi, K. K.; Bassi, R.; Fleming, G. R. Architecture of a Charge-Transfer State Regulating Light Harvesting in a Plant Antenna Protein. *Science* **2008**, *320* (5877), 794–797.

(13) Avenson, T. J.; Tae, K. A.; Zigmantas, D.; Niyogi, K. K.; Li, Z.; Ballottari, M.; Bassi, R.; Fleming, G. R. Zeaxanthin Radical Cation Formation in Minor Light-Harvesting Complexes of Higher Plant Antenna. *J. Biol. Chem.* **2008**, *283* (6), 3550–3558.

(14) Dall 'osto, L.; Cazzaniga, S.; Bressan, M.; Paleček, D.; Židek, K.; Niyogi, K. K.; Fleming, G. R.; Zigmantas, D.; Bassi, R. Two Mechanisms for Dissipation of Excess Light in Monomeric and Trimeric Light-Harvesting Complexes. **2017**.

(15) Cheng, Y. C.; Ahn, T. K.; Avenson, T. J.; Zigmantas, D.; Niyogi, K. K.; Ballottari, M.; Bassi, R.; Fleming, G. R. Kinetic Modeling of Charge-Transfer Quenching in the CP29 Minor Complex. *J. Phys. Chem. B* **2008**, *112* (42), 13418–13423.

(16) Betterle, N.; Ballottari, M.; Zorzan, S.; de Bianchi, S.; Cazzaniga, S.; Dall'Osto, L.;

Morosinotto, T.; Bassi, R. Light-Induced Dissociation of an Antenna Hetero-Oligomer Is Needed for Non-Photochemical Quenching Induction. *J. Biol. Chem.* **2009**, *284* (22), 15255–15266.

(17) Johnson, M. P.; Goral, T. K.; Duffy, C. D. P.; Brain, A. P. R.; Mullineaux, C. W.; Ruban, A. V. Photoprotective Energy Dissipation Involves the Reorganization of Photosystem II Light-Harvesting Complexes in the Grana Membranes of Spinach Chloroplasts. *Plant Cell Online* **2011**, *23* (4).

(18) Amarie, S.; Wilk, L.; Barros, T.; K?hlbrandt, W.; Dreuw, A.; Wachtveitl, J. Properties of Zeaxanthin and Its Radical Cation Bound to the Minor Light-Harvesting Complexes CP24, CP26 and CP29. *Biochim. Biophys. Acta - Bioenerg.* **2009**, *1787* (6), 747–752.

(19) Sylak-Glassman, E. J.; Zaks, J.; Amarnath, K.; Leuenberger, M.; Fleming, G. R. Characterizing Non-Photochemical Quenching in Leaves through Fluorescence Lifetime Snapshots. *Photosynth. Res.* **2016**, *127* (1), 69–76.

(20) Amarnath, K.; Zaks, J.; Park, S. D.; Niyogi, K. K.; Fleming, G. R. Fluorescence Lifetime Snapshots Reveal Two Rapidly Reversible Mechanisms of Photoprotection in Live Cells of Chlamydomonas Reinhardtii. *Proc. Natl. Acad. Sci.* **2012**, *109* (22), 8405–8410.

(21) Sylak-Glassman, E. J.; Malnoë, A.; De Re, E.; Brooks, M. D.; Fischer, A. L.; Niyogi, K. K.; Fleming, G. R. Distinct Roles of the Photosystem II Protein PsbS and Zeaxanthin in the Regulation of Light Harvesting in Plants Revealed by Fluorescence Lifetime Snapshots. *Proc. Natl. Acad. Sci.* **2014**, *111* (49), 17498–17503.

(22) Leuenberger, M.; Morris, J. M.; Chan, A. M.; Leonelli, L.; Niyogi, K. K.; Fleming, G. R. Dissecting and Modeling Zeaxanthin- and Lutein-Dependent Nonphotochemical Quenching inArabidopsis Thaliana. *Proc. Natl. Acad. Sci. U. S. A.* **2017**, *114* (33), E7009–E7017.

(23) Hill, T. J.; McGarvey, D. J.; Tinkler, J. H.; Truscott, T. G.; Land, E. J.; Schalch, W. Interactions between Carotenoids and the CCl3O2 Radical. *J. Am. Chem. Soc.* **1995**, *117* (32), 8322–8326.

(24) Jeevarajan, J. A.; Wei, C. C.; Jeevarajan, A. S.; Kispert, L. D. Optical Absorption Spectra of Dications of Carotenoids. *J. Phys. Chem.* **1996**, *100*, 5637–5641.

(25) Mortensen, A.; Skibsted, L. H. Free Radical Transients in Photobleaching of Xanthophylls and Carotenes. *Free Radic. Res.* **1997**, *26* (6), 549–563.

(26) Han, R.-M.; Tian, Y.-X.; Wu, Y.-S.; Wang, P.; Ai, X.-C.; Zhang, J.-P.; Skibsted, L. H. Mechanism of Radical Cation Formation from the Excited States of Zeaxanthin and Astaxanthin in Chloroform. *Photochem. Photobiol.* **2006**, *82* (2), 538–546.

(27) Danielsson, R.; Albertsson, P. Å.; Mamedov, F.; Styring, S. Quantification of Photosystem I and II in Different Parts of the Thylakoid Membrane from Spinach. *Biochim. Biophys. Acta - Bioenerg.* **2004**, *1608* (1), 53–61.

(28) Qin, X.; Suga, M.; Kuang, T.; Shen, J. R. Structural Basis for Energy Transfer Pathways in the Plant PSI-LHCI Supercomplex. *Science (80-.).* **2015**, *348* (6238), 989–995.

(29) Quax, T. E. F.; Daum, B. Structure and Assembly Mechanism of Virus-Associated Pyramids. *Biophys. Rev.* **2017**, *820* (August), 815–820.

(30) Havaux, M.; Niyogi, K. K. The Violaxanthin Cycle Protects Plants from Photooxidative Damage by More than One Mechanism. *Plant Biol.* **1999**, *96*, 8762–8767.

(31) Li, X. P.; Björkman, O.; Shih, C.; Grossman, A. R.; Rosenquist, M.; Jansson, S.; Niyogi, K. K. A

Pigment-Binding Protein Essential for Regulation of Photosynthetic Light Harvesting. *Nature* **2000**, *403* (6768), 391–395.
(32) Bergantino, E.; Segalla, A.; Brunetta, A.; Teardo, E.; Rigoni, F.; Giacometti, G. M.; Szabò, I.; Lorimer, G. H. Light-and pH-Dependent Structural Changes in the PsbS Subunit of Photosystem II. *Proc. Natl. Acad. Sci.* **2003**, *100* (25), 15265–15270.
(33) Li, X.-P.; Phippard, A.; Pasari, J.; Niyogi, K. K. Structure–function Analysis of Photosystem II Subunit S (PsbS) in Vivo. *Funct. Plant Biol.* **2002**, *29* (10), 1131.
(34) Li, X. P.; Gilmore, A. M.; Caffarri, S.; Bassi, R.; Golan, T.; Kramer, D.; Niyogi, K. K. Regulation of Photosynthetic Light Harvesting Involves Intrathylakoid Lumen pH Sensing by the PsbS Protein. *J. Biol. Chem.* **2004**, *279* (22), 22866–22874.
(35) Correa-Galvis, V.; Poschmann, G.; Melzer, M.; Stühler, K.; Jahns, P. PsbS Interactions Involved in the Activation of Energy Dissipation in Arabidopsis. *Nature Plants* **2016**, *2, 1-8*.
(36) Adams, W. W.; Demmig-Adams, B.; Winter, K.; Winter, K. Relative Contributions of Zeaxanthin-Related and Zeaxanthin-Unrelated Types of ;high-Energy-State' Quenching of Chlorophyll Fluorescence in Spinach Leaves Exposed to Various Environmental Conditions. *Plant Physiol.* **1990**, *92* (2), 302–309.
(37) Bilger, W.; Bjorkman, O. Role of the Xanthophyll Cycle in Photoprotection Elucidated by Measurements of Light-Induced Absorbance Changes, Fluorescence and Photosynthesis in Leaves of Hedera Canariensis. *Photosynth. Res.* **1990**, *25*, 173–185.
(38) Zaks, J.; Amarnath, K.; Kramer, D. M.; Niyogi, K. K.; Fleming, G. R. A Kinetic Model of Rapidly Reversible Nonphotochemical Quenching. *PNAS* **2012**, *109* (39), 15757-15762.
(39) Zaks, J.; Amarnath, K.; Sylak-Glassman, E. J.; Fleming, G. R. Models and Measurements of Energy-Dependent Quenching. *Photosynth. Res.* **2013**, *116* (2–3), 389–409.
(40) Pinnola, A.; Staleva-Musto, H.; Capaldi, S.; Ballottari, M.; Bassi, R.; Polívka, T. Electron Transfer between Carotenoid and Chlorophyll Contributes to Quenching in the LHCSR1 Protein from Physcomitrella Patens. *Biochimica et Biophysica Acta* **2016**, *1857*, 1870-1878.
(41) Bonente, G.; Ballottari, M.; Truong, T. B.; Morosinotto, T.; Ahn, T. K.; Fleming, G. R.; Niyogi, K. K.; Bassi, R. Analysis of LHcSR3, a Protein Essential for Feedback de-Excitation in the Green Alga Chlamydomonas Reinhardtii. *PLoS Biol.* **2011**, *9* (1).
(42) Wahadoszamen, M.; Berera, R.; Mane Ara, A.; Romero, E.; van Grondelle, R. Identification of Two Emitting Sites in the Dissipative State of the Major Light Harvesting Antennaw. *Phys. Chem. Chem. Phys.* **2012**, *14* (14), 759–766.
(43) Gilmore, A. M.; Yamamoto, H. Y. Linear Models Relating Xanthophylls and Lumen Acidity to Non-Photochemical Fluorescence Quenching. Evidence That Antheraxanthin Explains Zeaxanthin-Independent Quenching. *Photosynth. Res.* **1993**, *35*, 67–78.
(44) Bode, S.; Quentmeier, C. C.; Liao, P.-N.; Hafi, N.; Barros, T.; Wilk, L.; Bittner, F.; Walla, P. J. On the Regulation of Photosynthesis by Excitonic Interactions between Carotenoids and Chlorophylls. *Proc. Natl. Acad. Sci. U. S. A.* **2009**, *106* (30), 12311–12316.
(45) Holleboom, C.-P.; Walla, P. J. The Back and Forth of Energy Transfer between Carotenoids and Chlorophylls and Its Role in the Regulation of Light Harvesting. *Photosynth. Res.* **2014**, *119* (1–2), 215–221.
(46) Dreuw, A.; Fleming, G. R.; Head-Gordon, M. Charge-Transfer State as a Possible Signature of a Zeaxanthin-Chlorophyll Dimer in the Non-Photochemical Quenching Process in Green Plants. *J. Phys. Chem. B* **2003**, *107*, 6500-6503.

(47) Gilmore, A. M.; Shinkarev, V. P.; Hazlett, T. L.; Govindjee. Quantitative Analysis of the Effects of Intrathylakoid pH and Xanthophyll Cycle Pigments on Chlorophyll a Fluorescence Lifetime Distributions and Intensity in Thylakoids †. *Biochemistry* **1998**, *37* (39), 13582–13593.
(48) Müller-Moulé, P.; Conklin, P. L.; Niyogi, K. K. Ascorbate Deficiency Can Limit Violaxanthin De-Epoxidase Activity in Vivo 1. *Plant Physiol.* **2002**, *128*, 970–977.

Chapter 4: Chlorophyll-Carotenoid Excitation Energy Transfer in High-Light-Acclimating Thylakoid Membranes Investigated by Snapshot Transient Absorption Spectroscopy

Note: This work is adapted from a manuscript in preparation, coauthored by Soomin Park, Collin Steen, Masakazu Iwai, Jonathan Morris, Peter Walla, Kris Niyogi, and Graham Fleming. Soomin, Collin, Masa and I collected the data. All parties assisted with data analysis. Soomin, Collin, and I co-wrote the manuscript.

Abstract

Nonphotochemical quenching (NPQ) provides an essential photoprotection in plants, assuring safe dissipation of excess energy as heat under high light. Although excitation energy transfer (EET) between chlorophyll (Chl) and carotenoid (Car) molecules plays an important role in NPQ, detailed information on the EET quenching mechanism *in vivo* conditions, including triggering mechanism and activation dynamics, is very limited. In here, we observed EET from Chl Q_y state to Car S_1 state in high-light-acclimating spinach thylakoid membranes. The kinetic and spectral analyses using transient absorption (TA) spectroscopy revealed that the Car S_1 excited state absorption (ESA) signal after Chl excitation has a maximum absorption peak at around 540 nm and a lifetime of ~ 8 ps. Snapshot TA spectroscopy at multiple time delays allowed us to track the Car S_1 ESA signal as the thylakoid membranes acclimated to various light conditions. The Car S_1 ESA signal quickly rose and slightly dropped during the initial light-acclimation (< 3 min) and then gradually increased with a time constant of ~ 5 min after prolonged light exposure. This suggests the involvement of both rapidly-activated and slowly-activated mechanisms for EET quenching. DTT and DTSSP chemical treatments further revealed that the Car S_1 ESA signal (or the EET quenching mechanism) is primarily dependent on the accumulation of zeaxanthin and partially dependent on the reorganization of membrane proteins, perhaps due to the pH-sensing protein photosystem II subunit S.

Introduction

Photosynthetic organisms have a limited capacity to utilize the flow of excitation energy from absorbed sunlight. Under light-saturated conditions, the reaction center in photosystem II (PSII) closes due to lack of plastoquinones available for electron transfer.[1] As a consequence, the fluorescence lifetime (~ns) of excited chlorophyll (Chl) in the antenna increases, which in turn increases the probability of the formation of the Chl triplet state and reactive oxygen species, which will damage photosynthetic proteins.[2] Nonphotochemical quenching (NPQ) is a type of photoprotection in which absorbed light energy is safely converted into heat.[3] NPQ is a term which encapsulates many components, termed qE, qZ, qT, and qI, which were conventionally classified based on their induction and relaxation kinetics.[4] Among them, energy-dependent quenching (qE) is the fastest component, and is responsible for the largest portion of overall Chl de-excitation, providing relaxation pathways for the excited Chl on a timescale of a few seconds to minutes after excess light conditions occur. [4,5]

The carotenoid (Car) pigments in PSII serve an essential role in qE.[6] In higher plants, the enzymatic production of the carotenoid zeaxanthin (Zea) increases in response to high light, and Zea appears essential for maximum qE.[7,8] Direct involvement of Zea in Chl quenching has been suggested via evidence of interaction between Zea S_1 and Chl Q_y excited states.[9,10] To explain Chl-Zea energy transfer and subsequent Chl quenching, two mechanisms have been proposed: a charge-transfer (CT) quenching and excitation energy transfer (EET) quenching.[11] In the CT quenching mechanism, Chl and Zea are in close enough proximity to form a Chl-Zea heterodimer, which accepts excitation energy from the bulk Chl pool. Then, the heterodimer becomes charge-separated and forms a Zea radical cation ($Zea^{\bullet+}$) and a Chl radical anion ($Chl^{\bullet-}$).[12–15] This is followed by charge recombination which leads to energy dissipation. In the EET quenching mechanism, the excitation energy directly transferred from the Chl Q_y state to the Zea S_1 state.[16] The direction of energy transfer is not necessarily Chl $Q_y \rightarrow$ Zea S_1, as bidirectional energy transfer, Chl $Q_y \leftrightarrow$ Zea S_1, has been shown to occur when the two state energies are similar and there is strong electronic coupling between them.[17–19] After energy transfer, the Zea S_1 state rapidly relaxes to the ground state with a lifetime of ~ 9 ps.[16,20–22] Other carotenoids, such as lutein (Lut), have also been considered as direct quencher in CT and EET quenching mechanisms.[23,24] Although it has been speculated that both quenching mechanisms contribute to overall qE, specific information on the quenching sites, triggering factors, activation time courses, and relative contributions of individual mechanisms are not well understood.

Recently, we reported using snapshot transient absorption (TA) spectroscopy to gather quantitative and dynamic information on the $Zea^{\bullet+}$-mediated CT quenching mechanism in light-acclimating spinach thylakoid membranes.[15] Those experiments focused on one wavelength (1000 nm) and time delay (20 ps), and allowed us to collect the $Zea^{\bullet+}$ excited state absorption (ESA) signal within 10 second windows over the course of light-acclimation. The $Zea^{\bullet+}$ ESA signal reaches maximum intensity at the beginning ($\leq$ 2 min) of light-acclimation, which

suggests that $Zea^{\bullet+}$ formation is closely related to early qE. The evolution of the $Zea^{\bullet+}$ signal correlated well with the luminal $[H^+]$ and the rate of Chl fluorescence quenching. In addition, a cross-linking assay[25] arresting rearrangement of the pH-sensing PSII subunit S (PsbS) protein completely removed $Zea^{\bullet+}$ signals, and suggested that the CT quenching mechanism was triggered by a ΔpH → messenger protein(s) pathway.[5,26]

Here, to investigate a Chl-Car EET quenching mechanism in high-light-acclimating thylakoid membranes, we have modified our above-mentioned snapshot TA technique. Increased population of the Car S_1 state after Chl b excitation (650 nm) should provide evidence for the EET quenching mechanism.[19,20,27] Combining the new data with fluorescence lifetime snapshot data and our previous $Zea^{\bullet+}$ snapshot data,[15] we can provide a broader picture of the EET and CT quenching mechanisms.

Results and Discussion

In order to examine the feasibility of EET quenching involving a paired Chl-Car dimer, we have adapted our snapshot transient absorption setup to allow us to track changes in Car S1 absorption over the course of a light acclimation.

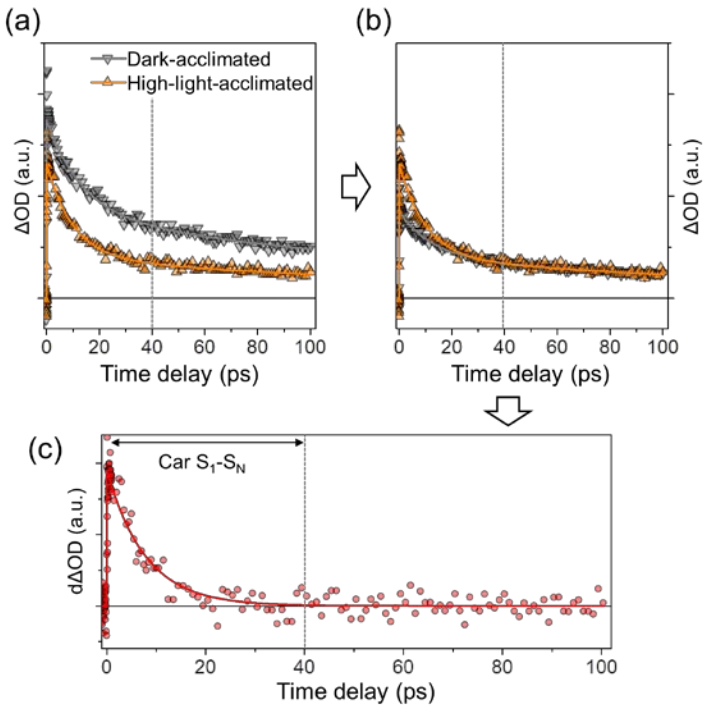

Figure 4.1: (a) Transient absorption (TA) kinetic trace for spinach thylakoid membranes under dark-acclimated (gray, down triangle) and high-light-acclimated (orange, up triangle) conditions. (b) Scaled TA kinetic trace obtained by matching the dark-acclimated thylakoids (gray, down triangle) to the respective trace measured under high-light-acclimated conditions (orange, up triangle) at 40 ps of time delay. (c) Difference between high-light-acclimated and dark-acclimated kinetic profiles. Samples were excited and probed at 650 nm and 540 nm, respectively. For the high-light-acclimation condition, thylakoids were continuously exposed to actinic light at 850 µmol photons·m^{-2}·s^{-1}.

Figure 4.1(a) shows the kinetic profiles of high-light- and dark-acclimated thylakoid membranes. At wavelengths longer than 520 nm, there is a considerable amount of Chl ESA signal detected in addition to Car S_1-S_N absorption.[28] As Chl Q_y excited states de-populate via quenching or another de-excitation pathway, the intensity of the ESA signal corresponding to Chl Q_y decreases significantly, which explains why light-acclimated samples have an overall

lower level of ESA signal compared to dark-acclimated samples. Correspondingly, the Car S_1-S_N transition becomes the more dominant signal at shorter time delays under light-acclimated conditions. We found that both TA kinetic profiles are kinetically indistinguishable at longer time delays ($\geq$ 40 ps) at which the Car S_1 ESA contribution should be negligible.[16,19] To account for the significant decrease in Chl ESA and clearly compare TA kinetic profiles, we scaled the profile of the dark-acclimated sample to match that of the light-acclimated profile based on signals at around 40 ps time delay. Figure 4.1(b) shows that the light-acclimated profile and scaled dark-acclimated profile overlap well at time delays greater than 40 ps.

Figure 4.1(c) shows the difference between the light-acclimated and dark-acclimated (scaled) profiles. The difference profile fits well to a single exponential decay, with a lifetime of 7.81 ps ($\pm$0.83 ps). This value agrees with the literature values of the S_1 lifetime of Zea, which range from 7 to 11 ps.[16,20,21] In this fit, there was no resolvable rise time within the time resolution ($\cong$120 fs) of our TA setup.[16,19] If we consider the difference decay profile as the excitation energy population in the Car S_1 state, a lack of resolvable rise time indicates near instantaneous excitation equilibrium near Chl-Car EET quenching sites. One possible scenario is that the mixing of Chl Q_y and Car S_1 states is reinforced by increased electronic coupling after light-acclimation, which eventually results in instantaneous excitation equilibrium via bidirectional energy transfer between Chl-Car at EET quenching sites. Such bidirectional Chl-Car EET was observed experimentally by Walla and co-workers.[17–19]

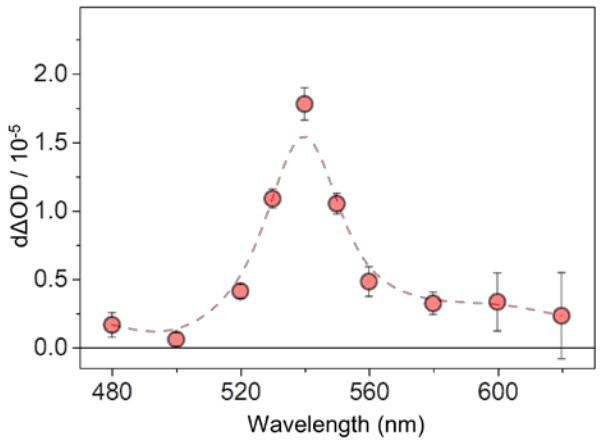

Figure 4.2: Difference TA spectrum reconstructed by subtracting the dark-acclimated signal from the high-light-acclimated signal. For the reconstruction, the TA signals from high-light-acclimated and dark-acclimated samples were collected at a time delay of 1 ps after Chl excitation. Before the subtraction, each data point of the dark-acclimated spectrum was scaled to match the corresponding data from the same sample after acclimation to high-light at a longer time delay ($\cong$ 40 ps). Data are presented as the mean$\pm$SE (n=5). The dashed line represents a b-spline interpolation among the experimental data points.

To determine the origin of the signal in Figure 4.1(c), we calculated the difference TA signal in the wavelength range 480 - 620 nm. Figure 4.2 shows the difference TA spectra reconstructed from data of light- and dark-acclimated samples measured at a 1 ps time delay. At each wavelength, the dark-acclimated data were scaled to match the high-light-acclimated data at a 40 ps time delay. The difference spectrum shows a distinct peak centered at 540 nm. The shape of the peak strongly resembles the S_1-S_N absorption spectrum of Zea in methanol from Polívka *et al.*, which features an asymmetric peak centered at 555 nm.[21,29] The peak in Figure 4.2 is slightly blue-shifted (~ 15 nm) from the spectra reported previously[21,29], likely due to differences in solvent vs. protein environments. A similar magnitude of blue-shift in the spinach thylakoid membrane environment has also been observed in previous studies.[16,19] Considering its lifetime (~ 8 ps) and spectrum, it seems likely that the observed ESA signal is from a Car S_1-S_N transition, and the Car is presumably Zea.

Considering that the Chl fluorescence lifetime of thylakoid membrane is in the range of 0.35 ~ 1.47 ns (Figure 4.5(a)), it is probable that exciton annihilation is the dominant factor in determining the rate of Chl* de-excitation and excitation diffusion length, which results in a shortened Chl ESA signal lifetime ($\tau_{average}$ < 0.1 ns). The signal decay difference between dark-acclimated and high-light-acclimated samples was negligible at 620 nm where Chl ESA signal dominates (Figure 4.7). If the light-acclimation process were to cause variations in Chl excitation energy dynamics beyond turning on quenching mechanisms (e.g. Chl*-Chl* annihilation), a significant change should appear at 620 nm. Therefore, it is reasonable to assume that Chl*-Chl* annihilation is consistent during the transition from a dark-acclimated state to a light-acclimated state.

Before continuing the analyses, we note that the relative timescales of excitation transport and/or trapping in the photosystem II antenna system would suggest that observing states with lifetimes as short as 8 ps would be very difficult, if not impossible, due to the extremely low steady state concentration of the short-lived species if the formation time is several hundred picoseconds. However, the presence of Chl*-Chl* annihilation in the TA measurement restricts the diffusion length of excitations in the antenna and enables the direct observation of short-lived intermediates. Valkunas and coworkers estimated an annihilation rate of $(16\ ps)^{-1}$ per LHCII trimer for extended aggregates.[30] If we assume that the annihilation in thylakoid membrane occurs on a much faster timescale than the exciton migration time through LHCII to an immobilized trap, excition-excition annihilation is the dominant process involved in the reduction of the excitation diffusion length. A key observation in our data is the lack of an observable rise time in the excited signal at 540 nm, in contrast to our data at 1000 nm.[12,15] Below we show that this difference arises from the differing lifetimes of the two quenching species.

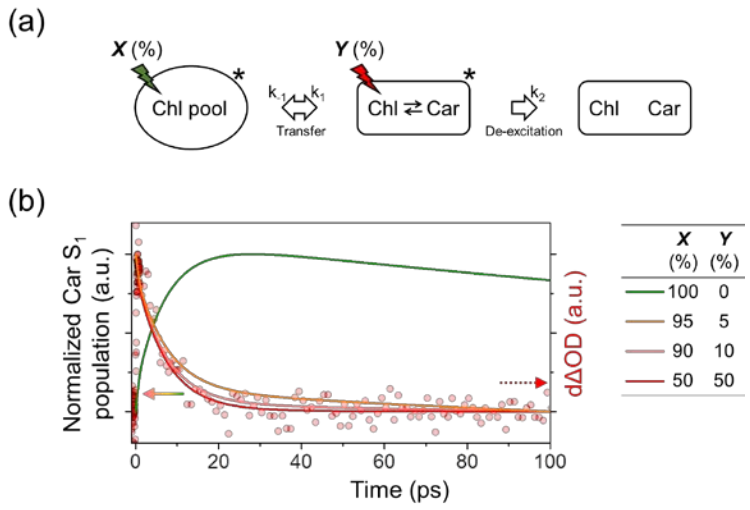

Figure 4.3: (a) Kinetic scheme for the EET quenching mechanism in light-acclimated thylakoid membranes, showing instantaneous excitation equilibrium via bidirectional Chl↔Car energy transfer at quenching sites. Relative percentages of Chl excitations between Chl pool and a Chl adjacent to Car are denoted as *X* and *Y*, respectively. The rate constants k_1 and k_{-1} were assumed to be $(350\ ps)^{-1}$ based on our bulk Chl fluorescence lifetime in the quenched state (Figure 4.5(a)). k_2 is $(8\ ps)^{-1}$ based on the lifetime of the Zea S_1 state.[16,20,21] (b) Dynamics of the Car S_1 state population calculated with various initial excitation populations at the bulk Chl pool vs. Chl close to Car. The solid curves represent the simulated dynamics. The difference TA kinetic data points (red dots) from Figure 4.1(c) are also displayed.

The dynamics of the Car S_1 state population were investigated using a linear chain model in which the instantaneous excitation equilibrium between a subset of Chl and Car was assumed (Figure 4.3(a)). In light-acclimated grana membranes, an excitation in the bulk Chl pool takes the 2.5×10^9 ~ $3\times10^9\ s^{-1}$ of rate constant to transfer to a quenching site of Chl-Car,[24] which is much slower than relaxation of the Car S_1 state ($k_2 \cong 1.125 \times 10^{11}\ s^{-1}$). In vivo, this would mean that there is no significant buildup of S_1 excited Car molecules, as they relax to ground state much faster than they are populated. However, in our TA measurements, the intense pump laser (20 nJ/pulse) produces significant Chl*-Chl* annihilation and significantly decreases the lifetime of the excited Chl pool, resulting in smaller excitation diffusion lengths and a lower probability of an excitation finding an EET quenching site. Therefore, only Chl that are excited very close to Car molecules will populate the Car S_1 state we observe. To model how these two different scenarios influence the Car S_1 population after Chl excitation, we divided the total Chl population into two groups. The ***Y*** group contains Chl molecules that are close enough to a Car molecule in a configuration consistent with downhill energy transfer such that EET would be very rapid, while the ***X*** group contains all other Chl molecules that are far enough away from a Car molecule in a quenching configuration that EET would be significantly slower. By varying the initial populations of the ***X*** and ***Y*** groups that are excited, which are depicted as the relative percentages of Chl excitations shown in Figure 4.3(b), we can observe the changes in the dynamics of the excited Car S_1 state. Increasing the proportion of Chl excited near a Car (***Y***) to

just 10% of the excited population in the bulk Chl pool (***X*** group) removes the rise component and results in a decay profile of the Car S_1 population that is well overlapped with the experimentally-observed difference decay profile (Figure 4.3(b)). The absence of a rise component in the Car S_1 kinetic profile differs from the previously observed $Car^{\bullet+}$ kinetic profiles, which are fitted with rise and decay components.[12–14] The difference can be attributed to the fact that a slower de-excitation rate ($\leq 2.5 \times 10^{10}$ s^{-1}) of the CT state allows for the observation of an increase in the excitation population after Chl excitation (Figure 4.8).

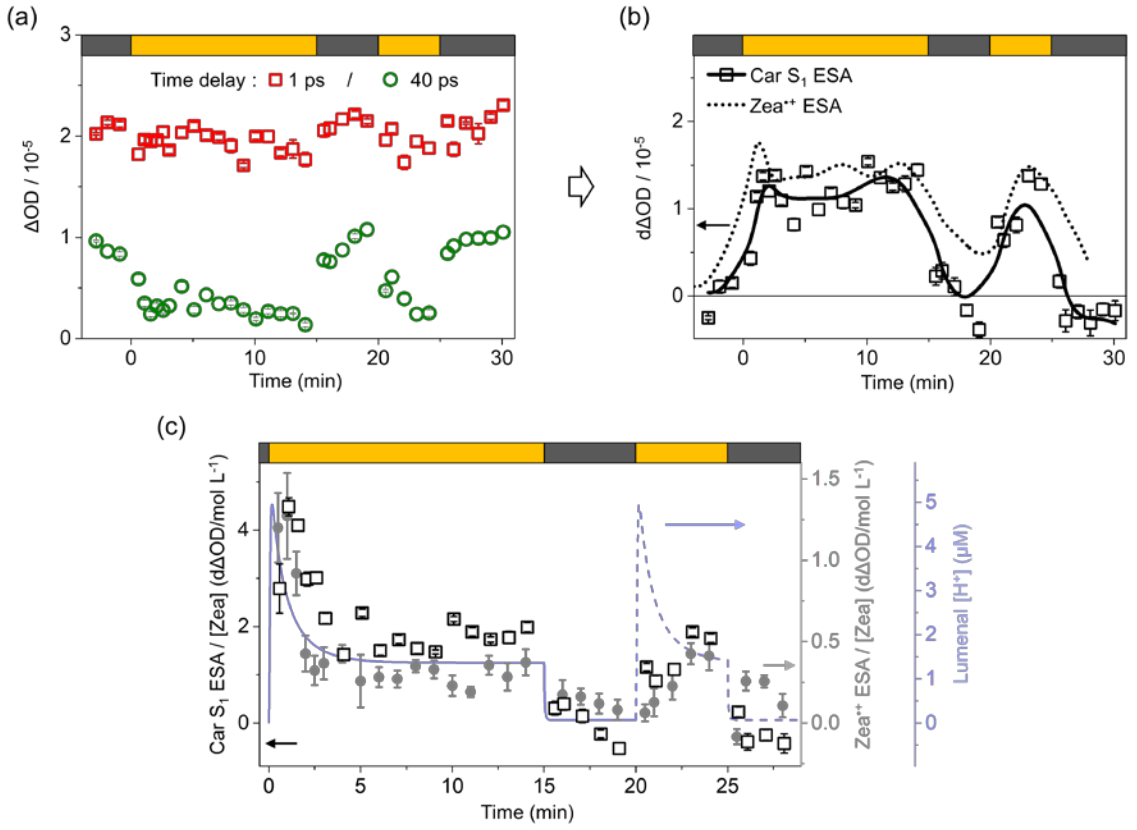

Figure 4.4: (a) Snapshot TA data obtained 1 ps (red, squares) and 40 ps (green, circles) after Chl excitation. (b) Difference (high-light-acclimated minus dark-acclimated) snapshot TA data at 1 ps (black, squares) with the zero line representing the average signal during the initial dark period. See Equation (1) in the text for the calculation of the difference snapshot TA data (dΔOD). The solid black line is a smoothed line from the data points corresponding to Car S_1 ESA. The smoothed line of $Zea^{\bullet+}$ absorption (dotted line) from light-acclimating spinach thylakoids is also displayed.[15] (c) Evolution of Zea S_1 ESA/[Zea] (black squares), $Zea^{\bullet+}$ ESA/[Zea] (gray circles), and lumenal $[H^+]$ (blue line) in response to high-light/dark exposures. [Zea] was determined by time-resolved HPLC measurements.[15] All data are presented as the mean±SE (n=5). The calculated lumenal $[H^+]$ (blue line) is based on the kinetic model described by Zaks *et al*.[5,26] Note that there is considerable uncertainty in the lumenal $[H^+]$ during the second high-light-acclimation period as the model was devised for completely dark-acclimated systems. Bars

at the top of the figures indicate the time sequence of actinic light on (yellow) and off (dark gray).

Using the previously described method for extracting the Car S_1 ESA signal from Chl ESA at 540 nm, we performed snapshot TA measurements at two different time delays after the excitation pulse. The Car S_1 ESA signal has a decay constant of less than 10 ps, while the Chl ESA signal decays on a much longer timescale.[16] Therefore, the TA signal was measured at 40 ps to account for the overall decrease in Chl ESA as thylakoids acclimated to high-light. The Car S_1 ESA signal has completely disappeared by this time delay (Figure 4.1(c)). Therefore, to measure Car S_1 ESA at 540 nm, the signal is measured at a delay time of 1 ps, then scaled using the 40 ps signal to account for the underlying decrease in Chl a ESA signal:

$$\boldsymbol{d\Delta OD_{Car\,S_1}(t)} = \Delta OD_{at\ 1\ ps}(t) - \Delta OD_{at\ 1\ ps}(dark) \times \left(\frac{\Delta OD_{at\ 40\ ps}(t)}{\Delta OD_{at\ 40\ ps}(dark)}\right) \quad (1)$$

where $\Delta OD_{at\ 1\ ps}(t)$ and $\Delta OD_{at\ 40\ ps}(t)$ represent the snapshot TA signal measured at time delays of 1 ps and 40 ps, respectively. $\Delta OD\ (dark)$ is the average of TA signals measured during the initial dark period.

Figure 4.4(a) shows individual snapshot TA results measured at 1 ps and 40 ps during a time sequence of the actinic light turning on and off. Each data point in the 1 ps trace is then scaled using the data point of the corresponding light acclimation time in the 40 ps trace, which gives the result shown in Figure 4.4(b), overlaid with data from the $Zea^{\bullet+}$ snapshot TA data of Park *et al.*.[15] Much like the $Zea^{\bullet+}$ signal, the Car S_1 ESA signal appears very rapidly (< 3 min) after the actinic light is turned on, well within the timescale of the qE response. Considering the fact that Zea accumulates exponentially with a rise time of 2~3 min,[15] it seems surprising that the amount of Zea S_1 ESA signal indicative of Chl-Zea EET quenching is substantial in the early stages ($\leq$ 3 min) of qE. This difference in timescale may result from ΔpH or ΔpH-triggered mechanisms,[26] such as a structural change in light-harvesting complex (LHC) proteins, which potentially enhance the appearance of the Car S_1 ESA signal in early qE. If this is so, during the first few minutes of light-acclimation, the amount of EET quenching is not significantly limited by the concentration of Zea. In this context we note that in the coarse grained model of qE in the grana membrane developed by Bennett *et al*,[31] wild-type levels of qE can be achieved with only 12-15% of potential LHCII quenching sites active as quenchers. Noticeably, both Car S_1 and $Zea^{\bullet+}$ ESA signals are well-correlated with ΔpH calculated from the model developed by Zaks et al. at early qE (Figure 4.4(c)), suggesting the important role of ΔpH or ΔpH-triggered mechanisms.

After the initial rapid response, the Car S_1 ESA signal appears to drop, then increases more slowly. This Car S_1 ESA could be indicative of both rapidly-activated and slowly-activated mechanisms. Two quenching timescales have been previously observed by Dall'Osto *et al.* in *Arabidposis thaliana* plants lacking minor-complexes.[32] Interestingly, the Car S_1 ESA signal

disappears very rapidly ($\leq$ 1 min) after turning the actinic light off. This is much faster than the $Zea^{\bullet+}$ signal, which is indicative of the CT quenching mechanism, and does not fully disappear even after the actinic light has been turned off for 5 min.[15] The rapid disappearance of Car S_1 ESA signal in response to dark acclimation indicates that the EET quenching mechanism plays a central role in rapidly reversible qE quenching, which is known to improve plant fitness under fluctuating light conditions.[33,34] It is conceivable that the CT and EET mechanisms involve different protein/carotenoid conformations with one able to relax more quickly than the other.[35]

As discussed above, the observed Car S_1 ESA signal suggests an electronic coupling between Chl Q_y and Car S_1 states, which would be required for the EET quenching mechanism. Under *in vivo* conditions, under this mechanism, the Chl excited state lifetime could significantly decrease as coupled Chl-Car molecules form in grana membranes during light-acclimation.[10,28] In order to compare the Car S_1 ESA data with data on the overall Chl fluorescence quenching, changes in the Chl fluorescence lifetime of same thylakoid samples used in snapshot TA were monitored during light-acclimation using fluorescence lifetime snapshot spectroscopy.[36–38] Examining the Chl fluorescence decay and corresponding lifetime value ($\tau_{average}$) at each time point allows for the assessment of Chl* quenching independent of Chl concentration, Chl*-Chl* annihilation, or photobleaching. Figure 4.5(a) and (b) present $\tau_{average}$ and calculated NPQ parameters (NPQτ), respectively. NPQτ values are comparable to the conventional NPQ parameter (see Experimental Methods).[15,37] Notably, the appearance time of the Car S_1 ESA presented in Figure 4.4(b) coincides with the Chl* quenching indicated by NPQτ (Figure 4.4(b)).

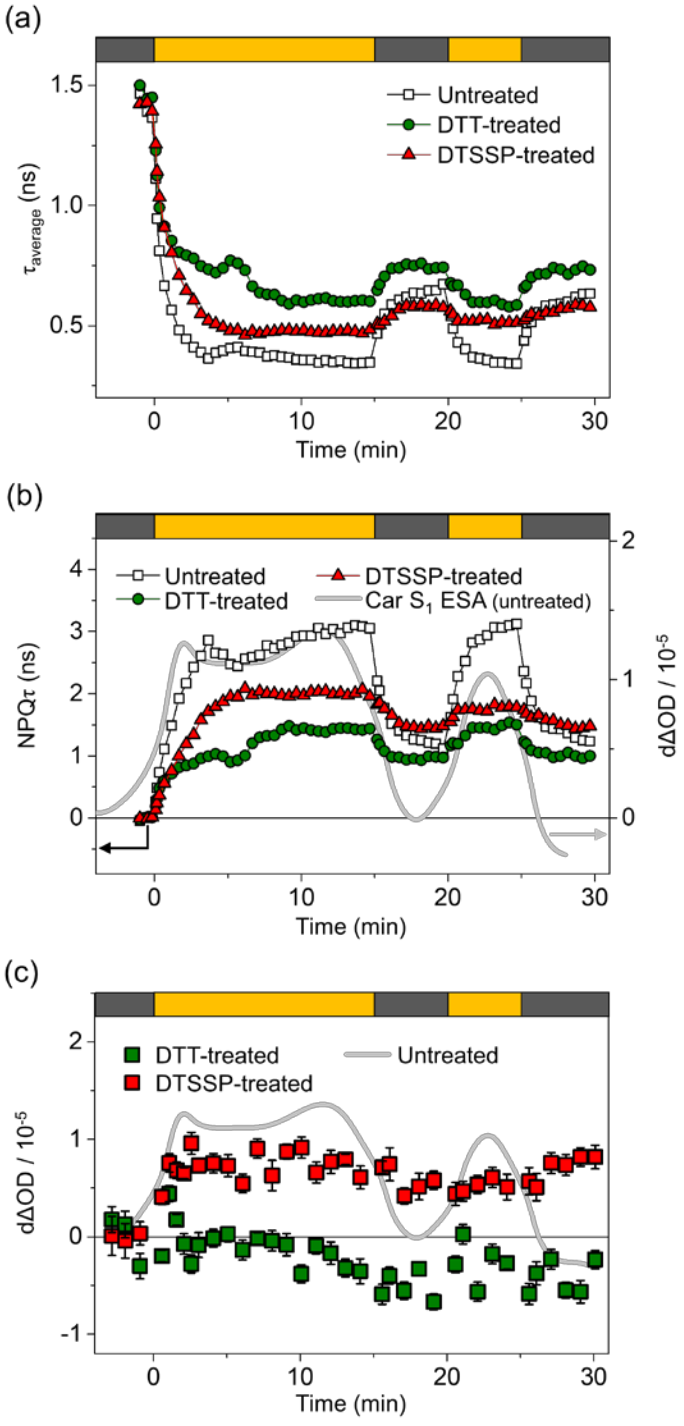

Figure 4.5: Fluorescence lifetime snapshot results presented as (a) average chlorophyll fluorescence lifetimes ($\tau_{average}$) and (b) calculated NPQτ values of untreated (square), DTT (circle)- and DTSSP (triangle)-treated thylakoids in response to high-light/dark exposure. See Experimental Methods for further discussion of $\tau_{average}$ and NPQτ values. (c) Difference (high-light-acclimated minus dark-acclimated) TA snapshot results of DTSSP (red)- and DTT (green)-

treated thylakoid membranes at 540 nm and 1 ps delay time. (b, c) The signal of the untreated sample shown in Figure 4.4(b) is displayed as a smoothed trajectory (gray curve). The zero line represents the averaged initial dark-adapted signal. See Equation (1) in the text for the calculation of the difference snapshot TA data (dΔOD). Data are presented as the mean $\pm$ SE (n=5). Bars at the top of the figures indicate the time sequence of the actinic light on (yellow) and off (dark grey).

Violaxanthin de-epoxidase (VDE) is a membrane-bound protein responsible for the accumulation of Zea, by de-epoxidizing violaxanthin in response to lumen acidification.[7,8] To examine Car S_1 ESA in thylakoids without accumulated Zea, samples were treated with 1,4-dithiothreitol (DTT) to inhibit VDE activity.[39,40] The DTT-treated thylakoid showed a substantially lowered NPQτ value compared to the untreated sample (Figure 4.5(b)). As shown in Figure 4.5(c), the snapshot TA data of the DTT-treated thylakoid showed the sharp spike in Car S_1 ESA signal in the first 2 min of light-acclimation. However, after the spike, there was no signal higher than that of the initial dark-acclimated state, suggesting that Zea accumulation is necessary to sustain the Chl-Car EET quenching process. This observation, together with its lifetime of ~ 8 ps, strongly suggests that the Zea S_1 state is directly involved in EET quenching of excited Chl. Nonetheless, we cannot completely rule out the possibility that accumulated Zea indirectly facilitates Lut S_1-mediated EET quenching and that both Zea S_1 and Lut S_1 states are involved in such quenching.[24] Slightly negative signals were observed with DTT after 10 min of light-acclimation. We speculate that the process of light-acclimation under the condition that few quenchers are available can slightly alter Chl ESA dynamics or Chl*-Chl* annihilation (Figure 4.9) which likely originates from a structural difference in dark- and light-acclimated grana membranes and/or the early onset of other quenching processes (e.g. phosphorylation and state transition[41]). The DTT treatment may alters the way the membrane responds to high-light and returns to low-light.

The cross-linking assay using 3,3'-dithiobis(sulfosuccinimidyl propionate) (DTSSP), likely stops the interactions of PsbS, resulting in behavior similar to the *npq4 Arabidposis thaliana* mutant.[15,25,42] As reported previously, DTSSP-treated and *npq4* thylakoids do not show any $Zea^{\bullet+}$ TA signal, consistent with the idea that the interactions of active PsbS are essential for $Zea^{\bullet+}$ formation that is indicative of CT quenching.[12,15] Interestingly, DTSSP-treated thylakoids showed a 50% lower amount of Car S_1 ESA signal compared to the untreated sample (Figure 4.5(c)). In addition, the signal was largely unchanged, even during subsequent changes in actinic light intensity. This result suggests that activated PsbS is not essential for EET quenching induction, but its presence allows for a greater amount of EET quenching and improves the reversibility.[37,43]

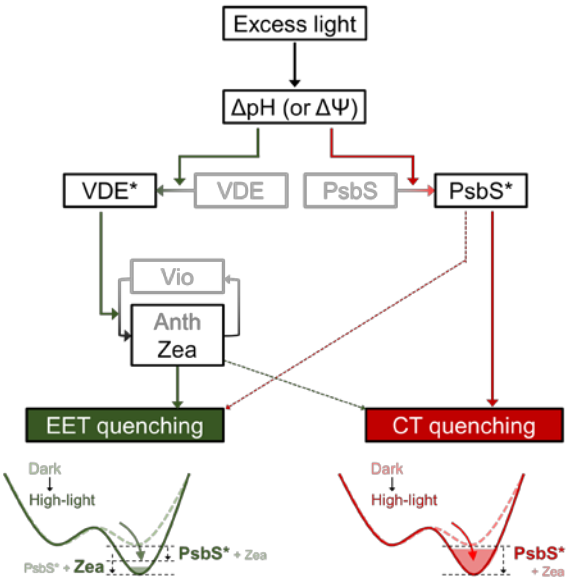

Figure 4.6: Proposed scheme for the triggering system of the EET and CT quenching mechanisms for qE. Regarding the involvement of PsbS and Zea, essential steps are denoted as solid arrows, and non-essential but influential steps are denoted as dashed arrows. VDE* and PsbS* represent activated proteins by ΔpH and protonation.

The activation of both Car S_1 (EET mechanism) and $Zea^{\bullet+}$ (CT mechanism) ESA signals within spinach thylakoids fundamentally require the accumulation of Zea and the interactions of activated PsbS, respectively. Zea accumulation is necessary for maximum $Zea^{\bullet+}$ signal, and activated PsbS is necessary for maximum Car S_1 ESA signal. This observation suggests that both EET and CT quenching mechanisms rely on Zea and PsbS, although to differing extents as evidenced by their different response to chemical treatments (Figure 4.5(c)). For example, the $Zea^{\bullet+}$ ESA signal, which responds more to pH-sensing PsbS, exhibits a faster response ($\leq$ 30 sec) to high-light exposure.[15] Meanwhile, the Car S_1 ESA signal has a relatively slow activation time ($\leq$ 1 min) due to a weaker dependence on PsbS, and then a slower activation mechanism follows with a time constant of ~5 min (Figure 4.9).

The biphasic activation of EET quenching possibly indicates its dependence on two different triggering pathways which are activated on different timescales. In this scenario, the fast pathway seems to be mainly directed by activated PsbS in response to ΔpH. The activation of this pathway is not significantly limited by the concentration of Zea, which is supported by the snapshot result of DTT-treated samples showing the positive Car S_1 ESA signal during early light-acclimation ($\leq$ 2 min) (Figure 4.5(c)). On the contrary, the slower pathway seems to be primarily dependent on the accumulation of Zea. Although active PsbS or membrane reorganization would be less influential factors in the activation of this pathway, PsbS likely plays an important role in dark recovery, as shown in Figure 4.5(c). Overall, we speculate that the operation of these two triggering pathways enables the fast establishment and sustained operation of the EET quenching mechanism, emphasizing its importance in qE (Figure 4.6).

Recently, Croce and co-workers reported that intense Chl*-Chl* annihilation and a higher excited state of Chl a within LHCII produced a (Chl a-Lut)* byproduct (referred to as ***Q***) which has a ESA peak at around 535 nm.[44] We closely examined the reported ***Q*** ESA and compared it to our Car S_1 ESA data in case the light-acclimation process significantly increases the extent of Chl*-Chl* annihilation, which would seem unlikely. The Car S_1 ESA signals observed in this study have decay time constants of ~ 8 ps, and almost disappear by 20 ps after Chl excitation (650 nm). These Car S_1 ESA kinetics remained unchanged when measured under various pump intensities. In contrast, the majority of the ***Q*** ESA signal remains after 20 ps as the species appears to be relatively long-lived. According to the species-associated difference spectrum of ***Q***, the measured ***Q*** state is populated with a time constant of several picoseconds. However, the rise time component of Car S_1 ESA signal was not resolvable with the time resolution (≅120 fs) of our TA setup. Consequently, the kinetics of the Car S_1 ESA signals are quite distinct from that of ***Q*** and exhibit a faster decay time constant equivalent to the values obtained in annihilation-free conditions in dilute solution.[20–22]

The signals in both this work and our previous study of CT quenching are observable because of the restricted diffusion length of excitation through moderate excitation annihilation. It is important to ask, then, if the intrinsic rate of CT or EET quenching is accurately obtained from the data reported here and in previous literature.[12,13,15,16,19,45] As the simple model calculation in Figure 4.3 shows, for quite small (~ 10%) and either direct or very rapid (≲ 120 fs) population of the quencher state, within our experimental error, the same decay time (≅ 8 ps) is observed for Zea S_1 as is observed in annihilation-free condition.[20–22] The CT ($Chl^{\bullet-}$-$Zea^{\bullet+}$) states in thylakoid membranes have been observed to have longer decay times (40 ~ 150 ps)[12,15] which could be influenced by Chl-Zea separation and the surrounding protein environment. We therefore consider that the time scales of the decay of the two trap states are the ones that should be used in quantitative models of qE such as that of Bennett et al.[31]

Methods

Isolation of thylakoid membrane. Fresh spinach leaves were purchased the day before the measurements and dark-acclimated at 4 °C overnight. Isolation of crude thylakoids membranes was performed in dark cold room (4 °C), following the protocol reported by Gilmore *et al*.[46] The final concentrations of all thylakoid samples were adjusted to 100 µg Chl/ml using reaction buffer before measurement. The reaction buffer contained 30 mM ascorbic acid, 0.5 mM ATP, and 50 µM methyl viologen. The working concentrations of DTSSP and DTT were 3 mM and 2 mM, respectively.

Pump-probe spectroscopy for transient absorption measurements. A description of the pump-probe transient absorption spectroscopy setup used in this study can be found in previous literature.[12–15] Briefly, the experiments were performed using a Ti:sapphire

regenerative amplifier (Coherent, RegA 9050) seeded by a Ti:sapphire oscillator (Coherent, MIRA Seed), generating an 800 nm pulse with a repetition rate of 250 kHz. The beam was split to generate the pump and probe beams. For the probe, the beam was focused on a 1 mm sapphire crystal to produce a visible continuum, and a 700 nm short pass filter was placed after continuum generation. For the pump, another beam pumped an optical parametric amplifier (Coherent, OPA 9450). The OPA was tuned to generate 20 nJ/pulse centered at 650 nm for the Chl b Q_y transition which yielded higher signal-to-noise ratio than 680 nm. The FWHM of pump pulses was 50 fs. The pump and probe were overlapped at the sample at the magic-angle (54.7°) polarization. The diameters of the pump and probe at the sample position were 150 µm and 65 µm, respectively. The cross-correlation time between the pump pulse and probe pulse was found to be ~ 120 fs. After the sample, a second polarization filter set to the probe polarization and a 658±26 nm notch filter were placed to minimize pump scattering and ensure a clean probe signal. After passing through a monochromator (Acton Research Corp., SpectraPro 300i), the signal was detected by a Si biased photodiode (Thorlabs, DET10A) which was connected to a lock-in amplifier (Stanford Research, SR830). The lock-in amplifier was synchronized with a chopper positioned in the pump beam path. An actinic light with a heat absorbing filter (KG1) was set to an intensity of 850 µmol photons·m^{-2}·s^{-1} at the sample position. For collecting snapshot TA data at fixed time delays (1 and 40 ps) and a wavelength (540 nm), a pump and probe shutter was controlled to open for 10 seconds at intervals ranging from 30 seconds to 1 minute throughout the light-acclimation sequence. The sample cell was translocated continuously to prevent sample damage. The path length of the cuvette was 1 mm.

Fluorescence lifetime snapshot. Fluorescence decay snapshots were recorded by a home-built time-correlated single photon counting (TCSPC) apparatus described previously.[36–38] First, 840 nm output pulses generated by Ti:sapphire oscillator (Coherent, Mira 900f, 76 MHz) were frequency-doubled using a beta barium borate (BBO) crystal. The resultant 420 nm pulses correspond to the Soret band region of Chl a. Before the sample, the beam was split by a beam splitter, so that a portion was directed to a photodiode providing SYNC for the TCSPC card (Becker-Hickl, SPC-630 and SPC-850). The remainder of beam was sent to excite sample and was intermittently blocked by a shutter controlled by a LabVIEW program. The excitation laser power was set to 1.6 mW (≅ 1650 µmol photons·m^{-2}·s^{-1}) at the sample, which is enough to close reaction centers.[47] The sample was intermittently exposed to an actinic light (Schott, KL1500) with an intensity of 850 µmol photons·m^{-2}·s^{-1}, also controlled by a shutter and LabVIEW program. After the sample, a monochromator set to 680 nm and a MCP PMT detector (Hamamatsu, R3809U) were placed for fluorescence detection. The fluorescence decay curves were measured at intervals varying from every 10 seconds to every 30 seconds. In each measurement, the sample was exposed to the laser for one second, divided up into five steps of 0.2 seconds. The step with the longest fluorescence lifetime was selected in data processing to ensure that the PSII reaction centers were closed.[38] Each fluorescence decay curve was fit to a sum of three exponential decay components (Picoquant, Fluofit Pro-4.6). Following data fitting, the amplitude-weighted average lifetime ($\tau_{average}$) and NPQ_τ values were calculated using the following equations:[15,37,38]

$$\tau_{avg} = \frac{\sum_i A_i \tau_i}{\sum_i A_i} \qquad (2)$$

where A_i and τ_i are the amplitudes and the fluorescence lifetime components, respectively.

$$NPQ_{\tau} = \frac{\tau_{avg,dark} - \tau_{avg,light}}{\tau_{avg,light}} \qquad (3)$$

where $\tau_{avg,dark}$ is the average of three lifetimes measured at initial dark period.

Acknowledgements

We thank Dr. Doran I. G. Bennett, Dr. Liang Guo, and Dr. Myeongkee Park for helpful discussions. This work was supported by US Department of Energy, Office of Science, Basic Energy Sciences, Chemical Sciences, Geosciences, and Biosciences Division under Field Work Proposal 449B. K.K.N. is an investigator of the Howard Hughes Medical Institute.

Supporting Information

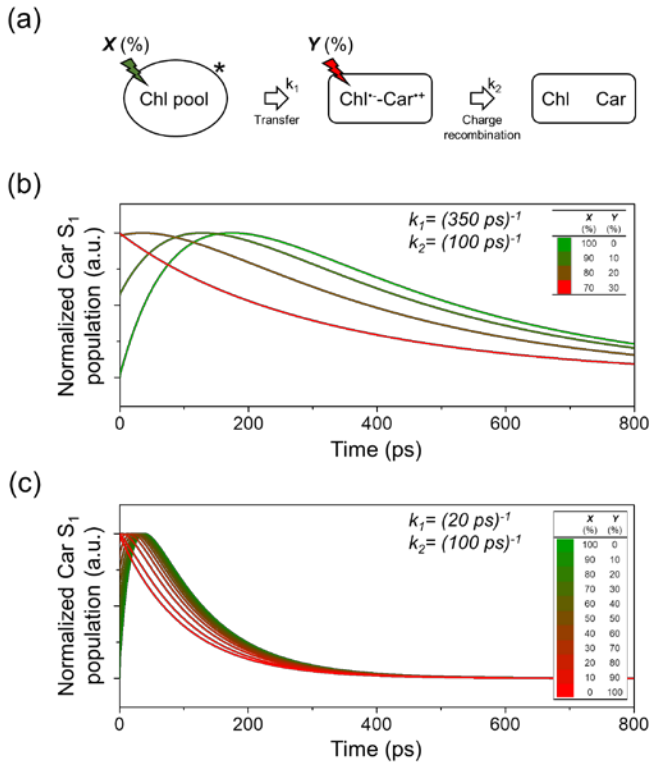

Figure 4.7. (a) Kinetic scheme for the CT quenching mechanism in light-acclimated thylakoid membranes, showing a slower de-excitation (charge recombination) rate ($k_2 \cong 10^{10}$ s^{-1}) at quenching sites. Relative percentages of Chl excitations between Chl pool and a Chl adjacent to Car are denoted as ***X*** and ***Y***, respectively. (b, c) Dynamics of the charge-transfer (CT) state population calculated with various initial excitation populations at the bulk Chl pool vs. Chl close to Car. The rate constant k_1 can vary as the PSII antenna structure changes during light-acclimation. (b) The k_1 was assumed to be $(350\ ps)^{-1}$ based on our bulk Chl fluorescence lifetime in quenched state (Figure 4.5(a)). (c) The k_1 was assumed to be $(20\ ps)^{-1}$ based on previous literature.[48] In both cases, due to the slower charge recombination (k_2), the rise components exist in the simulated dynamics even significant initial population (~ 20% and ~ 80% for (b) and (c), respectively) is placed on the ***Y*** group (a).

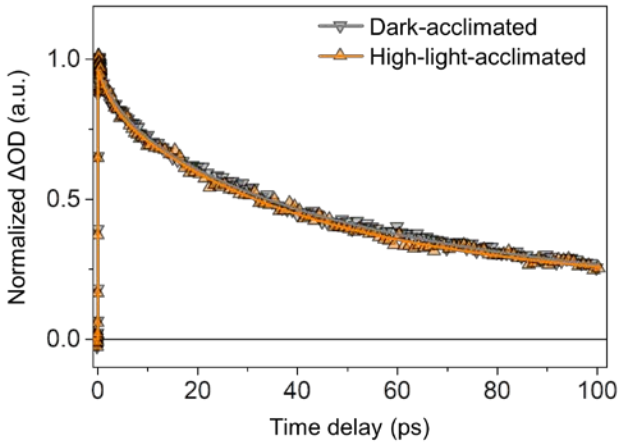

Figure 4.8. Transient absorption kinetics of spinach thylakoid membranes under dark-acclimated (gray, down triangle) and high-light-acclimated (orange, up triangle) conditions. Samples were excited and probed at 650 nm and 620 nm, respectively.

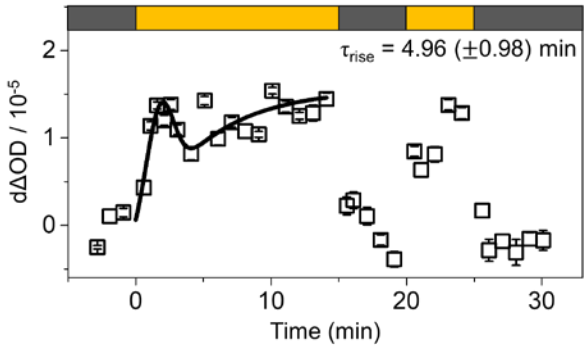

Figure 4.9. Snapshot TA data of untreated thylakoid samples with curve fit in the first high-light-acclimation period. Curve fittings use a combined single exponential rise and Gaussian peak function. The Gaussian peak function with a center at 1.9 min was included to account for the sharp rise and fall of the data which is likely a result of the sharp spike in ΔpH. The time constants of the single exponential rise component are denoted.

References

(1) Krause, G. H.; Weis, E. Chlorophyll Fluorescence as a Tool in Plant Physiology. II. Interpretation of Fluorescence Signals. *Photosynth. Res.* **1984**, *5* (2), 139–157.

(2) Tripathy, B. C. hara.; Oelmüller, R. Reactive Oxygen Species Generation and Signaling in Plants. *Plant Signal. Behav.* **2012**, *7* (12), 1621–1633.

(3) Muller, P. Non-Photochemical Quenching. A Response to Excess Light Energy. *Plant Physiol.* **2001**, *125* (4), 1558–1566.

(4) Müller, P.; Li, X.-P.; Niyogi, K. K. Non-Photochemical Quenching. A Response to Excess Light Energy 1. *Plant Physiol.* **2001**, *125*, 1558–1566.

(5) Zaks, J.; Amarnath, K.; Sylak-Glassman, E. J.; Fleming, G. R. Models and Measurements of Energy-Dependent Quenching. *Photosynth. Res.* **2013**, *116* (2–3), 389–409.

(6) Jahns, P.; Holzwarth, A. R. The Role of the Xanthophyll Cycle and of Lutein in Photoprotection of Photosystem II. *Biochim. Biophys. Acta* **2012**, *1817* (1), 182–193.

(7) Demmig-Adams, B. Carotenoids and Photoprotection in Plants: A Role for the Xanthophyll Zeaxanthin. *Biochim. Biophys. Acta* **1990**, *1020* (1), 1–24.

(8) Niyogi, K. K.; Grossman, A. R.; Björkman, O. Arabidopsis Mutants Define a Central Role for the Xanthophyll Cycle in the Regulation of Photosynthetic Energy Conversion. *Plant Cell* **1998**, *10* (7), 1121–1134.

(9) Young, A. J.; Frank, H. A. Energy Transfer Reactions Involving Carotenoids: Quenching of Chlorophyll Fluorescence. *J. Photochem. Photobiol. B Biol.* **1996**, *36* (1), 3–15.

(10) van Amerongen, H.; van Grondelle, R. Understanding the Energy Transfer Function of LHCII, the Major Light-Harvesting Complex of Green Plants. *J. Phys. Chem. B* **2001**, *105* (3), 604–617.

(11) Kloz, M.; Pillai, S.; Kodis, G.; Gust, D.; Moore, T. A.; Moore, A. L.; Van Grondelle, R.; Kennis, J. T. M. Carotenoid Photoprotection in Artificial Photosynthetic Antennas. *J. Am. Chem. Soc.* **2011**, *133* (18), 7007–7015.

(12) Holt, N. E.; Zigmantas, D.; Valkunas, L.; Li, X. P.; Niyogi, K. K.; Fleming, G. R. Carotenoid Cation Formation and the Regulation of Photosynthetic Light Harvesting. *Science (80-.).* **2005**, *307* (5708), 433–436.

(13) Avenson, T. J.; Ahn, T. K.; Zigmantas, D.; Niyogi, K. K.; Li, Z.; Ballottari, M.; Bassi, R.; Fleming, G. R. Zeaxanthin Radical Cation Formation in Minor Light-Harvesting Complexes of Higher Plant Antenna *. **2008**, *283* (6), 3550–3558.

(14) U nal, E.; Heidinger-Pauli, J. M.; Kim, W.; Guacci, V.; Onn, I.; Gygi, S. P.; Koshland, D. E. A Molecular Determinant for the Establishment of Sister Chromatid Cohesion. *Science (80-.).* **2008**, *321* (5888), 566–569.

(15) Park, S.; Fischer, A. L.; Li, Z.; Bassi, R.; Niyogi, K. K.; Fleming, G. R. Snapshot Transient Absorption Spectroscopy of Carotenoid Radical Cations in High-Light-Acclimating

Thylakoid Membranes. *J. Phys. Chem. Lett.* **2017**, *8* (22), 5548–5554.

(16) Ma, Y.-Z.; Holt, N. E.; Li, X.-P.; Niyogi, K. K.; Fleming, G. R. Evidence for Direct Carotenoid Involvement in the Regulation of Photosynthetic Light Harvesting. *Proc. Natl. Acad. Sci.* **2003**, *100* (8), 4377–4382.

(17) Bode, S.; Quentmeier, C. C.; Liao, P.-N.; Hafi, N.; Barros, T.; Wilk, L.; Bittner, F.; Walla, P. J. On the Regulation of Photosynthesis by Excitonic Interactions between Carotenoids and Chlorophylls. *Proc. Natl. Acad. Sci.* **2009**, *106* (30), 12311–12316.

(18) Holleboom, C.-P.; Walla, P. J. The Back and Forth of Energy Transfer between Carotenoids and Chlorophylls and Its Role in the Regulation of Light Harvesting. *Photosynth. Res.* **2014**, *119* (1–2), 215–221.

(19) Liao, P. N.; Holleboom, C. P.; Wilk, L.; Kühlbrandt, W.; Walla, P. J. Correlation of Car S1 Chl with Chl F Car S1 Energy Transfer Supports the Excitonic Model in Quenched Light Harvesting Complex II. *J. Phys. Chem. B* **2010**, *114* (47), 15650–15655.

(20) Billsten, H. H.; Pan, J.; Sinha, S.; Pascher, T.; Sundström, V.; Polívka, T. Excited-State Processes in the Carotenoid Zeaxanthin after Excess Energy Excitation. *J. Phys. Chem. A* **2005**, *109* (31), 6852–6859.

(21) Polívka, T.; Sundström, V. Ultrafast Dynamics of Carotenoid Excited States−From Solution to Natural and Artificial Systems. *Chem. Rev.* **2003**, *104*, 2021–2071.

(22) Polívka, T.; Herek, J. L.; Zigmantas, D.; Åkerlund, H.-E.; Sundström, V. Direct Observation of the (Forbidden) S1 State in Carotenoids. *Proc. Natl. Acad. Sci.* **1999**, *96* (9), 4914–4917.

(23) Li, Z.; Ahn, T. K.; Avenson, T. J.; Ballottari, M.; Cruz, J. A.; Kramer, D. M.; Bassi, R.; Fleming, G. R.; Keasling, J. D.; Niyogi, K. K. Lutein Accumulation in the Absence of Zeaxanthin Restores Nonphotochemical Quenching in the Arabidopsis Thaliana npq1 Mutant. *Plant Cell Online* **2009**, *21* (6), 1798–1812.

(24) Ruban, A. V.; Berera, R.; Ilioaia, C.; Van Stokkum, I. H. M.; Kennis, J. T. M.; Pascal, A. A.; Van Amerongen, H.; Robert, B.; Horton, P.; Van Grondelle, R. Identification of a Mechanism of Photoprotective Energy Dissipation in Higher Plants. *Nature* **2007**, *450* (7169), 575–578.

(25) Correa-Galvis, V.; Poschmann, G.; Melzer, M.; Stühler, K.; Jahns, P. PsbS Interactions Involved in the Activation of Energy Dissipation in Arabidopsis. *Nat. Plants* **2016**, *2* (2), 15225.

(26) Zaks, J.; Amarnath, K.; Kramer, D. M.; Niyogi, K. K.; Fleming, G. R. A Kinetic Model of Rapidly Reversible Nonphotochemical Quenching. *Proc. Natl. Acad. Sci.* **2012**, *109* (39), 15757–15762.

(27) Walla, P. J.; Linden, P. A.; Ohta, K.; Fleming, G. R. Excited-State Kinetics of the Carotenoid S1 State in LHC II and Two-Photon Excitation Spectra of Lutein and β-Carotene in Solution: Efficient Car S1→Chl Electronic Energy Transfer via Hot S1 States? *J. Phys. Chem. A* **2002**, *106* (10), 1909–1916.

(28) Gradinaru, C. C.; van Stokkum, I. H. M.; Pascal, A. A.; van Grondelle, R.; van Amerongen, H.

Identifying the Pathways of Energy Transfer between Carotenoids and Chlorophylls in LHCII and CP29. A Multicolor, Femtosecond Pump−Probe Study. *J. Phys. Chem. B* **2000**, *104* (39), 9330–9342.

(29) Polívka, T.; Zigmantas, D.; Sundström, V.; Formaggio, E.; Cinque, G.; Bassi, R. Carotenoid S1 State in a Recombinant Light-Harvesting Complex of Photosystem II. *Biochemistry* **2002**, *41* (2), 439–450.

(30) V. Barzda, V. Gulbinas, R. Kananavicius, V. Cervinskas, H. van Amerongen, R. van Grondelle, L. V. Singlet–Singlet Annihilation Kinetics in Aggregates and Trimers of LHCII. *Biophys. J.* **2001**, *80*, 2409–2421.

(31) Bennett, D. I. G.; Fleming, G. R.; Amarnath, K. Energy-Dependent Quenching Adjusts the Excitation Diffusion Length to Regulate Photosynthetic Light Harvesting. *Arxhiv eLife Submitt.* **2018**.

(32) Dall'Osto, L.; Cazzaniga, S.; Bressan, M.; Paleeèk, D.; Židek, K.; Niyogi, K. K.; Fleming, G. R.; Zigmantas, D.; Bassi, R. Two Mechanisms for Dissipation of Excess Light in Monomeric and Trimeric Light-Harvesting Complexes. *Nat. Plants* **2017**, *3* (April).

(33) Kulheim, C. Rapid Regulation of Light Harvesting and Plant Fitness in the Field. *Science (80-.).* **2002**, *297* (5578), 91–93.

(34) Kromdijk, J.; Glowacka, K.; Leonelli, L.; Gabilly, S. T.; Iwai, M.; Niyogi, K. K.; Long, S. P. Improving Photosynthesis and Crop Productivity by Accelerating Recovery from Photoprotection. **2016**, *354* (6314), 857–862.

(35) Hontani, Y.; Kloz, M.; Polívka, T.; Shukla, M. K.; Sobotka, R.; Kennis, J. T. M. Molecular Origin of Photoprotection in Cyanobacteria Probed by Watermarked Femtosecond Stimulated Raman Spectroscopy. *J. Phys. Chem. Lett.* **2018**, *9* (7), 1788–1792.

(36) Leuenberger, M.; Morris, J. M.; Chan, A. M.; Leonelli, L.; Niyogi, K. K.; Fleming, G. R. Dissecting and Modeling Zeaxanthin- and Lutein-Dependent Nonphotochemical Quenching in Arabidopsis Thaliana. *Proc. Natl. Acad. Sci. U. S. A.* **2017**, *114* (33), E7009–E7017.

(37) Sylak-Glassman, E. J.; Malnoë, A.; De Re, E.; Brooks, M. D.; Fischer, A. L.; Niyogi, K. K.; Fleming, G. R. Distinct Roles of the Photosystem II Protein PsbS and Zeaxanthin in the Regulation of Light Harvesting in Plants Revealed by Fluorescence Lifetime Snapshots. *Proc. Natl. Acad. Sci.* **2014**, *111* (49), 17498–17503.

(38) Sylak-Glassman, E. J.; Zaks, J.; Amarnath, K.; Leuenberger, M.; Fleming, G. R. Characterizing Non-Photochemical Quenching in Leaves through Fluorescence Lifetime Snapshots. *Photosynth. Res.* **2016**, *127* (1), 69–76.

(39) Adams, W. W.; Demmig-Adams, B.; Winter, K.; Winter, K. Relative Contributions of Zeaxanthin-Related and Zeaxanthin-Unrelated Types of ;high-Energy-State' Quenching of Chlorophyll Fluorescence in Spinach Leaves Exposed to Various Environmental Conditions. *Plant Physiol.* **1990**, *92* (2), 302–309.

(40) Bilger, W.; Björkman, O. Role of the Xanthophyll Cycle in Photoprotection Elucidated by

Measurements of Light-Induced Absorbance Changes, Fluorescence and Photosynthesis in Leaves of Hedera Canariensis. *Photosynth. Res.* **1990**, *25* (3), 173–185.

(41) Tikkanen, M.; Aro, E. M. Thylakoid Protein Phosphorylation in Dynamic Regulation of Photosystem II in Higher Plants. *Biochim. Biophys. Acta* **2012**, *1817* (1), 232–238.

(42) Li, X. P.; Björkman, O.; Shih, C.; Grossman, A. R.; Rosenquist, M.; Jansson, S.; Niyogi, K. K. A Pigment-Binding Protein Essential for Regulation of Photosynthetic Light Harvesting. *Nature* **2000**, *403* (6768), 391–395.

(43) Li, X.-P.; Muller-Moule, P.; Gilmore, A. M.; Niyogi, K. K. PsbS-Dependent Enhancement of Feedback de-Excitation Protects Photosystem II from Photoinhibition. *Proc. Natl. Acad. Sci.* **2002**, *99* (23), 15222–15227.

(44) van Oort, B.; Roy, L. M.; Xu, P.; Lu, Y.; Karcher, D.; Bock, R.; Croce, R. Revisiting the Role of Xanthophylls in Nonphotochemical Quenching. *J. Phys. Chem. Lett.* **2018**, 346–352.

(45) Ahn, T. K.; Avenson, T. J.; Ballottari, M.; Cheng, Y.-C.; Niyogi, K. K.; Bassi, R.; Fleming, G. R. Architecture of a Charge-Transfer State Regulating Light Harvesting in a Plant Antenna Protein. *Science* **2008**, *320* (5877), 794–797.

(46) Gilmore, A. M.; Shinkarev, V. P.; Hazlett, T. L.; Govindjee. Quantitative Analysis of the Effects of Intrathylakoid pH and Xanthophyll Cycle Pigments on Chlorophyll a Fluorescence Lifetime Distributions and Intensity in Thylakoids †. *Biochemistry* **1998**, *37* (39), 13582–13593.

(47) Schansker, G.; Tóth, S. Z.; Strasser, R. J. Dark Recovery of the Chl a Fluorescence Transient (OJIP) after Light Adaptation: The qT-Component of Non-Photochemical Quenching Is Related to an Activated Photosystem I Acceptor Side. *Biochim. Biophys. Acta - Bioenerg.* **2006**, *1757* (7), 787–797.

(48) Cheng, Y. C.; Ahn, T. K.; Avenson, T. J.; Zigmantas, D.; Niyogi, K. K.; Ballottari, M.; Bassi, R.; Fleming, G. R. Kinetic Modeling of Charge-Transfer Quenching in the CP29 Minor Complex. *J. Phys. Chem. B* **2008**, *112* (42), 13418–13423.

Chapter 5: Analyzing the dynamics of Carotenoid S1 absorption in *Nannochloropsis oceanica*

Collaborators

The data presented here was taken in collaboration with Dr. Dagmar Lyska from Prof. Kris Niyogi's lab, as well as Dr. Soomin Park and Collin Steen. Dagmar Lyska prepared the *N. oceanica* samples, and she and Ben Endelman created the mutants used for this work. Data collection was a collaborative effort between Soomin, Collin, Dagmar and myself. Dagmar analyzed the time-dependent HPLC measurements.

Introduction

To further investigate the details of Zea participation in charge transfer (CT) and excitation energy transfer (EET) quenching as well as the roles CT and EET quenching both play in the overall qE quenching response, we have applied our snapshot transient absorption technique to the algae *Nannochloropsis oceanica*. *N. oceanica* in particular is an excellent organism for this question, as it contains fewer types of pigments relative to land plants as well as other algae, which is helpful for identifying spectroscopic signatures.

N. oceanica is a small marine algae that is of particular interest as a potentially useful organism for biofuel production due to its high lipid content.[1–4] *N. oceanica* belongs to the group of algae called Heterokonts, which typically contain chlorophyll a and chlorophyll c.[5,6] *N. oceanica* however, only has Chl a. Furthermore, this species relies on the pigments in the xanthophyll cycle as primary light-harvesting carotenoids, rather than lutein.[2] However, essential components and mechanisms of non-photochemical quenching in *N. oceanica* are currently unknown.

Recently Dagmar Lyska and Ben Endelman have developed several sets of *N. oceanica* mutant strains, which can be divided into two categories. The first group of mutants contain altered amounts of the LHCX1 protein. The LHCX1 protein has previously been identified as an antenna of the violaxanthin-chlorophyll a protein (VCP), which is thought to be a light-harvesting protein with especially high carotenoid-to chlorophyll energy transfer efficiency.[5,7] It is unknown if VCP itself is a site of quenching in *N. oceanica*'s response to excess light. We characterized *lhcx1* knockout mutant, which I will refer to as *lhcx1*, as well as a mutant which overexpresses this protein, which I will refer to as *lhcx1 OE*. In her early work characterizing these mutants, Lyska found that removal of the *lhcx1* protein significantly reduced the

quenching ability of the cells (manuscript in preparation). It is unknown whether *lhcx1* is directly involved in quenching, and if so, the mechanism by which it performs this quenching.

The second set of mutant strains Lyska developed were designed to examine the effects of zeaxanthin accumulation on the quenching capacity as well as the quenching induction and relaxation dynamics in *N. oceanica*. First, she created a violaxanthin de-epoxidase knockout strain (*vde*) which cannot accumulate Zea in response to intense light. She also developed a series of zeaxanthin epoxidase mutants, which have a limited ability to convert accumulated Zea back to Vio after light acclimation.[8] These mutants will be referred to as *zep22*, *zep72*, and *zep74*. These mutants differ in their amount of residual zeaxanthin epoxidase activity.

See table 5.1 for a summary of *N. oceanica* strains discussed here.

Mutant name	Effect
lhcx1	Lacks *lhcx1* protein
lhcx1 OE	Excess *lhcx1* protein
vde	Lacks violaxanthin de-epoxidase, cannot accumulate Zea
zep22	Lower zeaxanthin epoxidase, less back conversion from Zea to Vio
zep72	Lower zeaxanthin epoxidase, less back conversion from Zea to Vio
zep74	Lower zeaxanthin epoxidase, less back conversion from Zea to Vio

Table 5.1: Summary of *N. oceanica* mutants and their effects

To investigate whether the LHCX1 protein may be directly involved in EET quenching as well as the relationship between zeaxanthin accumulation, NPQ, and EET quenching, we have examined wild-type *N. oceanica* as well as these mutants using snapshot transient absorption spectroscopy, fluorescence lifetime snapshots, and time-resolved HPLC. Snapshot transient absorption measurements designed to follow Car (assumed to be Zea) S1 signal evolution, were used to determine the likelihood of EET quenching (see chapter 4). Snapshot fluorescence lifetime data will provide insight into the speed of quenching induction as well as the relative quenching intensities across the *N. oceanica* strains. Lastly, time-resolved HPLC measurements were taken at various points during the light-acclimation sequence to determine the zeaxanthin concentration as a function of exposure to bright light. This chapter is a discussion of the progress made thus far to determine the mechanisms of quenching in *N. oceanica*, but there is significant work remaining.

Methods

All *N. oceanica* cells were grown in approximately 30 mL volumes in open flasks at 20°C, 30 µmol photons m^{-2} s^{-1}. Prior to experiment, each culture was concentrated to 80 mg of chlorophyll a per mL. All samples were dark-acclimated for 30 minutes immediately prior to experiment.

Fluorescence lifetime snapshot and and HPLC measurements were carried out using the apparatus and protocols discussed in chapters 2 and 3 with the following modifications. Fluorescence lifetime measurements were carried out with a light sequence consisting of 5 minutes of dark, then 10 minutes of actinic light at 850 µmol photons m^{-2} s^{-1}, followed by 5 minutes of dark re-acclimation. HPLC samples were taken in triplicate after 30 minutes of dark acclimation, halfway through the light acclimation period (5 mins), at the end of the light acclimation period, and at the end of the dark re-acclimation period.

The snapshot transient absorption measurements were taken using the same apparatus and process described in chapter 4 with the following changes. The pump and probe wavelengths were set to 650 nm and 540 nm to excite Chl a and the Zea S1 –SN transition, respectively. The light acclimation sequence used started with 3 minutes of darkness, 10 minutes of actinic light at 850 µmol photons m^{-2} s^{-1}, then 5 minutes of dark re-acclimation.

Results and Discussion

To investigate the dynamics of Car S1 population in *N. oceanica*, and by extension the role of EET quenching, we examined a series of *N. oceanica* mutants with snapshot transient absorption spectroscopy, fluorescence lifetime snapshot spectroscopy, and time-resolved HPLC measurements. In addition to wild-type *N. oceanica*, the mutants studied include *vde*, *lhcx1* KO, *lhcx1 OE*, as well as several mutants with altered zeaxanthin epoxidase activity, *zep22*, *zep72*, and *zep74*. All algae samples were dark-acclimated for 30 minutes prior to data collection. The average fluorescence lifetimes as a function of dark and light exposure for wild-type, *VDE*, *lhcx1*, *lhcx1 OE*, *zep22*, *zep72*, and *zep74* are shown in Figure 5.1.

The first strain of *N. oceanica* to respond to the actinic light turning on is *zep72*, whose average fluorescence lifetime (τ_{avg}) drops sharply within 10 seconds of light acclimation, then is reduced more slowly over the 10 minutes of light acclimation. The next-most-rapid response is in the *zep22*, strain, followed by wild-type, while *zep74* and *lhcx1 OE* both respond on similar (slower) timescales. The average fluorescence lifetime of the *VDE* mutant does show a small initial drop in response to the actinic light turning on, and a smaller slow drop over the course of the light acclimation, while the average fluorescence lifetime of the *lhcx1* mutant does not appear to immediately respond to the actinic light turning on, but shows a small and slow decrease as the sample acclimates to bright light.

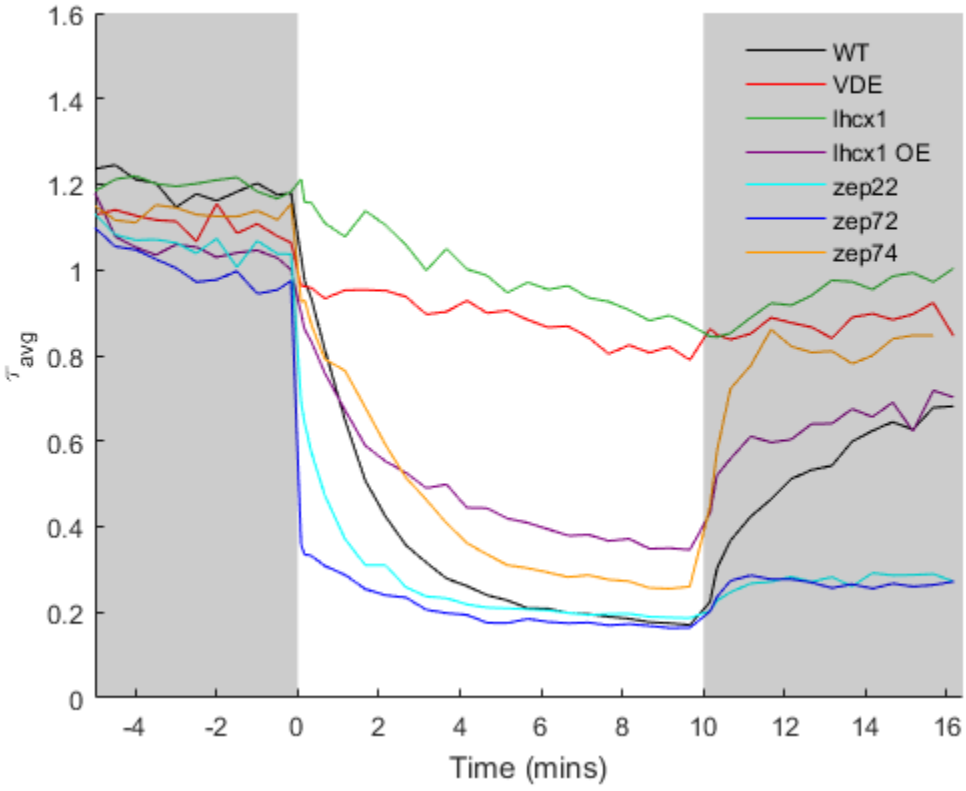

Figure 5.1. The average fluorescence lifetimes of wild-type (black), *vde* (red), *lhcx1* (green), *lhcx1 OE* (purple), *zep22* (cyan), *zep72* (blue), and *zep74* (orange). Dark grey background indicates dark-acclimation conditions, while white background indicates light-acclimation conditions. The intensity of the actinic light was set to 850 µE m^{-2} s^{-1}.

The difference in sample relaxation time across the various strains is also noteworthy. While *zep72* was the fastest to respond to actinic light turning on, it appears to relax much more slowly. There is a small increase in the average fluorescence lifetime, but only about the magnitude of the more slowly-responsive component rather. *Zep22* relaxes similarly, with only a small increase in the fluorescence lifetime when the dark-acclimation begins. However, though it did not reach as high a level of quenching, the *zep74* mutant relaxed extremely quickly and to a far greater extent than either *zep22* or *zep72*. In comparison, wild-type samples had a moderate relaxation speed. At first, the *lhcx1 OE* mutant relaxes quickly, but this relaxation is somewhat limited, as it then appears to relax more slowly after the first minute of re-acclimation to darkness. The *lhcx1* KO mutant does not have a fast initial relaxation, and instead appears to relax at a rate similar to the quenching turn-on rate. In contrast, the *VDE* mutant quenching appears to relax much more slowly than it turns on. The intensity of quenching as well as the varying rates of quenching induction and relaxation across mutants varies significantly, and will be useful when correlated with the strength and speed of the Car S1 signal, determined via snapshot transient absorption spectroscopy.

It is important to note that the Car S1 signal is only observable in snapshot transient absorption measurements due to the high pump laser intensity which causes significant

exciton-exciton annihilation in the samples and consequently shortens the average distance each excitation travels within the membrane. As the Car S1 relaxation process is very fast (<10 ps) compared to the amount of time it takes for excitation energy to reach a particular site of quenching (300 ps – 1ns), ordinarily the Car S1 site would not be sufficiently populated to be observed with transient absorption spectroscopy.[9–12] The relationship between annihilation, quenching, and Car S1 observation is still under discussion (see chapter 4), but for the purposes of this chapter I will assume that the amount of annihilation is constant over the course of the light acclimation sequence, and that the induction of non-EET quenching mechanisms does not affect the amount of Car S1 signal observed. Additional information characterizing the Car S1 signal in each *N. oceanica* strain can be found in the supplemental information.

In order to determine the timing and potential role of EET quenching in *N. oceanica*, the Car S1 absorption signal was monitored at 540 nm using snapshot transient absorption data for the *N. oceanica* strains as they acclimated to high light. Within the first subset of strains, the wild-type algae showed the most rapid growth in Car S1 signal, followed by *lhcx1 OE*, which also ultimately reached similar signal intensities (Figure 5.2). Notably, the Car S1 signals for these two stains did not show significant reduction during the dark re-acclimation period. Instead they stayed largely consistent with their final light acclimated intensity, with only a small reduction in *lhcx1 OE* and wild-type. The *lhcx1* KO mutant showed slow growth over the course of the light acclimation time, while the wild-type and *lhcx1 OE* strains reached maximum signal after approximately 4 minutes of light acclimation, then remained fairly constant. However, after the bright light was turned off, the Car S1 signal in the *lhcx1 OE* mutant quickly dropped, ultimately below zero. This could be due to several possible factors, which will be discussed in the next paragraph. Lastly, the *vde* mutant showed little-to-no signal over the course of the light acclimation sequence.

Within the second set of data, displayed in figure 5.3, the Car S1 absorption signal is shown for *zep22*, *zep72*, and *zep74*, as well as the wild-type signal for reference. Amongst the zep strains, the Car S1 signal appeared fastest in *zep22*. *Zep22* also reached the highest intensity of Car S1 absorption, growing fairly steadily and peaking after approximately 9 minutes of light acclimation. Wild-type Car S1 signal increased at a similar rate, but plateaus earlier and reaches about 70% of the intensity of *zep22*. In contrast, signals from *zep72* and *zep74* strains rise much more slowly than either wild-type or *zep22*. The *zep74* signal intensity reaches a similar level to wild-type after approximately 5 minutes of light acclimation, where it then plateaus. *Zep72* meanwhile, grows slowly and steadily over the entire course of light acclimation, but does not reach as high an intensity as WT or *zep74*. During the dark re-acclimation period, the Car S1 signal in all three of the *zep* mutants seems to increase slightly, while WT slightly decreases.

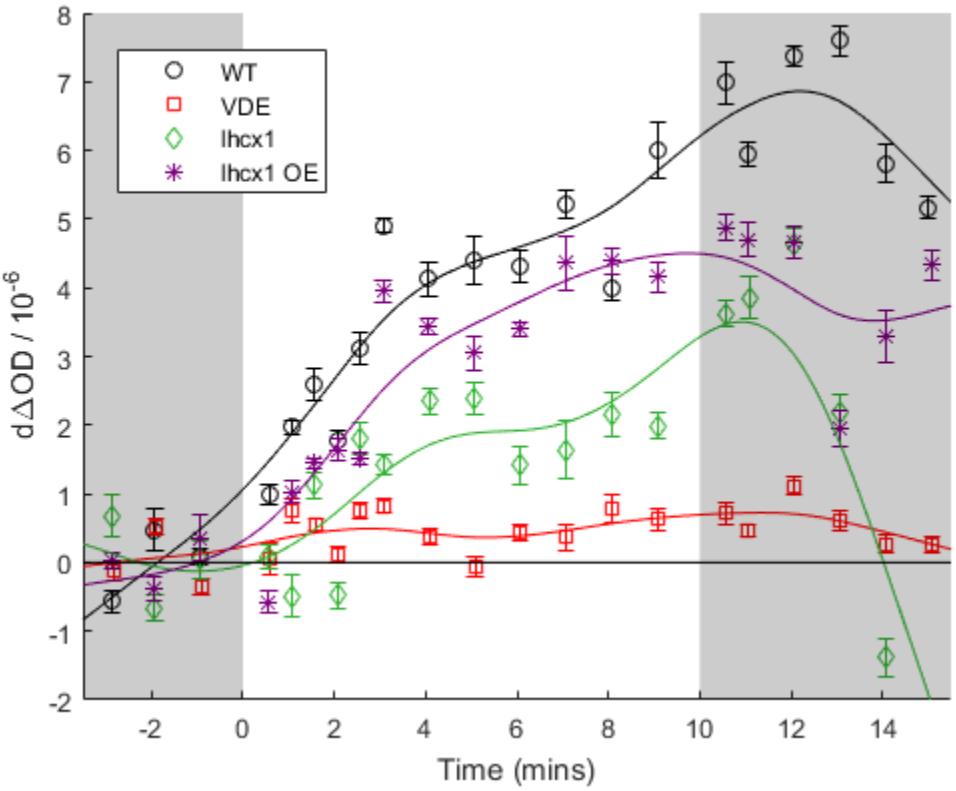

Figure 5.2: Evolution of the Car S1 signal in *N. oceanica* strains as they acclimate to high light. Data was taken at a probe wavelength of 540 nm and is the difference between the light acclimated signal and the dark-acclimated signal at 1 ps, scaled to account for underlying Chl ESA changes, as described in Chapter 4. In a) Wild-type is shown as black circles, *vde* knockout mutant as red squares, *lhcx1* knockout mutant as green diamonds, and *lhcx1* over-expresser is shown as purple stars. The solid lines are smoothed curve representations of the data. The zero line represents the average of the fully dark-acclimated signal. The grey background represents dark-acclimation conditions, while the white light represents high-light acclimating conditions. The intensity of the actinic light was set to 850 µmol photons m^{-2} s^{-1}.

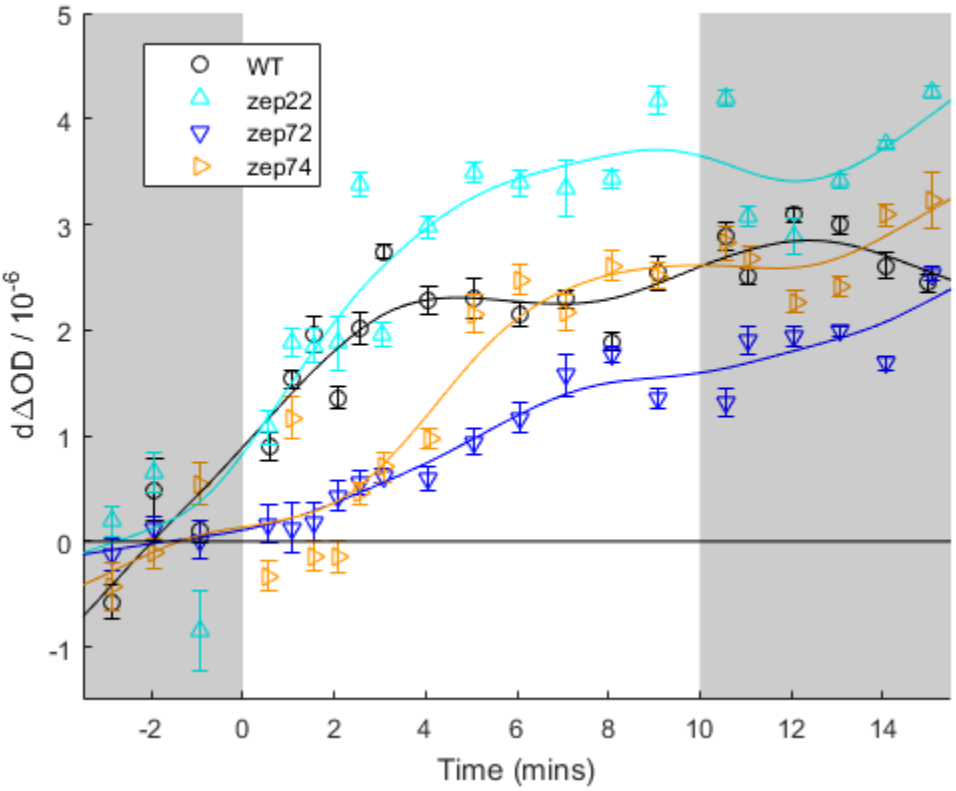

Figure 5.3: Evolution of the Car S1 signal in *N. oceanica* strains as they acclimate to high light. Probe wavelength was set to 540 nm. Data presented is the difference between the light acclimated signal and the dark-acclimated signal at 1 ps, scaled to account for underlying Chl ESA changes, as described in Chapter 4. Wild-type data from figure 5.X is shown as black circles for reference, *zep22* shown as cyan triangles, *zep72* as blue upside-down triangles, and *zep74* as orange sideways triangles. The solid lines are smoothed curve representations of the data. The zero line represents the average of the fully dark-acclimated signal. The grey background represents dark-acclimation conditions, while the white light represents high-light acclimating conditions. The intensity of the actinic light was set to 850 µmol photons m^{-2} s^{-1}.

To determine the relationship between Zea concentration, Car S1 signal evolution, and quenching intensity, we also collected HPLC measurements over the course of the light acclimation. The first samples were measured after 30 minutes of dark acclimation, then midway through the light-acclimation period, then at the end of the light acclimation period, and finally after 5 minutes of re-acclimation to darkness. These concentrations are shown in figure 5.4. The *vde* strain contained a small and unchanging amount of Zea throughout the entirety of the experiment, while all other strains accumulated significant Zea during the light-acclimation. At the end of the light-acclimation, *zep22* had the highest concentration of Zea, followed by wild-type, then *zep72*, while *lhcx1* and *lhcx1 OE* both accumulated a moderate amount. However, the Zea concentrations in wild-type, *zep22*, *zep72*, and *vde* strains did not

change significantly during the dark re-acclimation, while the concentration decreased in both *lhcx1* and *lhcx1 OE*.

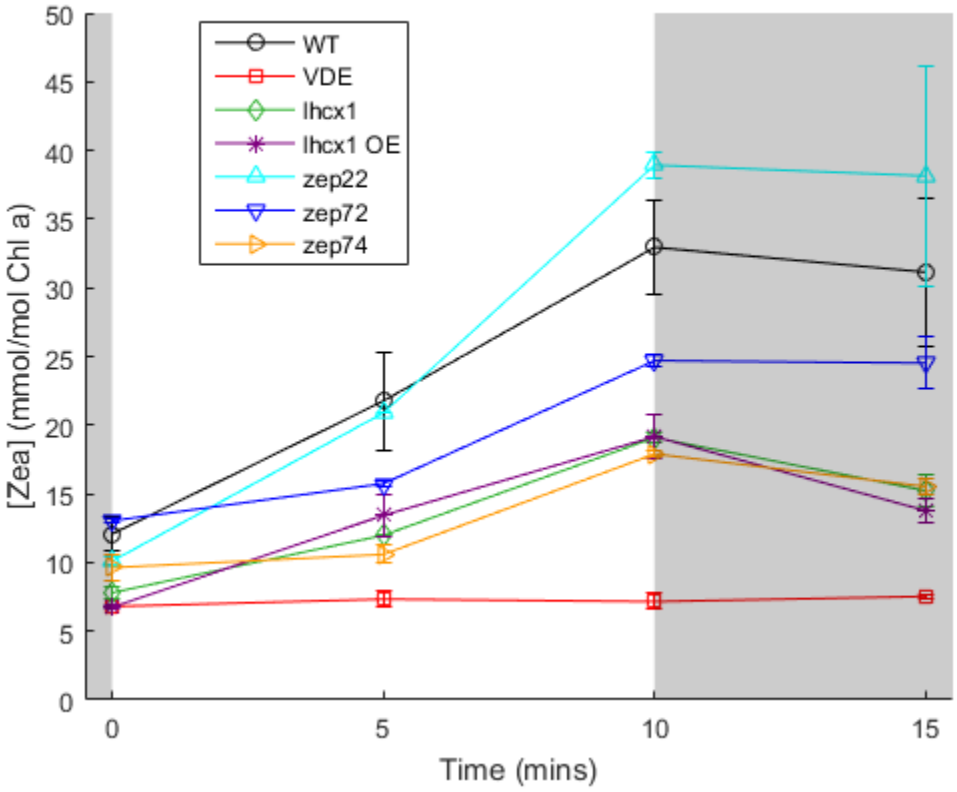

Figure 5.4: Time-dependent concentration of zeaxanthin of *N. oceanica* strains. Wild-type is shown as black circles, *vde* knockout mutant as red squares, *lhcx1* knockout mutant as green diamonds, *lhcx1* over-expresser as purple stars, *zep22* shown as cyan triangles, *zep72* as blue upside-down triangles, and *zep74* as orange sideways triangles. The grey background represents dark-acclimation conditions, while the white light represents high-light acclimating conditions. The intensity of the actinic light was set to 850 µmol photons m^{-2} s^{-1}. Samples were dark-acclimated for 30 minutes prior to time 0. N = 3, error bars shown are the standard deviation.

When the Car S1 absorption data is compared to the Chl fluorescence lifetime and time-resolved HPLC data, many interesting trends emerge. First, I will discuss the apparent relationship between the Car S1 signal intensity, the Zea concentration, and the Chl fluorescence lifetime dynamics. In wild-type cells, the majority of the maximum fluorescence quenching is reached after approximately 4 minutes of light acclimation, after which time there is a continued slow increase in quenching. In the corresponding Car S1 data, the majority of the maximum Car S1 signal appears after approximately 3 minutes of light acclimation, and may slowly increase over the rest of the light acclimation time, a similar timescale and behavior compared to the quenching. Lastly, the Zea concentration increases slowly and steadily during

the light acclimation. On the other hand, the *vde* knockout mutant showed a small amount of immediate quenching, and a very low and constant amount of Car S1 ESA after the light acclimation began. There was also a small and unchanging amount of zea during the course of the light acclimation sequence. This seems to indicate that Zea is necessary for the majority of quenching in *N. oceanica*, and that some of that quenching may be EET quenching. It also seems that if Zea is available, EET quenching responds quickly to increases in light intensity, and is unlikely to be responsible for the small amount of fast quenching seen in the *vde* mutant. Additionally, it does not appear that EET quenching relaxes very quickly once dark re-acclimation begins, as shown by the wild-type, *lhcx1 OE* mutant, and the trio of *zep* mutants.

Each of the *zep* mutants accumulates a different amount of Zea during the light acclimation period. *Zep22* accumulates the most, followed by *zep72*, then *zep74*. This is somewhat similar to the speed with which the Chl fluorescence quenching turns on. In terms of quenching induction, *zep72* is the fastest, followed by *zep22*, then *zep74*. This discrepancy can be explained by the fact that *zep72* starts the light acclimation period with the highest concentration of Zea (Fig 5.4). And indeed, after that initial acclimation, *zep22* and *zep72* show very similar quenching behavior, while *zep74* consistently quenches to a lesser extent (Figure 5.1). In terms of the Car S1 signal evolution, the *zep22* strain consistently has the highest signal intensity, while the Car S1 signal in *zep72* grows much more slowly and steadily, but ultimately is lower than either *zep22* or *zep74*. This indicates that the fast initial quenching in *zep72* may not actually be due to EET quenching, but is likely some other zea-dependent mode of quenching, such as CT quenching.[11,13,14] Additionally, during dark re-acclimation the Car S1 signal increased for all three *zep* mutants, despite the fact that during the same time period, the Zea concentration decreases or remains constant. The quenching relaxation behavior is also somewhat inconsistent with the trends observed in Car S1 data. For both *zep22* and *zep72*, the quenching relaxes rapidly, but only to a small extent. Meanwhile, *zep74* mutant quenching relaxes very rapidly and almost completely within 2 minutes of dark re-acclimation. This is very puzzling, as it seems that the relaxation of quenching during the short dark re-acclimation time is largely decoupled from the Car S1 behavior, especially in the *zep74* mutant. It may be that in *N. oceanica* EET quenching contributes only a very small amount to overall quenching, and thus its presence or absence does not significantly change the overall Chl fluorescence lifetime. Or, it may be that EET quenching is responsible for the more-slowly acclimating portion of NPQ, which also relaxes slowly. However, little is known about the thylakoid membrane proteins, or their organization, in *N. oceanica*. It may be that these mutations significantly alter protein structural features or arrangements, influencing observed quenching and Car S1 signal behavior.

Briefly, I shall also discuss potential quenching mechanisms of the LHCX1 protein, and its potential role in quenching in *N. oceanica*. In the wild-type strain, the Car S1 signal, the Chl fluorescence quenching, and the Zea concentration all appear to evolve on similar timescales, and at first glance the *lhcx1* KO mutant appears to behave similarly. The *lhcx1* KO strain shows only a small amount of slowly-acclimating quenching, and the Car S1 signal also grows steadily over the course of the light acclimation, but it reaches a similar amplitude to the wild-type signal at the end of the light acclimation period. This indicates that EET quenching is not dependent on the presence of the *lhcx1*, which is reinforced by the *lhcx1* overexpressor

mutant. The *lhcx1 OE* quenching data shows moderate quenching, but slower and less intense compared to wild-type. However, the shape and intensity of the *lhcx1 OE* Car S1 signal is extremely similar to that of wild-type, despite having half wild-type's maximum Zea concentration. Thus, the Car S1 signal does not appear to be influence by the absence or excess of the LHCX1 protein. These results also reinforce the notion that while the Car S1 signal appears to be related to the concentration of Zea, it is possible that EET quenching mechanism is either a slowly-accumulating type of quenching, or it is not responsible for a large portion of overall quenching in *N. oceanica*, though neither hypothesis can be confirmed definitely at this time.

Future work should focus on determining if Zea+ appearance is correlated with Chl fluorescence quenching, which would imply that Zea is participating in CT quenching, in addition to EET quenching. Further work exploring other possible factors influencing qE quenching in *N. oceanica* would also help contextualize these findings and further solidify the role EET quenching plays in the overall quenching response.

Supplemental Information

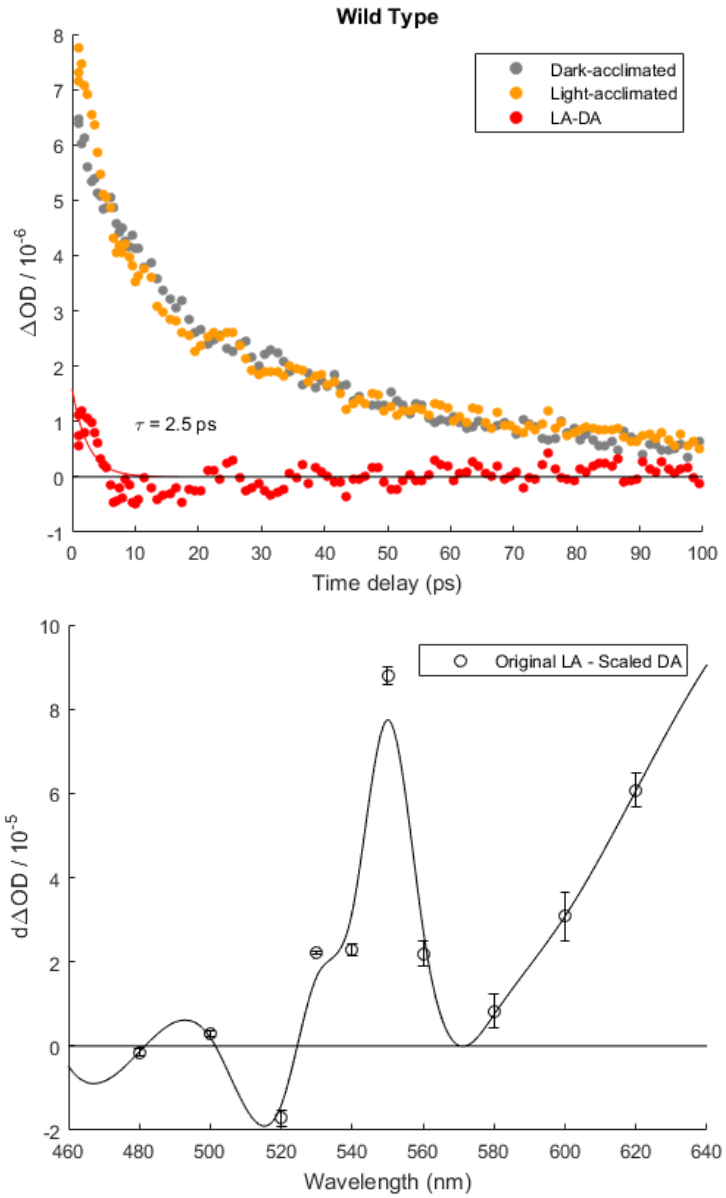

Figure 5.5: Transient absorption kinetic decays (top) and difference spectrum (bottom) of wild-type *N. oceanica* cells. Kinetic decays of dark-acclimated (grey) and light-acclimated (orange) as well as the difference (red) decay are shown in the upper image. Difference is fitted to a single exponential decay form. The lower image shows the wavelength-dependent absorption difference between light-acclimated sample and scaled dark-acclimated sample (black circles), as described in Chapter 4. Light acclimation consisted of 10 minutes of exposure to an actinic light set to 850 µE m^{-2} s^{-1}.

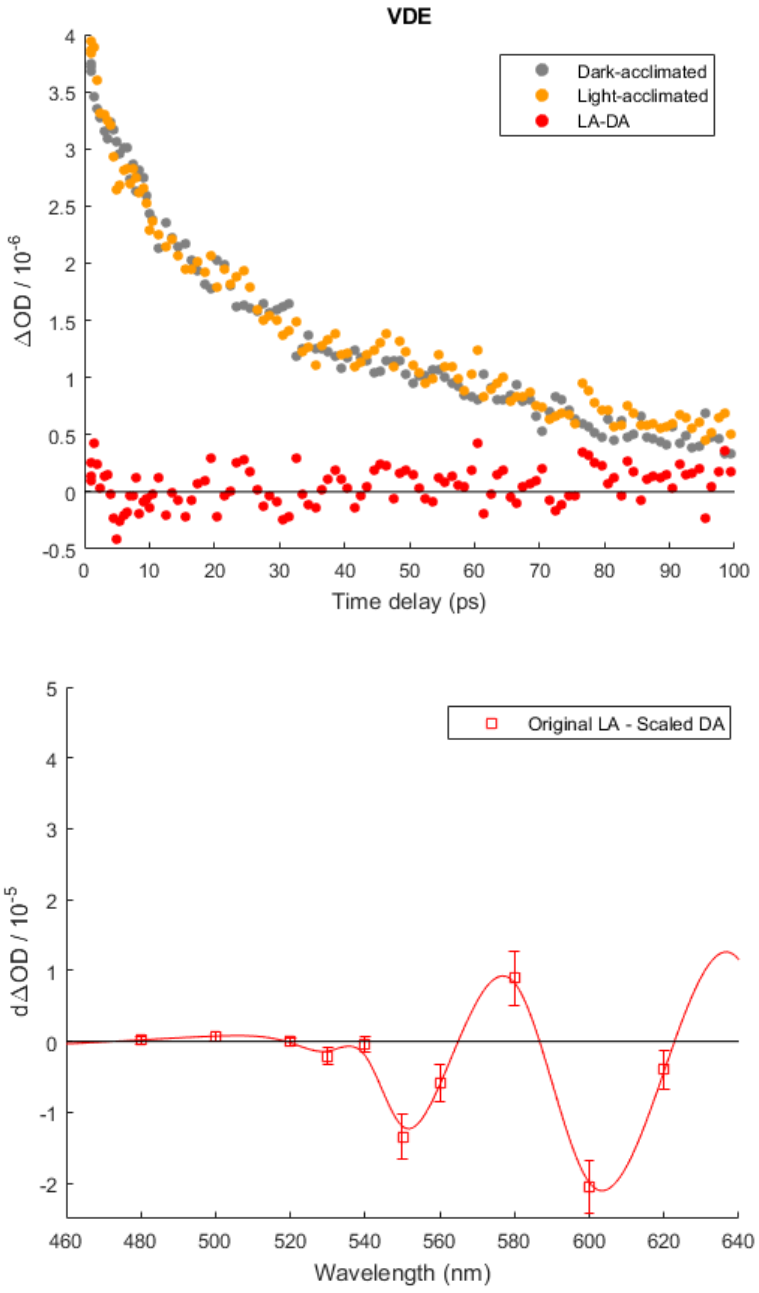

Figure 5.6: Transient absorption kinetic decays (top) as well as the difference spectrum (bottom) of *vde* mutant *N. oceanica* cells. Kinetic decays of dark-acclimated (grey) and light-acclimated (orange) as well as the difference (red) decay are shown in the upper image. The lower image shows the wavelength-dependent absorption difference between light-acclimated sample and scaled dark-acclimated sample (red squares), as described in Chapter 4. The solid line represents a smoothed average of the data points. Light acclimation consisted of 10 minutes of exposure to an actinic light set to 850 µE m^{-2} s^{-1}.

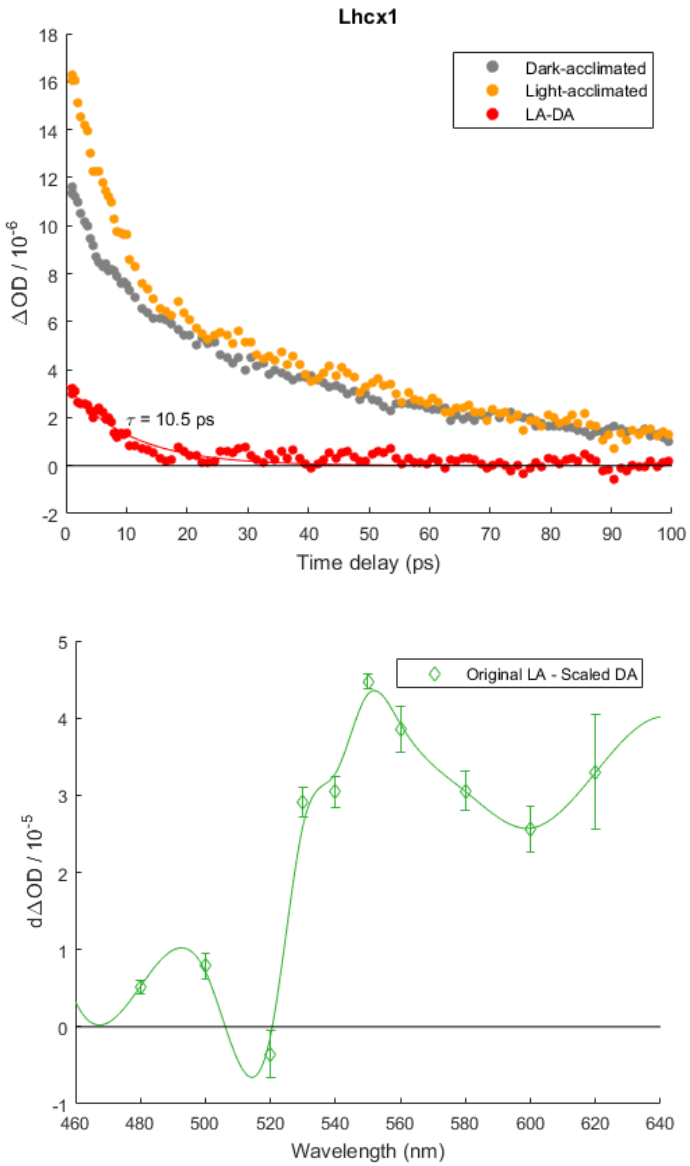

Figure 5.7: Transient absorption kinetic decays (top) as well as the difference spectrum (bottom) of *lhcx1* mutant *N. oceanica* cells. Kinetic decays of dark-acclimated (grey) and light-acclimated (orange) as well as the difference (red) decay are shown in the upper image. Difference is fitted to a single exponential decay. The lower image shows the wavelength-dependent absorption difference between light-acclimated sample and scaled dark-acclimated sample (green diamonds), as described in Chapter 4. The solid line represents a smoothed average of the data points. Light acclimation consisted of 10 minutes of exposure to an actinic light set to 850 µE m^{-2} s^{-1}.

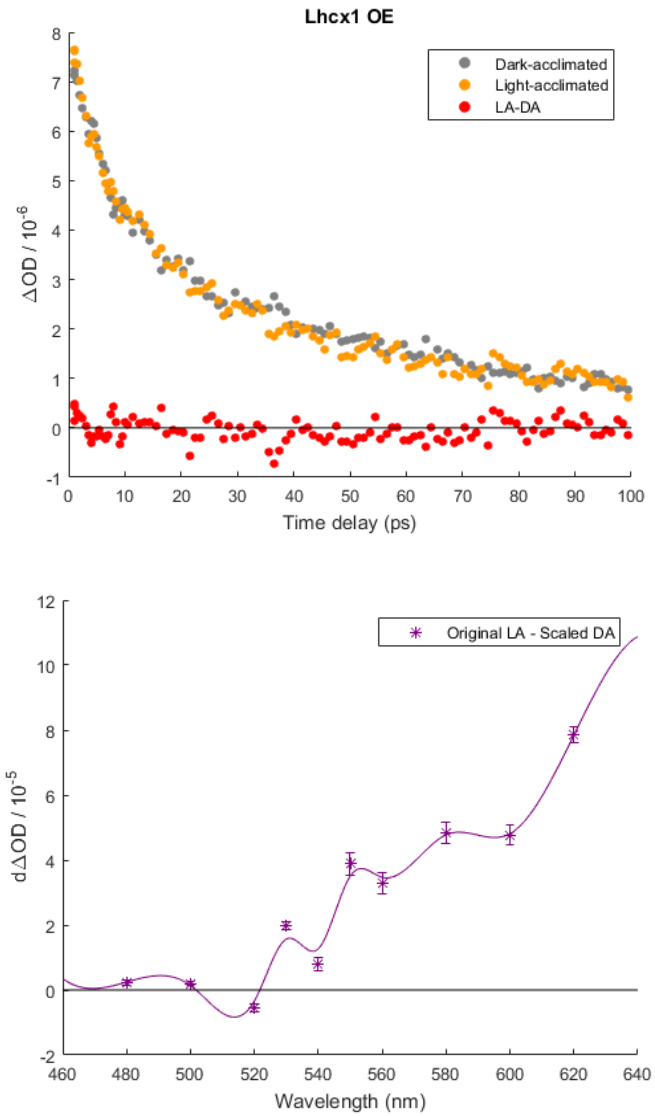

Figure 5.8: Transient absorption kinetic decays (top) and the difference spectrum (bottom) of *lhcx1 OE* mutant *N. oceanica* cells. Upper image shows kinetic decays of dark-acclimated (grey) and light-acclimated (orange) as well as the difference (red). The lower image shows the wavelength-dependent absorption difference between light-acclimated sample and scaled dark-acclimated sample (purple stars), as described in Chapter 4. The solid line represents a smoothed average of the data points. Light acclimation consisted of 10 minutes of exposure to an actinic light set to 850 µE m^{-2} s^{-1}.

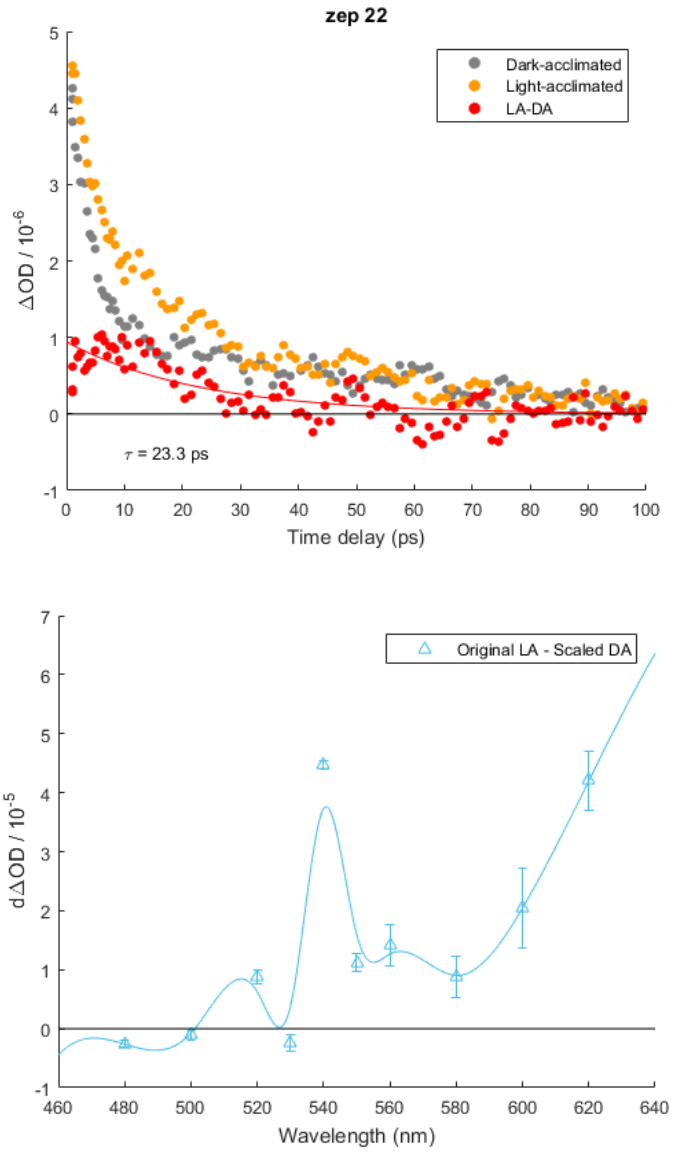

Figure 5.9: Transient absorption kinetic decays (top) and the difference spectrum (bottom) of *zep22* mutant *N. oceanica* cells. Upper image shows kinetic decays of dark-acclimated (grey) and light-acclimated (orange) as well as the difference (red). Difference decay is fitted to a single exponential decay. The lower image shows the wavelength-dependent absorption difference between light-acclimated sample and scaled dark-acclimated sample (light blue triangles), as described in Chapter 4. The solid line represents a smoothed average of the data points. Light acclimation consisted of 10 minutes of exposure to an actinic light set to 850 µE m^{-2} s^{-1}.

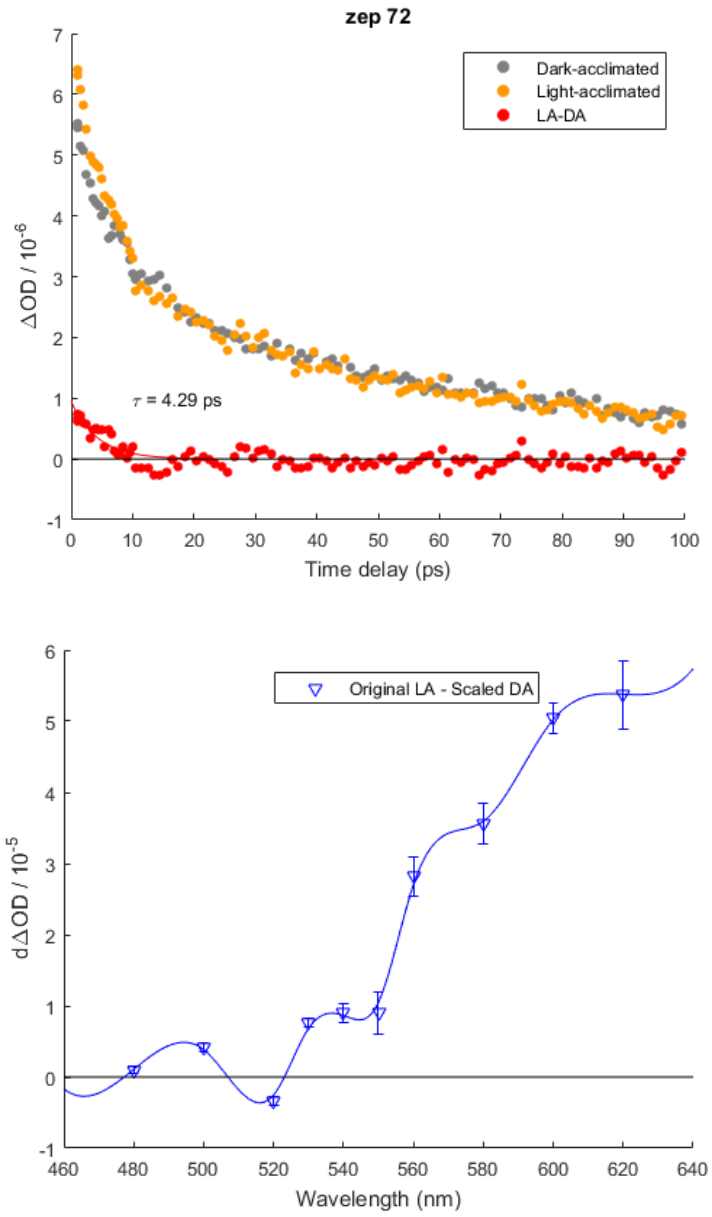

Figure 5.10: Transient absorption kinetic decays (top) and the difference spectrum (bottom) of *zep72* mutant *N. oceanica* cells. Upper image shows kinetic decays of dark-acclimated (grey) and light-acclimated (orange) as well as the difference (red). Difference decay is fitted to a single exponential decay. The wavelength-dependent absorption difference between light-acclimated sample and scaled dark-acclimated sample (blue inverted triangles), processed as described in Chapter 4, is shown in the lower image. The solid line represents a smoothed average of the data points. Light acclimation consisted of 10 minutes of exposure to an actinic light set to 850 µE m^{-2} s^{-1}.

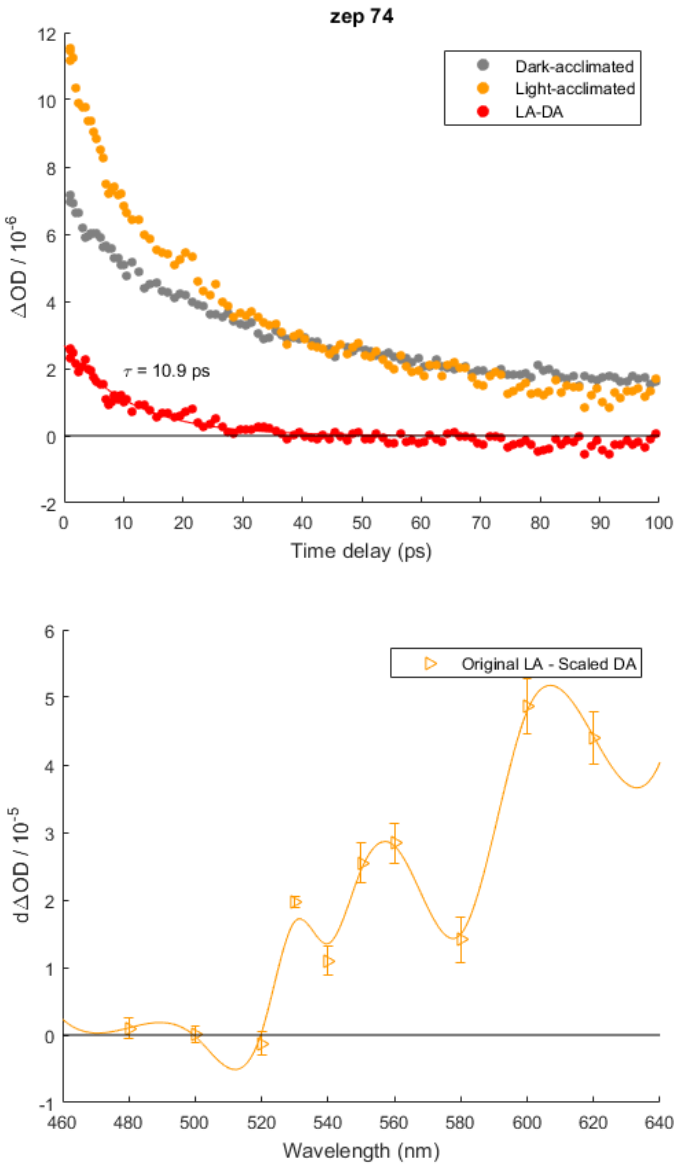

Figure 5.11: Transient absorption kinetic decays (top) and the difference spectrum (bottom) of *zep74* mutant *N. oceanica* cells. Upper image shows kinetic decays of dark-acclimated (grey) and light-acclimated (orange) as well as the difference (red). Difference decay is fitted to a single exponential decay. The lower image shows the wavelength-dependent absorption difference between light-acclimated sample and scaled dark-acclimated sample (orange sideways triangles), processed as described in Chapter 4. The solid line represents a smoothed average of the data points. Light acclimation consisted of 10 minutes of exposure to an actinic light set to 850 µE m^{-2} s^{-1}.

References:

(1) Basso, S.; Simionato, D.; Gerotto, C.; Segalla, A.; Giacometti, G. M.; Morosinotto, T. Characterization of the Photosynthetic Apparatus of the Eustigmatophycean Nannochloropsis Gaditana: Evidence of Convergent Evolution in the Supramolecular Organization of Photosystem I. *BBA - Bioenerg.* **2014**, *1837*, 306–314.

(2) Cao, S.; Zhang, X.; Xu, D.; Fan, X.; Mou, S.; Wang, Y.; Ye, N.; Wang, W. A Transthylakoid Proton Gradient and Inhibitors Induce a Non-Photochemical Fluorescence Quenching in Unicellular Algae Nannochloropsis Sp. *FEBS Lett.* **2013**, *587* (9), 1310–1315.

(3) Jia, J.; Han, D.; Gerken, H. G.; Li, Y.; Sommerfeld, M.; Hu, Q.; Xu, J. Molecular Mechanisms for Photosynthetic Carbon Partitioning into Storage Neutral Lipids in Nannochloropsis Oceanica under Nitrogen-Depletion Conditions. **2015**.

(4) Vieler, A.; Wu, G.; Tsai, C.-H.; Bullard, B.; Cornish, A. J.; Harvey, C.; Reca, I.-B.; Thornburg, C.; Achawanantakun, R.; Buehl, C. J.; et al. Genome, Functional Gene Annotation, and Nuclear Transformation of the Heterokont Oleaginous Alga Nannochloropsis Oceanica CCMP1779. *PLoS Genet* **2012**, *8* (11).

(5) Keşan, G.; Litvín, R.; Bína, D.; Durchan, M.; Šlouf, V.; Polívka, T. Efficient Light-Harvesting Using Non-Carbonyl Carotenoids: Energy Transfer Dynamics in the VCP Complex from Nannochloropsis Oceanica. *BBA - Bioenerg.* **2016**, *1857*, 370–379.

(6) Andersen, R. A. Biology and Systematics of Heterokont and Haptophyte Algae. *Am. J. Bot.* **2004**, *91* (10), 1508–1522.

(7) Litvín, R.; Bína, D.; Herbstová, M.; Gardian, Z. Architecture of the Light-Harvesting Apparatus of the Eustigmatophyte Alga Nannochloropsis Oceanica. *Photosynth. Res.* **2016**, *130*, 137–150.

(8) Leonelli, L.; Erickson, E.; Lyska, D.; Niyogi, K. K. Transient Expression in Nicotiana Benthamiana for Rapid Functional Analysis of Genes Involved in Non-Photochemical Quenching and Carotenoid Biosynthesis. *Plant J.* **2016**, *88* (3), 375–386.

(9) Polívka, T.; Sundström, V. Ultrafast Dynamics of Carotenoid Excited States−From Solution to Natural and Artificial Systems. *Chem. Rev.* **2003**, *104*, 2021–2071.

(10) Ma, Y.-Z.; Holt, N. E.; Li, X.-P.; Niyogi, K. K.; Fleming, G. R. Evidence for Direct Carotenoid Involvement in the Regulation of Photosynthetic Light Harvesting. *Proc. Natl. Acad. Sci.* **2003**, *100* (8), 4377–4382.

(11) Holt, N. E.; Zigmantas, D.; Valkunas, L.; Li, X. P.; Niyogi, K. K.; Fleming, G. R. Carotenoid Cation Formation and the Regulation of Photosynthetic Light Harvesting. *Science (80-.).* **2005**, *307* (5708), 433–436.

(12) Amarnath, K.; Bennett, D. I. G.; Schneider, A. R.; Fleming, G. R.; Barber, J.; Batista, V. S.;

Renger, T. Multiscale Model of Light Harvesting by Photosystem II in Plants. *Proc. Natl. Acad. Sci.* **2015**, *113* (5), 1156–1161.

(13) Andreas Dreuw, *; Graham R. Fleming, and; Head-Gordon, M. Charge-Transfer State as a Possible Signature of a Zeaxanthin−Chlorophyll Dimer in the Non-Photochemical Quenching Process in Green Plants. **2003**.

(14) Park, S.; Fischer, A. L.; Li, Z.; Bassi, R.; Niyogi, K. K.; Fleming, G. R. Snapshot Transient Absorption Spectroscopy of Carotenoid Radical Cations in High-Light-Acclimating Thylakoid Membranes. *J. Phys. Chem. Lett.* **2017**, *8* (22), 5548–5554.